DEPARTMENT OF OCEAN ENGINEERING

MASSACHUSETTS INSTITUTE OF TECHNOLOGY

CAMBRIDGE, MASSACHUSETTS 02139

AUTOMATIC CONTROL OF A SUBMERSIBLE

by

Kurt James Harris

SM (NAME)

SM (ME)

Course XIIIA

June 1984

AUTOMATIC CONTROL OF A SUBMERSIBLE

by

Kurt James Harris

B.S., Chemistry, Miami University

Submitted in Partial Fulfillment
of the Requirements for the
Degree of

MASTER OF SCIENCE IN NAVAL ARCHITECTURE
AND MARINE ENGINEERING

and the Degree of

MASTER OF SCIENCE IN MECHANICAL ENGINEERING

at the

MASSACHUSETTS INSTITUTE OF TECHNOLOGY

May 1984

AUTOMATIC CONTROL OF A
SUBMERSIBLE

by

Kurt James Harris

Submitted to the Departments of Ocean Engineering and Mechanical Engineering on May 1984 in partial fulfillment of the requirements for the Degree of Master of Science.

ABSTRACT

Multivariable control theory is used to design a controller for a modified drooping stern turning submersible. The procedure used is based on the LQG/LTR methodology. The controller is designed from a linear model and tested for performance on a nonlinear system model. Control variables are turning velocity, roll, and pitch. The resulting controller successfully minimizes roll and pitch for a turning submersible.

Thesis Supervisor: Dr. Lena Valavani
Research Scientist, Laboratory for Information and Decision Systems

Thesis Co-Supervisor: Dr. Damon E. Cummings
Visiting Lecturer, Department of Ocean Engineering

ACKNOWLEDGMENT

I would like to thank my supervisor, Dr. Lena Valavani, Dr. Damon Cummings, Dr. Martin Abkowitz, and Dr. Dana Yoerger for their help in shaping the ideas of this thesis and for their patience in seeing it through.

Additionally, I would like to thank Bill Bonnice for his many hours of assistance in computer programming of SUBMODEL. Without his help this thesis could not have been concluded.

Finally, I wish to thank Draper Laboratory for the opportunity to utilize their computer and administrative facilities.

Publication of this thesis does not constitute approval by The Charles Stark Draper Laboratory, Inc. of the findings or conclusions contained herein. It is published solely for the stimulation and exchange of ideas.

TABLE OF CONTENTS

TABLE OF CONTENTS (Cont.)

LIST OF FIGURES

LIST OF FIGURES (Cont.)

LIST OF TABLES

CHAPTER 1

INTRODUCTION

1.1 Introduction

In the present age of high technology and sophisticated development of vehicles, both air and submersible, designers continue to push the performance limits of their designs, due to increased demands on system requirements. Aircraft are required to perform faster, at higher and lower altitudes. Submersibles, especially submarines, are being designed to dive deeper and faster. It is this last category of vehicles that this thesis addresses.

The operating envelope of a submarine is predicated on its design depth and speed plus its ability to handle a mechanical casualty with enough time to recover before exceeding test depth of the hull. Currently, submarines have the capability to operate at depths greater than 700 feet and speeds in excess of 30 knots.

The current hull design has been determined to be the most efficient hydrodynamic design and has evolved from the Albacore. Additionally, the rudder and sternplane cnfiguration has basically been unchanged from the cruciform design for decades. The cruciform stern is quite a sensible design in case of a casualty situation. When one wants to climb or dive, all one has to do is either command rise or dive on the sternplanes. To turn, a similar situation exists. One just needs to turn the rudder in the desired direction one wants to go which also causes the boat to dive. However, the cruciform stern arrangement has

its drawbacks. There is no differential control, i.e., both the upper and lower rudders are mechanically tied together as are the right and left sternplane control surfaces. A severe casualty such as a sternplane jam on dive does not allow for independent action on the sternplane control surface. The corrective action to combat this casualty is to quickly reverse propulsion power direction and command full rise on the sailplanes. All of this corrective action must be accomplished fast enough, before the boat exceeds test depth. Finally, the cruciform stern does not effectively allow the boat to maintain a level attitude in a turn. The boat has a natural tendency to roll thereby causing the rudder to contribute to pitch as if it were a stern surface.

In order to effectively correct the drawbacks of the cruciform stern, an alternative stern configuration could be used employing differential control of its surfaces, i.e., each surface independently operated. The independent action would allow the operator to deflect the control surfaces that effect depth in a casualty. Also, if a sternplane jam casualty occurred, then the plane that did not suffer the casualty could be used to control the rate of depth excursion, while the propulsion plant is used to slow the vehicle. Differential action of the stern control surfaces can also be used to counteract the forces that cause roll, thereby prohibiting undesirable depth changes of the vehicle.

The stern configuration that will be considered in this thesis is called a modified drooping stern (MDS). The MDS consists of a single rudder surface with two dihedral surfaces 37.5° below the horizontal. In theory the MDS should be able to effectively control roll and enable the operator to combat a sternplane casualty. However, the MDS presents the operator with a coordination problem in that its movement is not so straightforward; for example, for normal cruising, how should one deflect the dihedral surfaces to control the effects of roll? It therefore becomes of considerable importance to design an automatic control system that handles such a vehicle in operation.

In this thesis a truly multivariable automatic controller will be designed for the MDS configuration. Since there exists a number of operating points within the submerged envelope, we have selected as a nominal design point that which describes the situation of a two degree deflection of the rudder and small deflections of the dihedrals, while the boat is at a velocity of 21 knots.

A sketch of the proposed submersible is located in Figure 1. The overall length is 180 feet with a top speed of 21 knots. Mass properties are summarized in Appendix A. The convention for positive deflections of the control surfaces are shown in Figure 2, using the right hand rule system. The rudder and dihedral surfaces will be referred to as D1, D2, and D3 and will be limited to a maximum deflection of plus or minus forty degrees.

The mathematical model used for the control design utilizes the six degree-of-freedom nonlinear differential equations as developed by Gertler and Hagen known as the NSRDC Model 2510 [1]. The linear hydrodynamic coefficients employed in the 2510 equations are derived in Chapter 2. All nonlinear coefficients used are based on submersibles of similar size and shape. Since this submersible has never been constructed on scale basis or tested in a tow tank, the accuracy of the coefficients could not be verified. However, the computer model behaved in a reasonable manner as one would expect with a full scale equivalent model.

The origin of the submarine fixed axes is located at the center of gravity. The positive directions of axes are: x-direction, forward; y-direction to starboard; z-direction downward. The linear and angular velocity components, forces and moments are shown in Figure 2 [6].

This thesis will develop and design a multivariable automatic controller for the submarine model in Chapter 2. Chapter 2 consists of the development of the linear hydrodynamic coefficients and explains the modifications made to the six degree-of-freedcm equations of motion.

SCALE: 1/16 in. = 1.875 ft

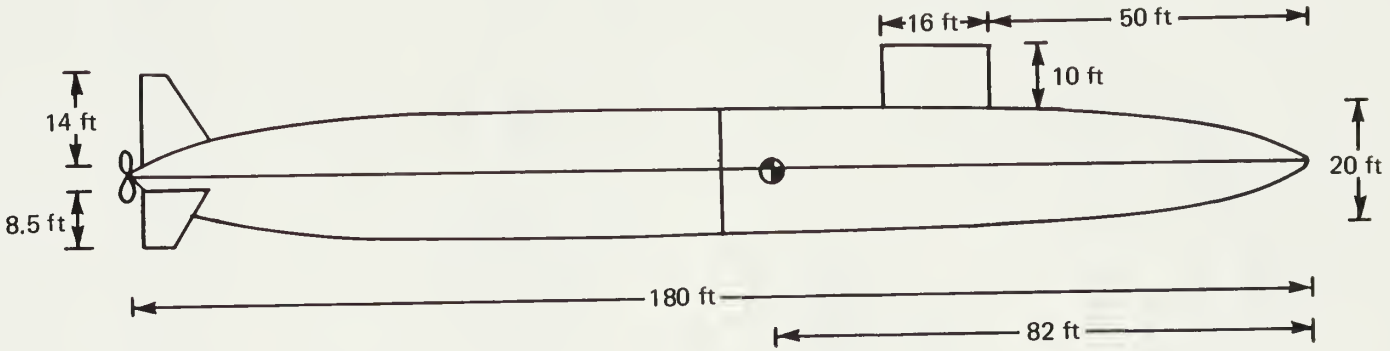

Figure 1. Submarine profile.

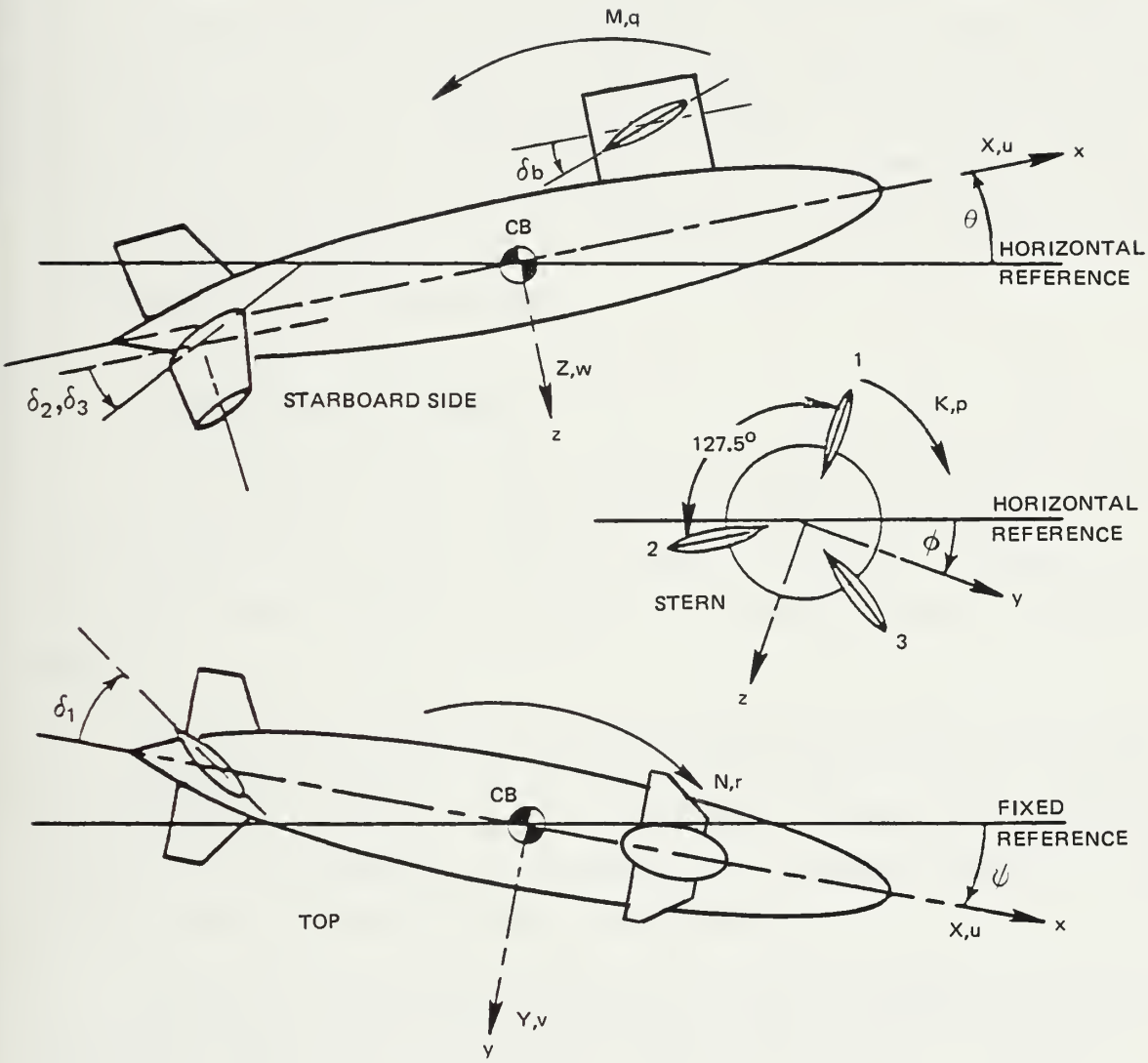

Figure 2. Sketch showing positive directions of axes, angles, velocities, forces, and moments.

Additionally, an explanation is provided as to how the equations of motion were linearized. Chapter 3 consists of the controller (compensator) design. It includes a brief explanation of the control variables, system augmentation, and calculation of the control gain matrix, $\underline{G}$, and the filter gain matrix, $\underline{H}$, which result from the frequency domain loop shaping methodology employed for the design. The design methodology itself is also discussed briefly. Chapter 4 summarizes the results of the nonlinear controller simulations. Finally, Chapter 5 lists the conclusions and recommendations as drawn from the resultant submarine model and controller design.

1.2 Contributions of Thesis

The contributions of this thesis is twofold: (i) evaluation of the MDS configuration for a submersible in a high speed turn, (ii) design of an automatic control system to facilitate the MDS operation using Linear Quadratic Gaussian/Loop Transfer Recovery (LQG/LTR) methods.

The emphasis is on the frequency-domain properties of the state-space based LQG designs. Simple and efficient tools for loop shaping are employed that lead to satisfactory designs. These tools accomplish singular value "pinching" in the high and low frequency ranges, so as to satisfy stability and performance requirements.

Moreover, this thesis tests the controller designed on the basis of a linear model on the nonlinear process model which is a better approximation to the actual system.

CHAPTER 2

THE SUBMARINE MODEL

2.1 Nonlinear Equations of Motion

The equations of motion describing the design vehicle in this thesis as already mentioned, were the six degree-of-freedom equations contained in the NSRDC document 2510 [1]. The coefficients of the equations, as developed in Section 2.3, describe the vehicle's geometry. Modification was made to the equations to account for the geometry of the MDS configuration. The terms that involved both rudder and sternplane action were combined; these can be seen in the lateral force, pitching moment and yawing moment equations. The factors that premultiply the corresponding surface deflections were based upon the geometry depicted in Figure 3.

D1 is primarily used for rudder control while control surfaces D2 and D3 are used for depth and roll control. However, D2 and D3 can also act as an additional rudder and their potential contribution can be seen from the lateral force equation where the multiplying coefficient is given by sin 37.5° = 0.6088. The resulting term looks like the following, D1 - 0.6088D2 + 0.6088D3. Additionally, this term takes into account the sign of the hydrodynamic coefficients Y_{δ} and $Y_{\delta\eta}$. In this case both Y_{δ} and $Y_{\delta\eta}$ are positive and employ the sign convention as established in Figure 2. Likewise, the stern contribution terms in the pitching and yawing moment equations have similar form.

For depth control, surfaces D2 and D3 are used. The factor cos 37.5° = 0.7934 appears. Depending on the sign of the hydrodynamic coefficients Z_δ, $Z_{\delta\eta}$, M_δ, $M_{\delta\eta}$, N_δ, and $N_{\delta\eta}$, the sign of the deflecting term is assigned.

One must keep in mind that, not all hydrodynamic coefficients involving a control surface have a value that can be predicted or measured in model tests. If a value could be determined, then one would assign the additive or subtractive nature to the contribution of the control surface based upon the sign of the corresponding hydrodynamic coefficient. The resulting nonlinear and auxiliary force equations are given in Appendix B.

2.2 Linearized Equations of Motion

Control design requires that the nonlinear equations of motion be linearized about a nominal operating point. The nonlinear equations are of the form

$$\underline{E}\dot{\underline{x}} = \underline{f}(\underline{x}, \underline{u}) \tag{2.1}$$

from which one can derive the linearized equations in the form

$$\underline{E}\Delta\dot{\underline{x}} = \underline{A}\Delta\underline{x} + \underline{B}\Delta\underline{u} \tag{2.2}$$

which represents a Taylor Series expansion of the nonlinear equations about a nominal point $\underline{x}_o$ and $\underline{u}_o$, by retaining only the first order terms. More specifically, expanding Equation (2.1) in a first order Taylor Series around a nominal point, one gets

$$\underline{E}\dot{\underline{x}}_o + \underline{E}\Delta\dot{\underline{x}} = \underline{f}(\underline{x}_o, \underline{u}_o) + \frac{\partial \underline{f}(\underline{x}_o, \underline{u}_o)}{\partial \underline{x}} (\underline{x} - \underline{x}_o) + \frac{\partial \underline{f}(\underline{x}_o, \underline{u}_o)}{\partial \underline{u}} (\underline{u} - \underline{u}_o) \tag{2.3}$$

If one lets $\Delta\underline{x} = (\underline{x} - \underline{x}_o)$ and $\Delta\underline{u} = (\underline{u} - \underline{u}_o)$ where $\underline{x}_o$ is the nominal state vector and $\underline{u}_o$ the nominal input which, furthermore, are known to satisfy the original nonlinear equations, then one is left with

$$\underline{E}\Delta\dot{\underline{x}} = \frac{\partial \underline{f}(\underline{x}_o, \underline{u}_o)}{\partial \underline{x}} \Delta\underline{x} + \frac{\partial \underline{f}(\underline{x}_o, \underline{u}_o)}{\partial \underline{u}} \Delta\underline{u} \qquad (2.4)$$

where $\underline{A} \equiv \frac{\partial \underline{f}(\underline{x}_o, \underline{u}_o)}{\partial \underline{x}}$ and $\underline{B} \equiv \frac{\partial \underline{f}(\underline{x}_o, \underline{u}_o)}{\partial \underline{u}}$. The linearized equations are listed in Appendix C.

Additionally, the full nonlinear equations include crossflow and vortex shedding terms. For the purpose of this thesis, the crossflow term was linearized while the vortex shedding term was omitted. The reason for this was to be able to compare the results of this submersible to a full scale model, whose linearized equations did not include vortex shedding, either.

2.3 Hydrodynamic Coefficients

The hydrodynamic coefficients that comprise the linear and nonlinear equations of motion are very important in the mathematical model. The linear coefficients can be estimated using equations based on the geometry of the submersible. The nonlinear coefficients are normally the result of model tests either in a tow tank or wind tunnel. The coefficients not calculated in this thesis are taken from past designs of similar size and shape vehicles.

2.3.1 Body Coefficients [2]

We assume a prolate ellipsoid for the hull shape, where the major and minor axes are given by

$$a = 90 \text{ ft} \quad b = 10 \text{ ft}$$

$$V = \frac{4}{3} \pi a b^2$$

$$V = 37{,}699 \text{ ft}^3$$

The buoyant force of the ellipsoid is

$$B = \rho V$$

$$B = 2.4283 \times 10^6 \text{ lbf.}$$

The surface area of the ellipsoid is given by

$$S = 2\pi b^2 + 2\pi \frac{ab}{e} \sin^{-1} e$$

where

$$e = \text{eccentricity} = \frac{c}{a}$$

$$c = (a^2 - b^2)^{\frac{1}{2}}$$

$$e = 0.9938$$

$$S = 8932.4 \text{ ft}^2$$

From Lamb [3] with $\frac{a}{b} = 9$, the factors

$$K' = 0.8645$$

$$K_1 = 0.0241$$

$$K_2 = 0.9538$$

can be obtained. The moments of inertia for the body are as follows:

$I_{yy} = I_{zz}$ for a prolate ellipsoid

$$m = \frac{B}{32.17 \frac{ft}{s^2}} = \frac{2.4283 \times 10^6 \text{ lbf}}{32.17 \frac{ft}{s^2}} = 75483 \text{ slugs}$$

$$I_{yy} = \frac{m(a^2 + b^2)}{5} = 1.2379 \times 10^8 \text{ slugs-ft}^2$$

$$I_{zz} = 1.2379 \times 10^8 \text{ slugs-ft}^2$$

$$I_{xx} = \frac{m(2b^2)}{5}$$

$$I_{xx} = 3.0193 \times 10^6 \text{ slugs-ft}^2$$

The mass and moments of inertia can be nondimensionalized by dividing with the appropriate factor.

$$I' = \frac{I}{\left(\frac{\rho \ell^5}{2}\right)}$$

$$m' = \frac{m}{\left(\frac{\rho \ell^3}{2}\right)}$$

Therefore,

$$I'_{yy} = I'_{zz} = 0.000654$$

$$I'_{xx} = 0.000016$$

$$m' = 0.1293$$

The center of gravity is assumed to be located in the port-starboard plane of symmetry, 12 inches below the centerline.

$$X_G = 0$$

$$Y_G = 0$$

$$Z_G = 1 \text{ ft}$$

Nondimensionalizing,

$$Z'_G = \frac{Z_G}{\ell} = 0.00556$$

From Newman [4], the Reynolds number for a body in 10°C seawater at 21 KTS, is given by

$$R_e = \frac{U\ell}{\gamma}$$

$$= \frac{(21)(1.689)(180)}{1.35 \times 10^{-6}(3.281)^2}$$

$$= 4.3931 \times 10^8$$

Assuming that the frictional drag coefficient is equal to the drag coefficient and using the ITTC frictional resistance line gives

$$C_D = C_F = \frac{0.075}{(\log_{10} R - 2)^2}$$

$$C_D = C_F = 0.0017$$

for the coefficient of drag.

The body hydrodynamic coefficients can now be calculated [5].

$$Y'_v = -0.234(m')^{0.79} - \frac{C_D S}{\ell^2} = -0.008009 \qquad (2.5)$$

$$Y'_r = -(0.10 - K_1)m' = 0.000981 \qquad (2.6)$$

$$Z'_w = Y'_v = -0.008009 \qquad (2.7)$$

$$Z'_q = -Y'_r = 0.000981 \qquad (2.8)$$

$$M'_w = 0.87(K_2 - K_1)m' = 0.010458 \qquad (2.9)$$

$$M'_q = 0.045(m') = 0.000582 \qquad (2.10)$$

$$N'_v = -M'_w = -0.010458 \tag{2.11}$$

$$N'_r = M'_q = -0.000582 \tag{2.12}$$

$$X'_{\dot{u}} = -K_1 m' = -0.000312 \tag{2.13}$$

$$Y'_{\dot{v}} = -K_2 m' = -0.012333 \tag{2.14}$$

$$Y'_{\dot{p}} = \frac{Y'_{\dot{v}} Z_g}{\ell} = -0.000069 \tag{2.15}$$

$$K'_{\dot{v}} = Y'_{\dot{p}} = -0.000069 \tag{2.16}$$

$$Z'_{\dot{w}} = Y'_{\dot{v}} = -0.012333 \tag{2.17}$$

$$M'_{\dot{q}} = -K' I'_y = -0.000565 \tag{2.18}$$

$$N'_{\dot{r}} = M'_{\dot{q}} = -0.000565 \tag{2.19}$$

2.3.2 Fin Coefficients [6]

The MDS stern configuration introduces asymmetry about the centerline of the vertical plane. Several views have been depicted to allow calculation of areas, aspect ratios and planes of motion. Figures 3 and 4 depict fin dimensions.

For a single fin:

$$A_f = \text{Projected area}$$

$$= 100.4 \text{ ft}^2$$

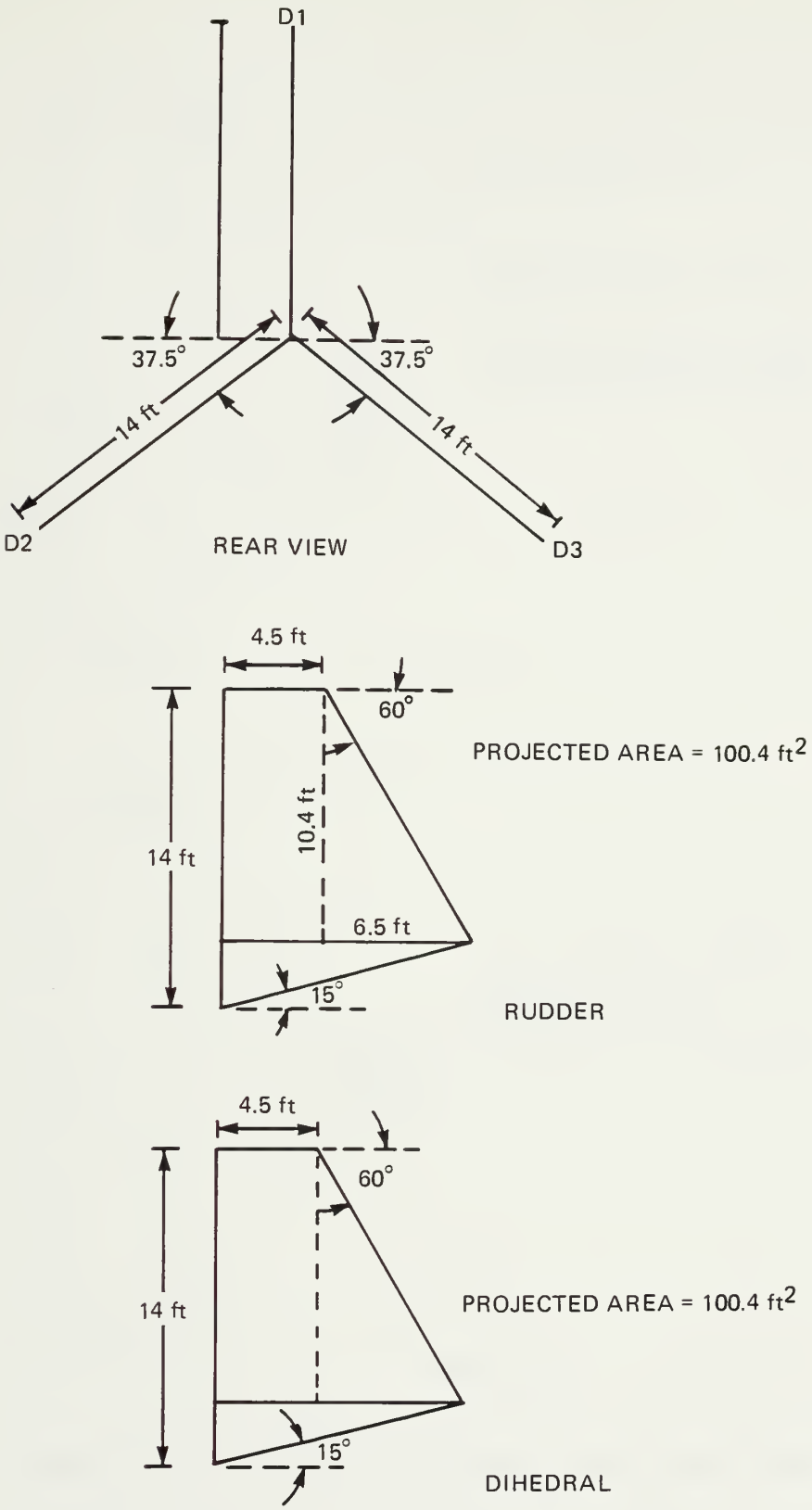

Figure 3. Rear view, rudder, and dihedral fin dimensions.

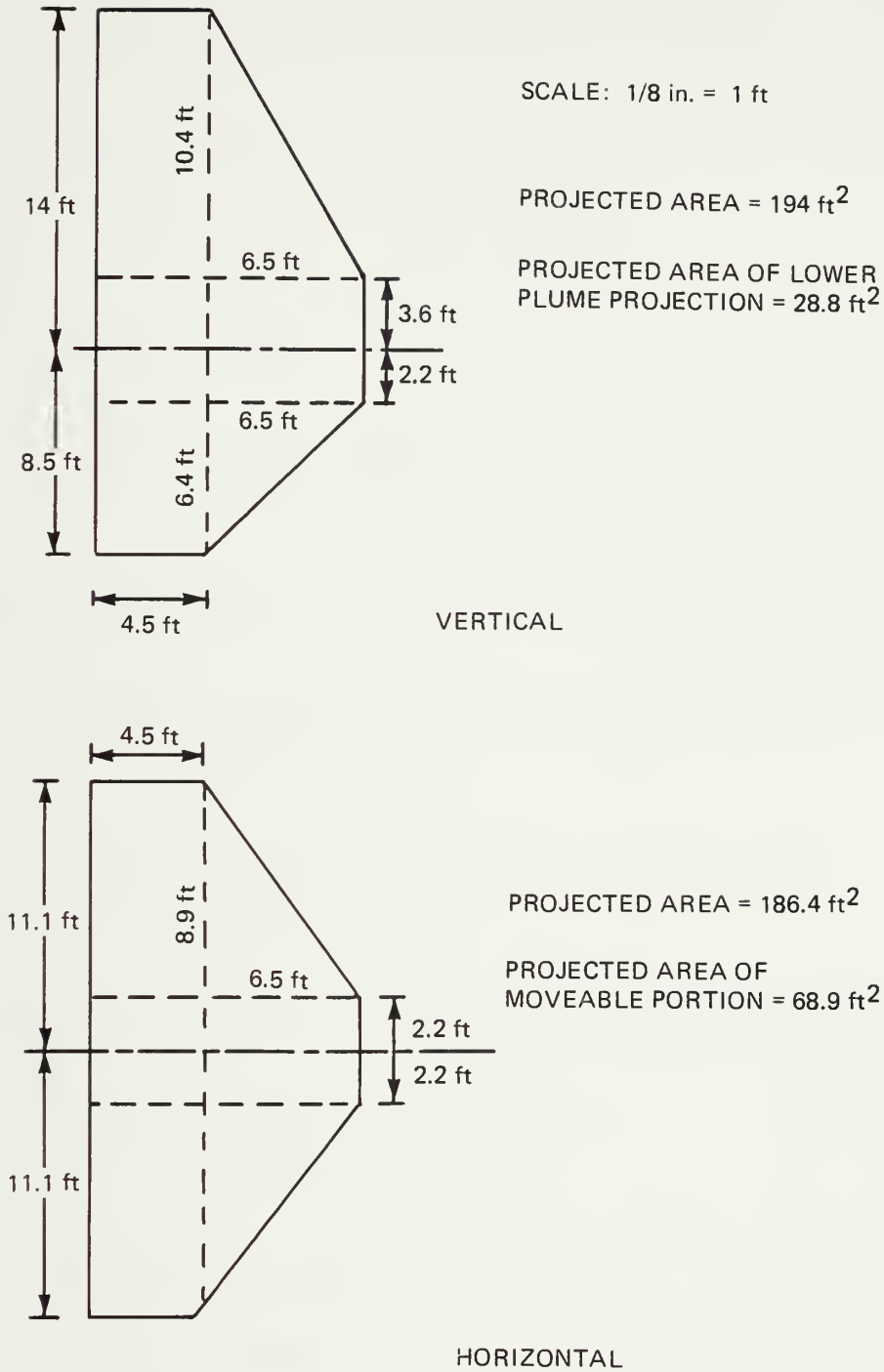

Figure 4. Vertical and horizontal plane projections.

A_m = Projected area of movable portion

= 80.6 ft^2

AR_f = aspect ratio of fin = $\frac{\bar{s}}{\bar{c}}$

$\bar{s}$ = 28 ft $\bar{c}$ = 8.25 ft

AR_f = 3.394

AR_m = aspect ratio of the movable portion

= 6.222

For the horizontal plane projection contributions, one has:

A_{HP} = projected area of the horizontal plane

= 186.4 ft^2

AR_{HP} = aspect ratio in the horizontal plane

= 2.69

The following definitions are used in calculating A and $C_{L\alpha}$.

$$C_{L\alpha} = \frac{2\pi}{1 + \frac{2}{AR}}$$

In the vertical plane

AR_f = 3.394

A_f = 100.4 ft^2

$C_{L\alpha}$ = 3.953

x_{cp} = distance from center of buoyancy to center of pressure of the stern

The center of pressure is assumed to be 1/2 the mean chord length forward of the hailing edge. For this vehicle

$$x_{cp} = -94.5 \text{ ft}$$

$$Y'_v = \frac{-C_{L\alpha}(A_f)}{\ell^2} = -0.012249 \tag{2.20}$$

$$N'_v = \frac{Y'_v X_{CP}}{\ell} = 0.006431 \tag{2.21}$$

The contribution to roll due to asymmetry is

$$K'_v = \frac{Y'_v Z_{cp}}{\ell}$$

where Z_{cp} was calculated by summing the different components of the vertical projection times their moment arm and then divided by the total area.

For this vehicle a value for Z_{cp} was found as

$$Z_{cp} = 10.9 \text{ ft}$$

Therefore

$$K'_v = -0.000742 \tag{2.22}$$

For the horizontal plane projection

$$a = 2.64$$

$$A = 186.4 \text{ ft}^2$$

$$C_{L\alpha} = 3.604$$

whereby

$$Z'_w = \frac{-C_{L\alpha} A}{\ell^2} = -0.020733 \tag{2.23}$$

$$M'_w = \frac{-Z'_w x_{cp}}{\ell} = -0.010885 \tag{2.24}$$

$$Z'_q = M'_w = -0.008673 \tag{2.25}$$

$$Y'_r = N'_v = 0.006276 \tag{2.26}$$

$$K'_r = \frac{-K'_v x_{cp}}{\ell} = -0.000380 \tag{2.27}$$

$$M'_q = \frac{-Z'_q x_{cp}}{\ell} = -0.004553 \tag{2.28}$$

$$N'_r = \frac{Y'_r x_{cp}}{\ell} = -0.003295 \tag{2.29}$$

In order to calculate K'_p, the method will be applied to an individual fin.

$$A = 100.4 \text{ ft}^2$$

$$C_{L\alpha} = 3.953$$

$$Y_v'' = \frac{-C_{L\alpha} A}{\ell^2} = -0.012249$$

then

$$K_p' = Y_v'' \left(\frac{Z_{cp}'}{\ell}\right)^2$$

Z_{cp}' is the distance from centerline to center of pressure of the individual fin. For this fin $Z_{cp}' = 7.44$ ft

$$K_p' = -0.000021$$

The K_p' for the design vehicle will be three times the above value.

$$K_p' = -0.000063 \qquad (2.30)$$

Abkowitz [7] provides a means for calculating the acceleration derivatives. In the horizontal plane

$$Z_{\dot{w}} = \frac{\pi \rho s^2 c^2}{4\sqrt{s^2 + c^2}} \left(1 - \frac{0.54}{\left(1 + \frac{s}{c} + \frac{c}{s}\right)}\right)$$

where s is the span and c is the chord.

$$s = 11.1 \text{ ft} + 11.1 \text{ ft} = 22.2 \text{ ft} \qquad c = 8.25 \text{ ft}$$

$$Z_w^{\cdot\prime} = \frac{Z_w^{\cdot}}{\frac{1}{2}\rho\ell^3} = 0.000331 \tag{2.31}$$

In the vertical plane,

$$Y_v^{\cdot\prime} = \frac{\pi\rho s^2 c^2}{4\sqrt{s^2 + c^2}} \frac{\left(1 - \frac{0.54}{\left(1 + \frac{s}{c} + \frac{c}{s}\right)}\right)}{\frac{1}{2}\rho\ell^3}$$

where

$$s = 14 \text{ ft} + 8.5 \text{ ft} = 22.5 \text{ ft} \qquad c = 8.25 \text{ ft}$$

Hence,

$$Y_v^{\cdot\prime} = -0.000336 \tag{2.32}$$

$$M_w^{\cdot\prime} = \frac{Z_w^{\cdot\prime} x_{cp}}{\ell} = -0.000174 \tag{2.33}$$

$$N_v^{\cdot\prime} = \frac{-Y_v^{\cdot\prime} x_{cp}}{\ell} = -0.000176 \tag{2.34}$$

$$Z_q^{\cdot\prime} = -M_w^{\cdot\prime} = 0.000174 \tag{2.35}$$

$$M_q^{\cdot\prime} \approx -Z_w^{\cdot\prime} \left(\frac{x_{cp}}{\ell}\right)^2 = -0.000091 \tag{2.36}$$

$$N_r^{\cdot\prime} = Y_v^{\cdot\prime} \left(\frac{x_{cp}}{\ell}\right)^2 = -0.000093 \tag{2.37}$$

$$K_v^{\cdot\prime} = \frac{Y_v^{\cdot\prime} z_{cp}}{\ell} = -0.000020 \tag{2.38}$$

$$Y_r' = N_v' = 0.000176 \tag{2.39}$$

Contributions due to the deflections of the fins result in the following coefficients, for which it suffices to calculate those for one fin only.

$$Y_\delta' = \frac{C_{L\alpha} A_M}{\ell^2}$$

$$a = AR_{MP} = 3.394$$

$$C_{L\alpha} = 3.95$$

$$A_M = 46.8 \text{ ft}^2$$

$$Y_\delta' = 0.005706$$

$$Z_\delta' = \frac{C_{L\alpha} A_M}{\ell^2} = -0.007656 \tag{2.40}$$

where $C_{L\alpha} = 3.6$ and $A_M = 68.9 \text{ ft}^2$.

$$K_\delta' = \frac{Y_\delta' |Z_{cp}''|}{\ell} = 0.000269 \tag{2.41}$$

where Z_{cp}'' is the distance for the moveable portion, -8.46 ft.

$$M_\delta' = \frac{-Z_\delta' x_{cp}}{\ell} = -004019 \tag{2.42}$$

$$N_\delta = \frac{C_{L\alpha} A_M}{\ell^2} \times \frac{|x_{cp}|}{\ell}$$

where $A_M = 28.8 \text{ ft}^2$.

$$N_\delta = -0.001680 \tag{2.43}$$

When the fins are deflected, drag forces are induced. The drag force of a body is given by

$$x = \frac{1}{2} C_D \rho A u^2$$

From Comstock [8],

$$C_D = C_{DO} + \frac{C_L^2}{\pi a e}$$

where

$a = AR_M = 1.182$

$e = 0.9$ (Oswald efficiency factor)

Since

$$C_L = \left(\frac{dC_L}{d\delta}\right) \delta = 1.65\delta$$

then

$$C_D = C_{DO} + 0.8146\delta^2$$

Substituting this into the X equation,

$$X = \frac{\left(C_{DO} + 0.8146\ ^2\right)\rho A_M u^2}{2}$$

and, taking the second derivative with respect to δ_1, one gets

$$X_{\delta\delta} = 0.8146\rho A_M u^2$$

Next, nondimensionalizing,

$$X'_{\delta\delta} = \frac{-X_{\delta\delta}}{\left(\frac{\rho \ell^2 u^2}{2}\right)} = -0.004053 \qquad (2.44)$$

2.3.3 Sail Coefficients

Figure 5 shows the dimensions of sail used. Using the method described in Reference 8, to evaluate $C_{L\alpha}$ for the sail one calculates the following.

$$\Lambda = 0 \text{ radian for sail}$$

$$AR_s = a = \frac{(2)(10)}{16} = 1.25$$

$$A = 160 \text{ ft}^2$$

$$C_{L\alpha} = \frac{2\pi}{1 + \frac{2}{AR}} = 2.42$$

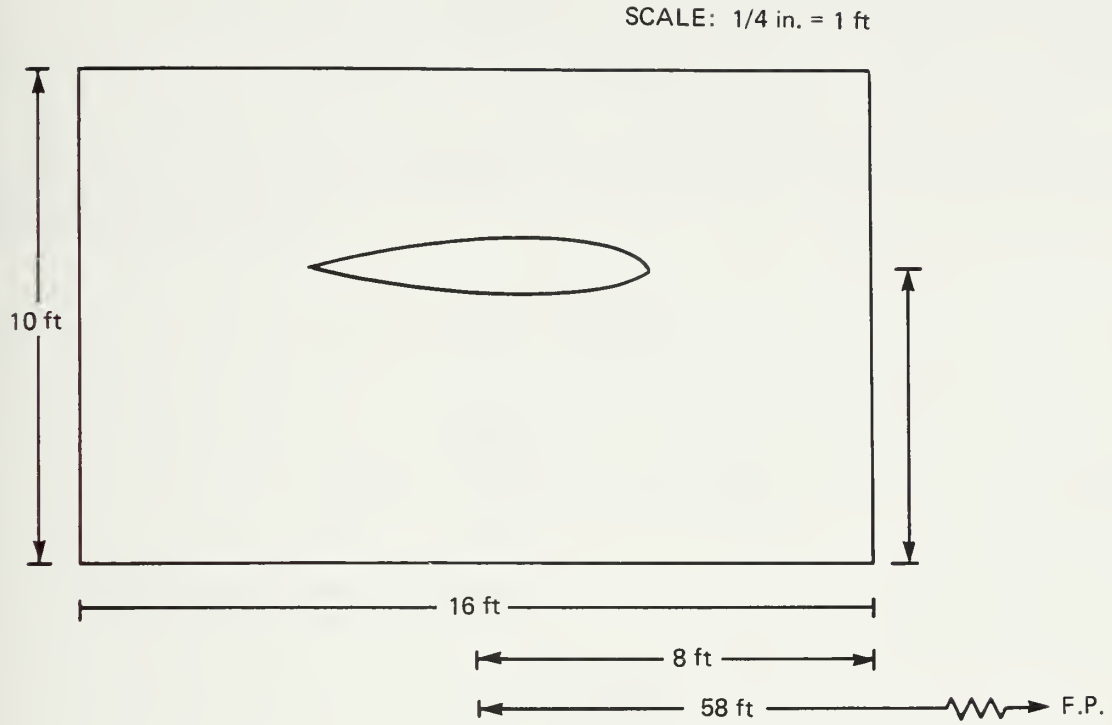

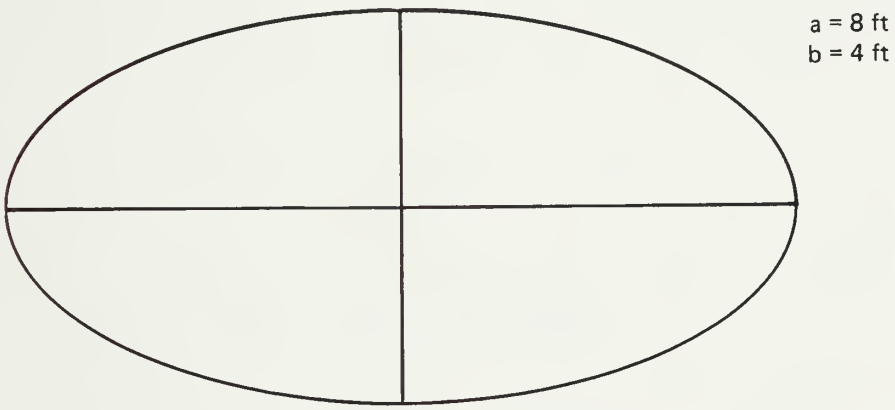

$$\text{SURFACE AREA} = 2\pi\sqrt{1/2\,(a^2 + b^2)} \cdot h$$

$$A_s = 397.4\ \text{ft}^2$$

Figure 5. Sail geometry.

$$Y'_v = \frac{-C_{L\alpha} A}{\ell^2} = -0.011934 \qquad (2.45)$$

The center of pressure is assumed to be located at the 1/4 chord length from the forward edge.

$$x_{cp} = 28 \text{ ft}$$

$$N'_v = \frac{-Y'_v x_{cp}}{\ell} = 0.001856 \qquad (2.46)$$

The contribution to roll is

$$K'_v = \frac{Y'_v z_{cp}}{\ell}$$

where z_{cp} is the distance from the centerline of the vehicle to the vertical center of pressure, and $z_{cp} = z'_{cp} = -15$ ft for this submersible. Then,

$$K'_v = 0.000155 \qquad (2.47)$$

$$Y'_r = N'_v = 0.001856 \qquad (2.48)$$

$$N'_r = \frac{Y'_r x_{cp}}{\ell} = 0.000289 \qquad (2.49)$$

$$K'_p = Y'_v \left(\frac{z'_{cp}}{\ell}\right)^2 = -0.000083 \qquad (2.50)$$

The acceleration derivatives, according to Abkowitz can be derived analogously as for the stern control surfaces. In this case, the span will be twice the height of the sail and the resulting derivative will be divided in half and then nondimensionalized. In the vertical plane one gets

$$Y_v^{\bullet\prime} = \frac{\pi\rho s^2 c^2}{4\sqrt{s^2 + c^2}} \frac{\left(1 - \frac{0.54}{\left(1 + \frac{s}{c} + \frac{c}{s}\right)}\right)}{\frac{1}{2}\rho\ell^3}$$

$$Y_v^{\bullet\prime} = -0.000886 \tag{2.51}$$

where

$s = 20$ ft

$c = 16$ ft

Hence

$$N_v^{\bullet\prime} = \frac{-Y_v^{\bullet\prime} x_{cp}}{\ell} = 0.000138 \tag{2.52}$$

$$K_v^{\bullet\prime} = \frac{Y_v^{\bullet\prime} z_{cp}}{\ell} = 0.000074 \tag{2.53}$$

$$N_r^{\bullet\prime} \approx Y_v^{\bullet\prime} \left(\frac{x_{cp}}{\ell}\right)^2 = -0.000021 \tag{2.54}$$

$$Y_r^{\bullet\prime} = N_v^{\bullet\prime} = -0.000138 \tag{2.55}$$

$$K_p^{\bullet\prime} = Y_v^{\bullet\prime} \left(\frac{z_{cp}}{\ell}\right)^2 = -0.000006 \tag{2.56}$$

2.3.4 Sailplane Coefficients

Figure 6 shows the geometry of the sailplane. The center of pressure is assumed to be 1/2 mean chord length forward of the trailing edge. For this vehicle,

$$x_{cp} = 24 \text{ ft}$$

The following definitions are used in calculating A and $C_{L\alpha}$.

b = tip of fin to hull centerline

= 11 ft

d = maximum diameter of hull

= 20 ft

a = aspect ratio = 2.67 for a single plane

$A = 31.5 \text{ ft}^2$

$C_{L\alpha} = 3.59$

$$Z'_w = \frac{-C_{L\alpha} A}{\ell^2} = -0.003490 \qquad (2.57)$$

$$M'_w = \frac{-Z'_w x_{cp}}{\ell} = 0.000465 \qquad (2.58)$$

There is no contribution to roll in the horizontal plane.

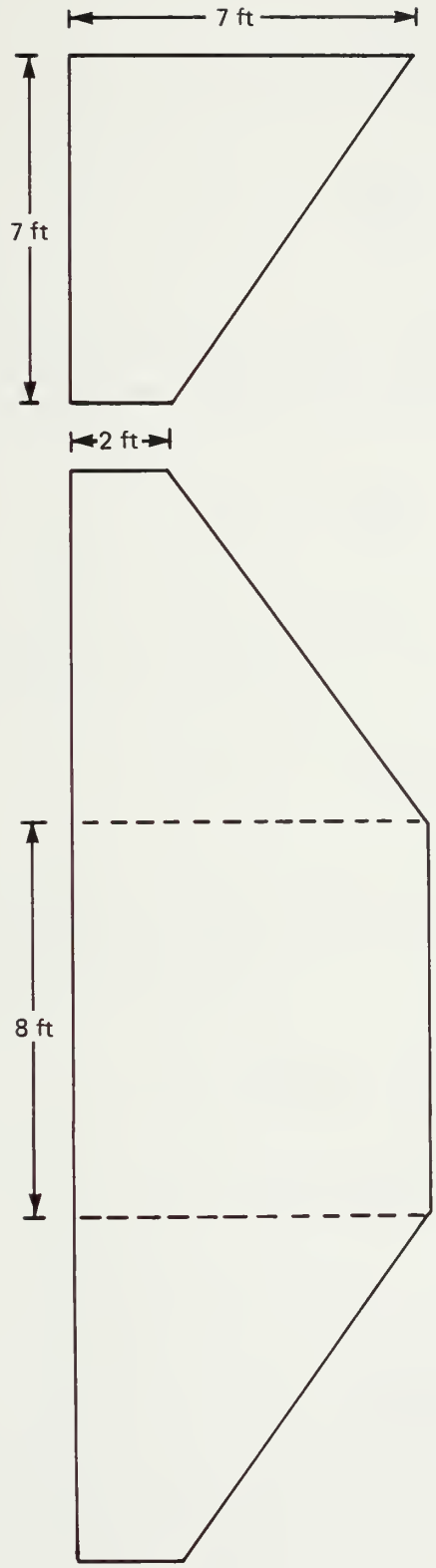

SCALE: 1/4 in. = 1 ft

PROJECTED AREA OF
SINGLE FIN = 31.5 ft^2

Figure 6. Sailplane geometry.

$$Z'_q = \frac{-Z'_w x_{cp}}{\ell} = 0.000465 \qquad (2.59)$$

$$M'_q = \frac{Z'_q x_{cp}}{\ell} = 0.000097 \qquad (2.60)$$

The contributions due to the deflection of the fins are calculated in a similar fashion as before.

$$Z'_{\delta b} = \frac{C_{L\alpha} A}{\ell^2} = -0.005429 \qquad (2.61)$$

where z''_{cp} for the sailplane is 16 ft.

$$M'_\delta = \frac{Z'_\delta |x_{cp}|}{\ell} = 0.000724 \qquad (2.62)$$

As with the stern control surfaces, when the fins are deflected, drag forces are induced.

$$a = AR_{msp} = \frac{\bar{s}}{\bar{c}} = 1.2727$$

$$e = 0.9 \text{ (Oswald efficiency factor)}$$

Since

$$C_L = \left(\frac{dC_L}{d\delta}\right)\delta = 3.20\delta$$

then

$$C_D = C_{DO} + \frac{C_L^2}{\pi ae}$$

$$= C_{DO} + 0.4501\delta^2$$

Substituting this into the expression for the drag force of a body $x = \frac{1}{2} C_D \rho A u^2$ gives

$$x = \frac{\left(C_{DO} + 0.4501\delta^2\right)\rho A_{msp} u^2}{2}$$

Taking the second derivative with respect to δ,

$$X_{\delta\delta} = 0.4501 \rho A_{msp} u$$

Nondimensionalizing,

$$X'_{\delta\delta} = \frac{-X_{\delta\delta}}{\left(\frac{\rho \ell^2 u^2}{2}\right)} = -0.001750 \qquad (2.63)$$

The acceleration derivatives for the sailplanes are calculated as follows, with c = 5.25 ft and s = 14 ft. In the horizontal plane,

$$Z_w^{\cdot\prime} = \frac{\pi\rho(14)^2(5.5)^2}{4\sqrt{(14)^2 + (5.5)^2}} \frac{\left(1 - \frac{0.54}{\left(1 + \frac{14}{5.25} + \frac{5.25}{14}\right)}\right)}{\frac{1}{2}\rho\ell^3}$$

$$Z_{\dot{w}}' = 0.000092 \tag{2.64}$$

$$M_{\dot{w}}' = \frac{z_{\dot{w}}' x_{cp}}{\ell} = 0.000012 \tag{2.65}$$

$$Z_{\dot{q}}' = M_{\dot{w}}' = 0.000012 \tag{2.66}$$

$$M_{\dot{q}}' \approx Z_{\dot{w}}' \left(\frac{x_{cp}}{\ell}\right)^2 = -0.000002 \tag{2.67}$$

The hydrodynamic data to be utilized by the SUBRUN computer program, that will generate the linear dynamics, requires that the coefficients be input in a dimensionalized form rather than a nondimensionalized form. Appendix D contains a listing of dimensionalized hydrodynamic data and dimensionalizing factors for this purpose.

2.4 Computer Program Description

The computer program, SUBMODEL, used for this thesis was developed at Draper Laboratory [9]. The program has the capability to integrate the nonlinear equations of motion of a submarine; search for a local equilibrium point in the nonlinear equations of motion; calculate the linearized dynamics of the linearized equations about a nominal point; integrate the linearized equations of motion; simulate the compensated vehicle using either the nonlinear or linear equations.

As previously stated, the nonlinear equations take the form of Equation (2.1)

$$\underline{E}\dot{\underline{x}} = \underline{f}(\underline{x}, \underline{u})$$

where

$\underline{x}$ = 10 × 1 state vector with states u, v, w, p, q, r, phi, theta, psi and z, the last four describing the vehicle attitude with respect to an inertial reference frame.

$\underline{u}$ = 4 × 1 control vector with DB, D1, D2, D3 as members

$\underline{f}$ = 10 × 1 vector that is a nonlinear function of the states and the controls

$\underline{E}$ = 10 × 10 matrix

The nonlinear equations were integrated with the RPS propulsion model, as described in Appendix E, using as input a velocity in feet/second (corresponding to 21 knots) with initial values of zero for all states, with the exception of D1 deflected to 2 degrees, D2 deflected to 0.5 degree and D3 deflected to -0.4744 degrees. The assumption is made in the propulsion data that wake and thrust deduction factors vary slightly and are therefore considered constant. The nominal point is then determined by integrating the nonlinear equations with the eta propulsion model using as inputs for the states, the final value of the states from the RPS integration.

Once the nominal point has been determined, the linearized dynamics can be calculated by linearizing about that nominal point (see Appendix E for a description of Nominal Point). Recall that the linearized equations are of the form

$$\underline{E}\Delta\dot{\underline{x}} = \underline{A}'\Delta\underline{x} + \underline{B}'\Delta\underline{u} \tag{2.68}$$

or, equivalently, the conventional representation form

$$\dot{\underline{x}} = \underline{E}^{-1}\underline{A}'\underline{x} + \underline{E}^{-1}\underline{B}'\underline{u} = \underline{A}\underline{x} + \underline{B}\underline{u} \tag{2.69}$$

On can easily see that $\underline{A}$ in state space form equates to $\underline{E}^{-1}\underline{A}'$ and $\underline{B}$ equates to $\underline{E}^{-1}\underline{B}'$. It is $\underline{E}^{-1}\underline{A}'$ and $\underline{E}^{-1}\underline{B}'$ that define the linear system dynamics, on which the control design is based.

To validate the resulting linear model, one perturbs the states of the nominal point and compares the resulting responses of the perturbed linear and nonlinear models. Perturbation from the nominal point on the order of 10% is adequate for checking validity of the linear model behavior in comparison to the nonlinear model. Figure 7 shows the graphical responses of the two models for comparison.

Once the controller has been designed, the effectiveness of its operation can be tested by using it on the previously derived linear and nonlinear models and analyzing their responses to step and ramp inputs. A description of the controller development is given in Chapter 3 with the results of the subsequent testing in Chapter 4.

Figure 7. Linear and nonlinear submarine model responses.

NON-LINEAR RESPONSE

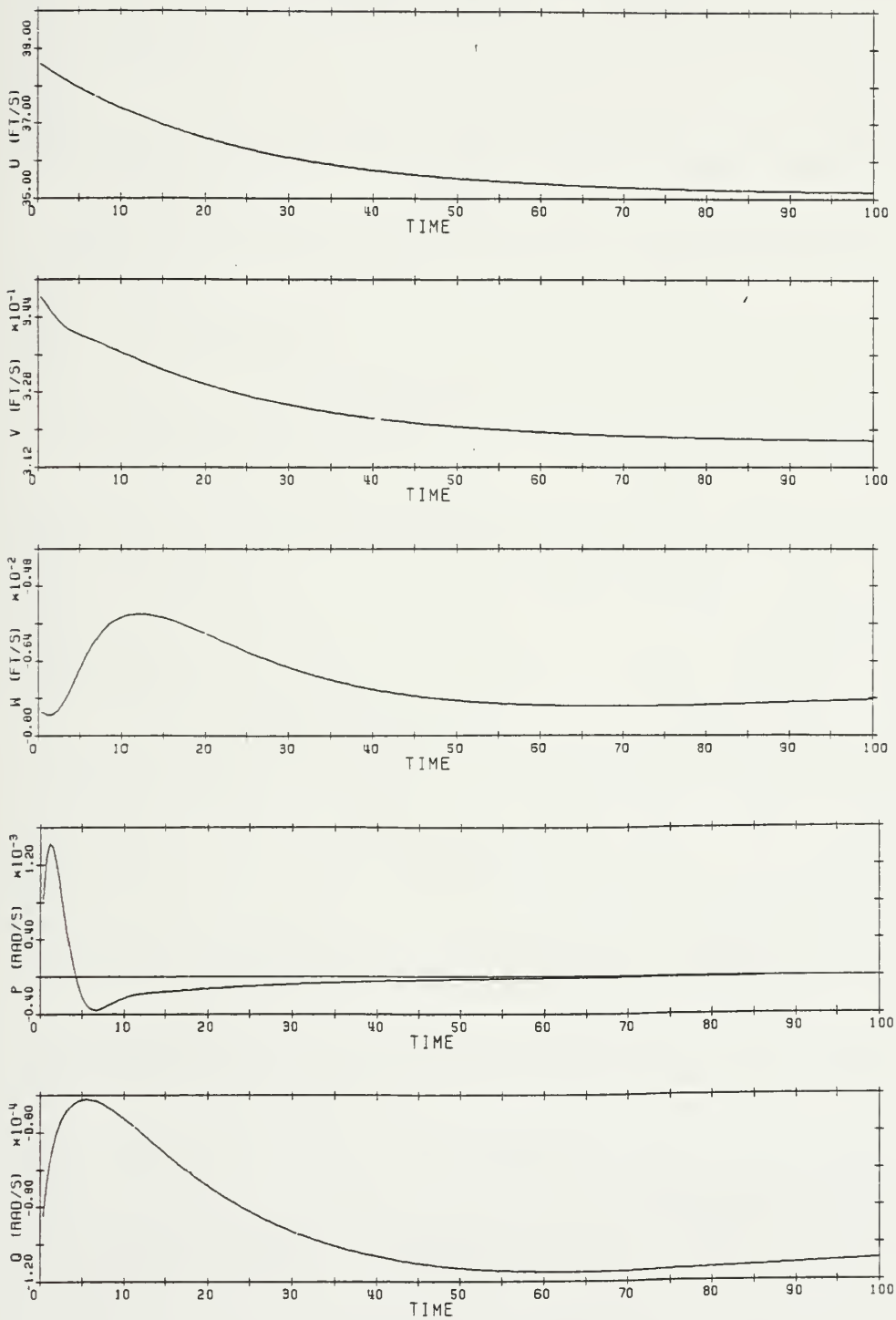

Figure 7. (Cont.)

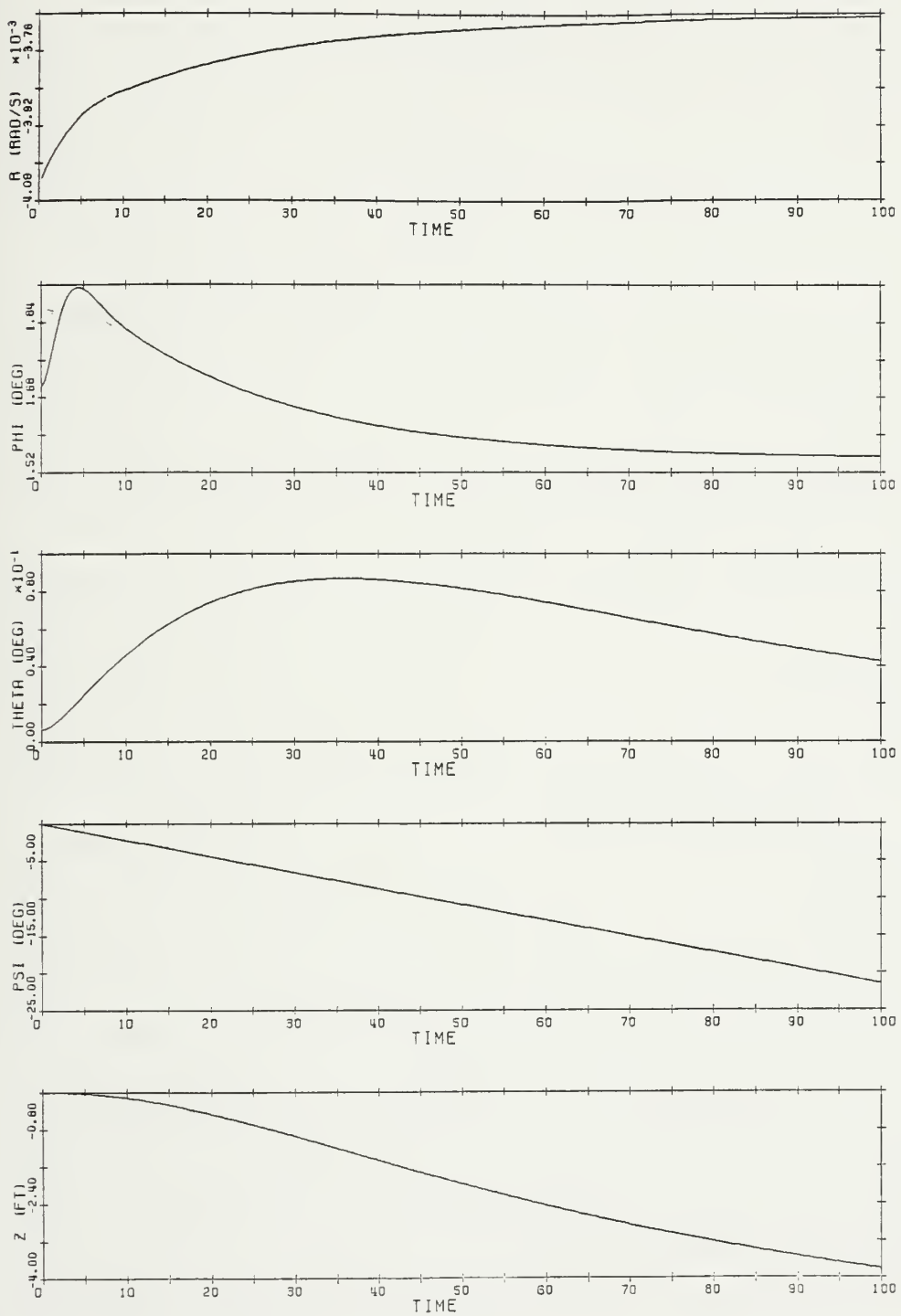

Figure 7. (Cont.)

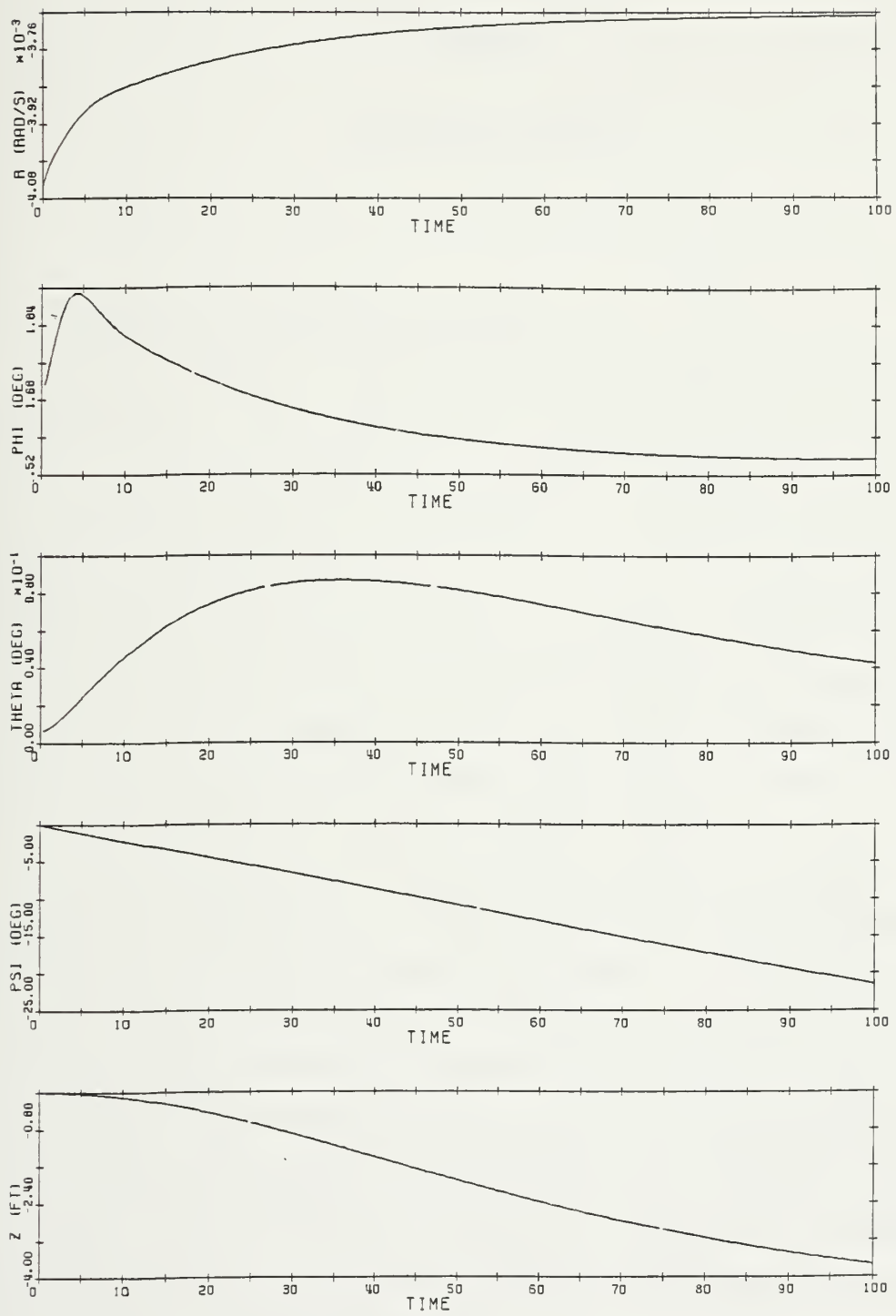

Figure 7. (Cont.)

CHAPTER 3

COMPENSATOR DESIGN

3.1 Overview of the LQG/LTR Procedure [10]

In this chapter, a controller will be designed using the LQG/LTR design procedure. The singular value loop shaping approach will be used to mold the singular values of the system open-loop transfer function to meet the specifications of performance and robustness to plant uncertainty and modeling errors. In order to meet the performance specifications of small steady state errors, one desires high DC gains. To minimize the effect of wave encounter and modeling errors at high frequancies, we desire crossover at about 0.1 radians per second with a large roll-off after crossover. This will ensure attenuation of high frequency modeling errors and sensor noise, as well as wave effects which typically occur in the 0.2 to 2 radian range.

The LQG procedure is a mathematical method of designing a robust multivariable controller for a state space system. The designer, however, has the flexibility to pick the parameters of the design motivated from a frequency domain setting. An iterative design process is then carried out, during which the designer is able to match desired frequency domain characteristics, captured by the singular values of the multivariable system, which are equivalent to the SISO Bode plots, by using time-domain mathematics as derived for the solution of the original optimal control problem. In this way, a systematic procedure can be carried out, with the mathematical solution kept simple and in closed form for even a complex MIMO design.

The design is based on the feedback loop as represented in Figure 8. The plant $\underline{G}(s)$ has an input $\underline{u}$, and output $\underline{y}$, a disturbance $\underline{d}$ as seen at the output, and measurement noise vector $\underline{n}$. The compensator is designated as $\underline{K}(s)$.

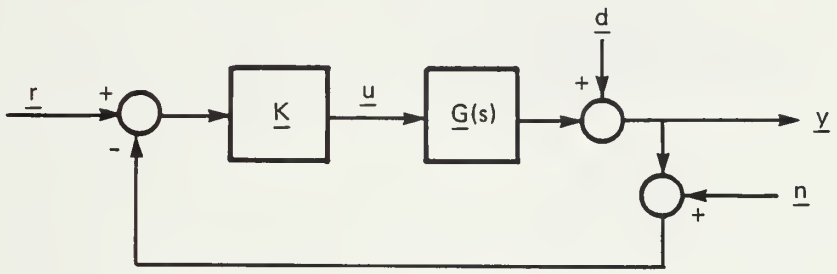

Figure 8. Generalized feedback loop.

The plant $\underline{G}$ is the physical system to be controlled and can therefore behave in a complex manner, as implied by the term nonlinear, infinite dimensional and time-varying which are used for its modeling. To simplify the situation, we desire $\underline{G}$ to be linear, finite and time-invariant (as results from the linearization procedure described in the preceding chapter), with a transfer function $\underline{G}(s)$.

The design objective will be to provide good command-following, good disturbance rejection, and small responses to sensor noise, all subject to the constraints imposed by modeling errors. Hence we need large loop gains in the frequency ranges where commands and disturbances are large and small loop gains in the frequency ranges where modeling errors are large, as well as a well-behaved crossover. These frequency domain requirements can be captured as shown in Figure 9, where the maximum and minimum singular values of the loop transfer matrix envelope the MIMO system performance, and can be directly interpreted as SISO Bode plots. For a good design, it becomes necessary to use techniques which directly take plant descriptions and performance specifications

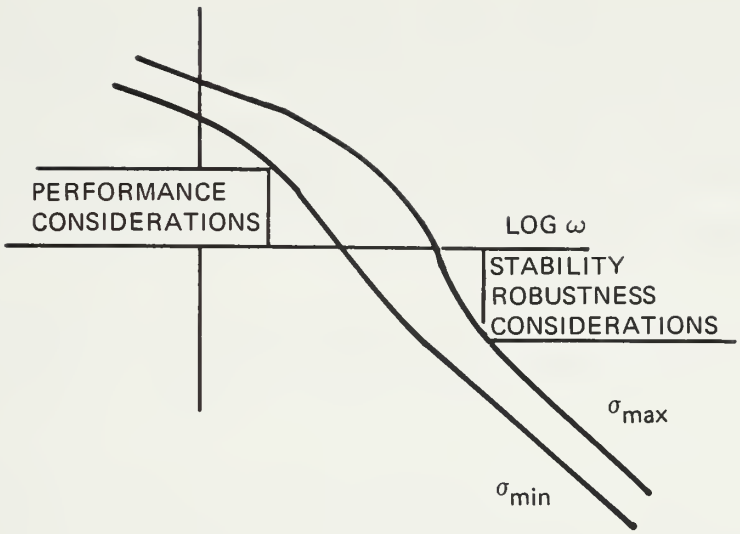

Figure 9. Frequency domain requirements.

into consideration and systematically produce a controller which satisfies the singular value requirements of Figure 9. The multivariable design technique, LQG with Loop Transfer Recovery, is able to perform such a direct singular value loop-shaping.

As previously stated, the LQG/LTR methodology was developed to perform control system design on the basis of time-domain optimization. The method uses the following state space description of the plant, $\underline{G}$:

$$\dot{\underline{x}} = \underline{A}\underline{x} + \underline{B}\underline{u} + \underline{\xi} \tag{3.1}$$

$$\underline{y} = \underline{C}\underline{x} + \underline{\eta} \tag{3.2}$$

where $\underline{x}$ is an n-dimensional state vector, $\underline{u}$ and $\underline{y}$ are m-dimensional control inputs and outputs, and $\underline{\xi}$ and $\underline{\eta}$ are white noise processes. The $\underline{A}$, $\underline{B}$, and $\underline{C}$ matrices satisfy

$$\underline{G}(s) = \underline{C}\phi(s)\underline{B} \tag{3.3}$$

where $\underline{\phi}(s) = (S\underline{I} - \underline{A})^{-1}$. The feedback design task is to find a control law $\underline{u}(t)$ that satisfies the specifications. For this purpose, the mathematics developed for the solution of the following optimization problem are employed, although the design is geared towards loop-shaping and clearly cannot claim optimality as will be seen in the sequel.

$$\text{Min } J = \int_0^T [\underline{x}^T(t)\underline{Q}\underline{x}(t) + \underline{u}^T(t)\underline{R}\underline{u}(t)]\, dt \tag{3.4}$$

where the $\underline{R}$ matrix is the control weighting matrix and $\underline{Q}$ is the state weighting matrix. The solution of this optimization problem is given by

$$\underline{u}(t) = -\underline{G}\underline{x}(t) \tag{3.5}$$

where $\underline{G}$ is a full-state linear quadratic regulator (LQR) gain as defined in the Control Algebraic Riccati equation (CARE). However, in the LQG/LTR procedure, the solution is carried out in two stages. First, the filter gain matrix, $\underline{H}$, is found by solving the Filter Algebraic Riccati equation (FARE).

The objective in this first step is to shape the singular values of the Kalman filter (filter gain) matrix according to the specifications, as suggested in Figure 9, and then recovering the same loop transfer matrix shape for the singular values of the overall system loop transfer matrix $\underline{T}(s)$, which includes the plant, any augmentation, and the controller gain matrix $\underline{G}$, which is obtained as a second stage solution, by solving the CARE, for a given filter design. This compensator structure is referred to as a Model Based Compensator (MBC), because it makes explicit use of the plant linear model (i.e. $\underline{A}$, $\underline{B}$, $\underline{C}$ matrices). At the end of the second stage, the overall system matrix is obtained as

$$\underline{T}(s) = \underline{G}p(s)\underline{K}(s) \tag{3.6}$$

where $\underline{K}(s) = \underline{G}(S\underline{I} - \underline{A} + \underline{BG} + \underline{HC})^{-1}\underline{H}$. Once the shape meets the design specifications, we are further guaranteed that the poles of [$\underline{A}$ - $\underline{HC}$] and [$\underline{A}$ - $\underline{BG}$] will lie in the left half plane, i.e., no instabilities will be introduced into the nominal system, provided [$\underline{A}$, $\underline{B}$] are stabilizable and [$\underline{A}$, $\underline{C}$] detectable.

3.2 Modal Analysis

Since this thesis emphasizes primarily the influence of the MDS configuration, the decision was made not to address the effect of the sailplanes. Additionally, the states psi and z are of no direct interest because of their non-effect on the other (body) states. The original plant $\underline{A}$ matrix contained zeroes in the columns designated for psi and z. By ignoring psi and z, this reduces the plant matrix to an (8 × 8) matrix, the control matrix to an (8 × 3), and the output matrix to a (3 × 8). It then becomes necessary to determine which states to use for the purposes of control.

The MDS arrangement has the unique potential to control roll, ϕ, (and pitch, θ) via D2 and D3. Finally, for the third variable, turning velocity, r, (yaw rate), could be controlled with D1.

At the outset, the corresponding poles and zeroes of the plant were determined. The variable combination ϕ, θ, and r provided no non-minimum phase zeroes and no unstable poles. Table 1 lists both poles and zeroes for the open-loop plant.

A modal analysis was then conducted to ascertain the relative controllability and observability of the system. To examine the controllability of a system, one is interested in the ability of (a) particular input(s), in this case, D1, D2 and/or D3, to control the (entire) state of a system. The observability of a system tests the possibility of observing the complete state of the system through a particular output, i.e., r, ϕ or θ. Using the augmented system $\underline{A}$, $\underline{B}$ and $\underline{C}$ matrices

Table 1.

Augmented Plant Poles

-2.029353579E-02
-4.377357711E-02
-1.803910515E-01
-1.843174783E-01
-6.227811352E-01
-6.583723063E-01
-5.085034079E-01 ± 5.224757797E-01
0.000 (Multiple of 3)
-1.000E-01 (Multiple of 3)

Augmented Plant Zeroes

-4.421289192E-02
-1.984634951E-01
-2.583928560E-01

(augmentation to be described in Section 3.3), the corresponding eigenvalues and eigenvectors were calculated and a modal analysis performed in order to study the controllability and observability properties of the system. The eigenvalues give the response time of a system's modes while the eigenvectors represent the relative contributions of each state to a particular mode, represented by the corresponding (normalized) eigenvector. For example, the plant can be described in state space from by,

$$\dot{\underline{x}} = \underline{Ax} + \underline{Bu} \tag{3.7}$$

$$\underline{y} = \underline{Cx} \tag{3.8}$$

If we let $\underline{x} = \underline{Tz}$, for any nonsingular $\underline{T}$, we can define a new system. However, one must remember that $\underline{z}$ does not describe the physical state space. $\underline{T}$ can be chosen to be the matrix of eigenvectors. Using this change of variable transformation, one gets that $\dot{\underline{x}} = \underline{T\dot{z}}$. So if one makes this change of variable substitution into the state space equations (3.7) and (3.8), one is left with

$$\dot{\underline{x}} = \underline{T\dot{z}} = \underline{ATz} + \underline{Bu} \tag{3.9}$$

$$\underline{y} = \underline{CTz} \tag{3.10}$$

To complete the transformation, $\underline{T}^{-1}$ is multiplied through (3.9) and (3.10) thus yielding

$$\dot{\underline{z}} = \underline{T}^{-1}\underline{ATz} + \underline{T}^{-1}\underline{Bu} \tag{3.11}$$

The net effect of the above procedure is the diagonalization of the state equation where the elements on the diagonal correspond to the eigenvalues of the system, if they are distinct. Rewriting the modal-domain state and output equations for MIMO system, one gets

$$\dot{\underline{z}} = \underline{\Lambda z} + \underline{B}^{*}\underline{u} \tag{3.12}$$

$$\underline{y} = \underline{C}^{*}\underline{z} \tag{3.13}$$

where $\underline{B}^{*} = \underline{T}^{-1}\underline{B}$, $\underline{C}^{*} = \underline{CT}$, and $\underline{\Lambda}$ is a diagonal matrix of eigenvalues. For a system to be controllable by an input $\underline{u}$ or observable by output $\underline{y}$, the column matrix $\underline{B}^{*}$ or the row matrix $\underline{C}^{*}$ must not contain zeroes in a SISO setting. In a MIMO setting, if zeroes appear, then there must be at least one nonzero entry in the $\underline{B}^{*}$ matrix and one nonzero entry in the

$\underline{C}^*$ matrix for a particular state to be controllable and observable by at least one corresponding input or output.

Another method could be used to determine the degree of controllability and observability for a MIMO system and that is the rank method. If one forms the matrices

$$[B, AB, A^2B, \ldots, A^{n-1}B]$$

and

$$\begin{bmatrix} C \\ CA \\ CA^2 \\ \cdot \\ \cdot \\ \cdot \\ CA^{n-1} \end{bmatrix}$$

and their rank is equal to the order of the system, then the system is both controllable and observable. If the rank is less than the order of the system, then that difference is the number of uncontrollable and unobservable states [11]. Appendix F contains the eigenvalues (excluding augmentation) and the corresponding eigenvector matrix, TEMP. The matrix $\underline{\Lambda}$ is the diagonalized modal domain matrix with the eigenvalues located along the main diagonal. The new $\underline{B}^*$ and $\underline{C}^*$ matrices are also included and one can observe that no zeroes exist in either matrix. Thus one can conclude that control inputs D1, D2, and D3 can each control all the states of the plant while the entire state vector can be observed by any of the r, ϕ, and θ outputs.

3.3 System Augmentation

Before setting off to design a compensator for the control system, one must examine the behavior of the plant singular values. Figure 11 shows the open loop singular values with the system augmented with an integrator for each input. In order to further improve the model, one must take into account the actuator dynamics. Actuators are normally modeled as second order systems, however, when one takes into account the high damping in a real actuator, one can then approximate the dynamics of the actuator as a first order system. Pictorially this situation looks like Figure 10.

The state-space equations for this open loop representation are:

$$\dot{\underline{x}}_p = \underline{A}_p \underline{x}_p + \underline{B}_p \underline{u}_p \tag{3.14}$$

$$\underline{y}_p = \underline{C}_p \underline{x}_p \tag{3.15}$$

$$\dot{\underline{x}}_a = \underline{A}_a \underline{x}_a + \underline{B}_a \underline{u}_a \tag{3.16}$$

$$\underline{y}_a = \underline{C}_a \underline{x}_a \tag{3.17}$$

$$\dot{\underline{x}}_I = \underline{A}_I \underline{x}_I + \underline{B}_I \underline{u}_I \tag{3.18}$$

$$\underline{y}_I = \underline{C}_I \underline{x}_I \tag{3.19}$$

Combining the above and putting into matrix form, one gets

$$\dot{\underline{x}} \equiv \begin{bmatrix} \dot{\underline{x}}_p \\ \dot{\underline{x}}_a \\ \dot{\underline{x}}_I \end{bmatrix} = \begin{bmatrix} \underline{A}_p & \underline{B}_p\underline{C}_a & 0 \\ 0 & \underline{A}_a & \underline{B}_a\underline{C}_I \\ 0 & 0 & \underline{A}_I \end{bmatrix} \begin{bmatrix} \underline{x}_p \\ \underline{x}_a \\ \underline{x}_I \end{bmatrix} + \begin{bmatrix} 0 \\ 0 \\ \underline{B}_I \end{bmatrix} \begin{bmatrix} \underline{u}_p \\ \underline{u}_a \\ \underline{u}_I \end{bmatrix}$$

$$\underline{y}_p = [\underline{C}_p \quad 0 \quad 0] \begin{bmatrix} \underline{x}_p \\ \underline{x}_a \\ \underline{x}_I \end{bmatrix}$$

The modeling of each actuator to a first order approximation will be of the form

$$G_a = \frac{1}{\tau s + 1} = \frac{\frac{1}{\tau}}{s + \frac{1}{\tau}} = \frac{x_a}{u} \tag{3.20}$$

Therefore

$$Sx_a + \frac{x_a}{\tau} = \frac{u}{\tau} \tag{3.21}$$

In state space form, this will be represented as

$$\dot{x}_a = -\frac{x_a}{\tau} + \frac{u}{\tau} \tag{3.22}$$

For a system with three control surfaces, in matrix form, we get

$$\underline{A}_a = \begin{bmatrix} -\frac{1}{\tau} & 0 & 0 \\ 0 & -\frac{1}{\tau} & 0 \\ 0 & 0 & -\frac{1}{\tau} \end{bmatrix} \quad \underline{B}_a = \begin{bmatrix} \frac{1}{\tau} & 0 & 0 \\ 0 & \frac{1}{\tau} & 0 \\ 0 & 0 & \frac{1}{\tau} \end{bmatrix}$$

$$\underline{C}_a = \begin{bmatrix} 1 & 0 & 0 \\ 0 & 1 & 0 \\ 0 & 0 & 1 \end{bmatrix}$$

The addition of three integrators is needed to provide high enough gains at low frequencies for good command following and disturbance rejection.

$$G_I = \frac{1}{s} = \frac{x_I}{u} \tag{3.23}$$

Thus for each control variable $x_I s = u$ or $\dot{x}_I = u$. Then for a system with three control inputs, the associated matrices will look like

$$\underline{A}_I = \begin{bmatrix} 0 & 0 & 0 \\ 0 & 0 & 0 \\ 0 & 0 & 0 \end{bmatrix} \quad \underline{B}_I = \begin{bmatrix} 1 & 0 & 0 \\ 0 & 1 & 0 \\ 0 & 0 & 1 \end{bmatrix}$$

$$\underline{C}_I = \begin{bmatrix} 1 & 0 & 0 \\ 0 & 1 & 0 \\ 0 & 0 & 1 \end{bmatrix}$$

The augmented system in state-space form is consequently given by

$$\dot{\underline{x}} = \begin{bmatrix} \underline{A}_{p(8\times 8)} & \underline{B}_p\underline{C}_a \; (8\times 3)(3\times 3) & \underline{0}\;(8\times 3) \\ \underline{0}\;(3\times 8) & \begin{matrix} -\frac{1}{\tau} & 0 & 0 \\ 0 & -\frac{1}{\tau} & 0 \\ 0 & 0 & -\frac{1}{\tau} \end{matrix} & \begin{matrix} \frac{1}{\tau} & 0 & 0 \\ 0 & \frac{1}{\tau} & 0 \\ 0 & 0 & \frac{1}{\tau} \end{matrix} \\ & & \begin{matrix} 0 & 0 & 0 \\ 0 & 0 & 0 \\ 0 & 0 & 0 \end{matrix} \\ \underline{0}\;(3\times 3) & \underline{0}\;(3\times 3) & \end{bmatrix} \underline{x} + \begin{bmatrix} \underline{0}\;(8\times 3) \\ \\ \underline{0}\;(3\times 3) \\ \\ \begin{matrix} 1 & 0 & 0 \\ 0 & 1 & 0 \\ 0 & 0 & 1 \end{matrix} \end{bmatrix} \underline{u} \tag{3.24}$$

$$\underline{y} = \begin{bmatrix} 0 & 0 & 0 & 0 & 0 & 1 & 0 & 0 \\ 0 & 0 & 0 & 0 & 0 & 0 & 1 & 0 \\ 0 & 0 & 0 & 0 & 0 & 0 & 0 & 1 \end{bmatrix} \begin{matrix} \underline{0}\;(3\times 3) & \underline{0}\;(3\times 3) \end{matrix} \underline{x}$$

Note that the $\underline{c}_I$ matrix was not included in the output matrix because the desired outputs are r, ϕ, and θ.

The time constant, τ, is defined as $\frac{1}{w_\eta \xi}$ [12]. Recall that the projected crossover frequency is about 0.1 radian per second so as to avoid the natural frequency of ocean waves of 0.14 radians per second. A typical value for the natural frequency and damping ratio for an actuator is 3.14 radians per second and $\xi = 0.9$. The resultant time constant for the actuator then becomes 0.354 sec. This is clearly above the desired bandwidth. It was consequently decided to ignore the actuators and instead use lag compensation at 0.1 radians per second to improve roll-off near crossover. This will have the effect of making the vehicle less susceptible to modeling errors and high frequency noise. Therefore, the system is augmented with three lag compensators whose dynamics are as shown in Figure 12.

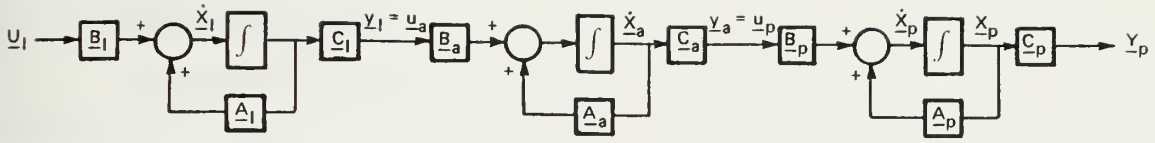

Figure 10. Augmentation representation.

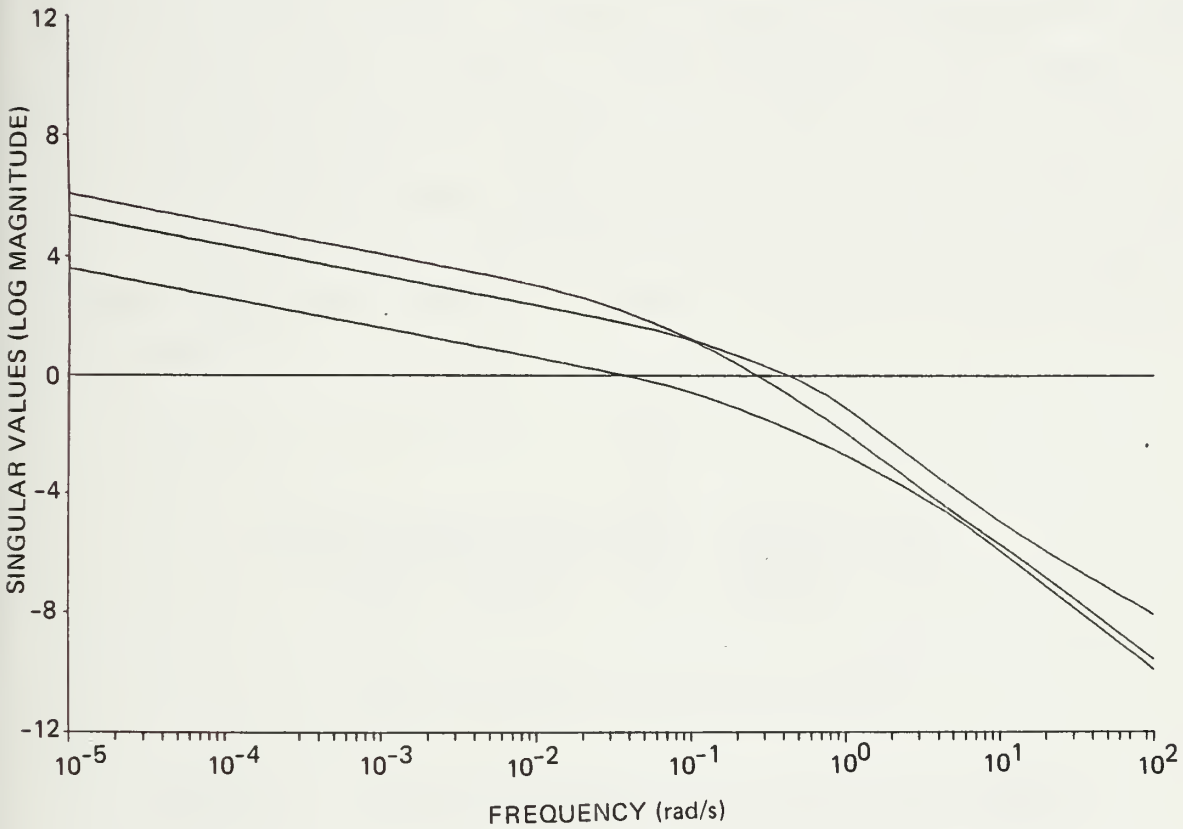

Figure 11. Singular values of open loop plant.

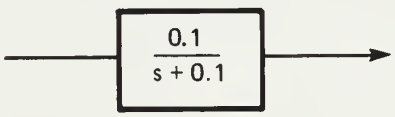

Figure 12. First order lag compensator.

3.4 Controller Design

The method employed to design the controller uses the Model-Based Compensator approach [13]. Two very important points must be kept in mind. First, the controller must be able to maintain the stability of the closed loop system and, secondly, be able to achieve desirable singular value loop shapes, in the frequency domain which translate to performance specifications. This can be achieved by appropriately shaping the system singular values in a manner analogous to the single input-single output Bode plot shaping. Pictorially, the controller and system look like Figure 13. Figure 14 illustrates the state-space description of the Model-Based Compensator, $\underline{K}(s)$, and the open-loop plant, $\underline{G}_p(s)$. It should be noted that the $\underline{A}$, $\underline{B}$, and $\underline{C}$ matrices that appear in the plant also appear in $\underline{K}(s)$ in a similar fashion and thus the term "model-based."

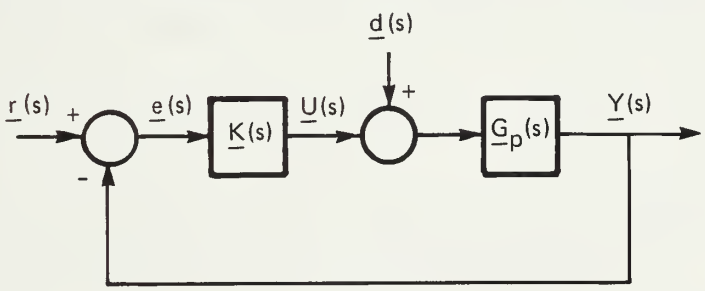

Figure 13. Feedback structure of a MIMO control system.

The dynamics of the open loop plant can be written as

$$\dot{\underline{x}}(t) = \underline{A}\underline{x}(t) + \underline{B}\underline{u}(t) + \underline{L}\underline{d}(t) \tag{3.25}$$

$$\underline{y}(t) = \underline{C}\underline{x}(t) \tag{3.26}$$

The open-loop transfer matrix is then

$$\underline{G}p(s) = \underline{C}(S\underline{I} - \underline{A})^{-1}\underline{B} \tag{3.27}$$

so that

$$\underline{y}(s) = \underline{G}p(s)\underline{u}(s) \tag{3.28}$$

The Model Based Compensator dynamics utilizes the state vector $\underline{z}(t)$ which has the same dimension as the plant state $\underline{x}(t)$. The dynamics of the MBC can be written as

$$\dot{\underline{z}}(t) = \underline{A}\underline{z}(t) + \underline{B}\underline{u}(t) + \underline{H}\underline{v}(t) \tag{3.29}$$

$$\underline{v}(t) = -\underline{e}(t) - \underline{C}\underline{z}(t) = \underline{y}(t) - \underline{C}\underline{z}(t) - \underline{r}(t) \tag{3.30}$$

$$\underline{u}(t) = -\underline{G}\underline{z}(t) \tag{3.31}$$

In the above, the augmented dynamics of the plant as described by Eq. (3.24) are used. Combining the above three expressions we get

$$\dot{\underline{z}}(t) = [\underline{A} - \underline{B}\underline{G} - \underline{H}\underline{C}]\underline{z}(t) - \underline{H}\underline{e}(t) \tag{3.32}$$

Thus the input to the controller is the error, $\underline{e}(t)$ and the output is $\underline{u}(t)$. The input-to-output relation can be written as

$$\underline{u}(s) = \underline{K}(s)\underline{e}(s) \tag{3.33}$$

where $K(s) = \underline{G}(s\underline{I} - \underline{A} + \underline{B}\underline{G} + \underline{H}\underline{C})^{-1}\underline{H}$. If one uses an appropriate change of variable, one can determine the stabilizing nature of the gain matrices $\underline{G}$ and $\underline{H}$. The appropriate variable change is

$$\underline{w}(t) = \underline{x}(t) - \underline{z}(t) \tag{3.34}$$

It follows that $\dot{\underline{w}}(t) = \dot{\underline{x}}(t) - \dot{\underline{z}}(t)$. After making the appropriate substitution for $\dot{\underline{x}}(t)$ and $\dot{\underline{z}}(t)$, one is left with

$$\dot{\underline{w}}(t) = [\underline{A} - \underline{HC}]\underline{w}(t) + \underline{Ld}(t) - \underline{Hr}(t) \qquad (3.35)$$

This resulted in the decoupling of the dynamics of $\underline{w}(t)$ from that of $\underline{x}(t)$. Then $\dot{\underline{x}}(t)$ can be written as

$$\dot{\underline{x}}(t) = [\underline{A} - \underline{BG}]\underline{x}(t) - \underline{BGw}(t) + \underline{Ld}(t) \qquad (3.36)$$

The dynamics of the closed-loop system in matrix form is then given by

$$\begin{bmatrix} \dot{\underline{x}}(t) \\ \dot{\underline{w}}(t) \end{bmatrix} = \begin{bmatrix} \underline{A} - \underline{BG} & -\underline{BG} \\ \underline{0} & \underline{A} - \underline{HC} \end{bmatrix} \begin{bmatrix} \underline{x}(t) \\ \underline{w}(t) \end{bmatrix} + \begin{bmatrix} \underline{L} & \underline{0} \\ \underline{L} & -\underline{H} \end{bmatrix} \begin{bmatrix} \underline{d}(t) \\ \underline{r}(t) \end{bmatrix}$$

The eigenvalues of the closed loop matrices $[\underline{A} - \underline{BG}]$ and $[\underline{A} - \underline{HC}]$ constitute the system poles. Therefore, the det $(\lambda\underline{I} - \underline{A} + \underline{BG})$ and det $(\lambda\underline{I} - \underline{A} + \underline{HC})$ provide the needed insight into the stability of the closed-loop system. In order for the closed-loop system to be stable

$$\mathrm{Re}\lambda_i[\underline{A} - \underline{BG}] < 0; \qquad i = 1, 2, \ldots, n \qquad (3.37)$$

and

$$\mathrm{Re}\lambda_i[\underline{A} - \underline{HC}] < 0; \qquad i = n + 1, n + 2, \ldots, 2n$$

If we are given matrices $\underline{A}$, $\underline{B}$ and $\underline{C}$ with $[\underline{A}, \underline{B}]$ stabilizable and $[\underline{A}, \underline{C}]$ detectable, then matrices $\underline{G}$ and $\underline{H}$ exist that stabilize the open loop system, i.e. $[\underline{A} - \underline{HC}]$ and $[\underline{A} - \underline{BG}]$ are stable. The methodology used to calculate $\underline{G}$ and $\underline{H}$ is outlined in sections 3.5 and 3.6 [13, 14]. This provides in fact the underlying mathematical basis of the LQG/LTR obtained solutions.

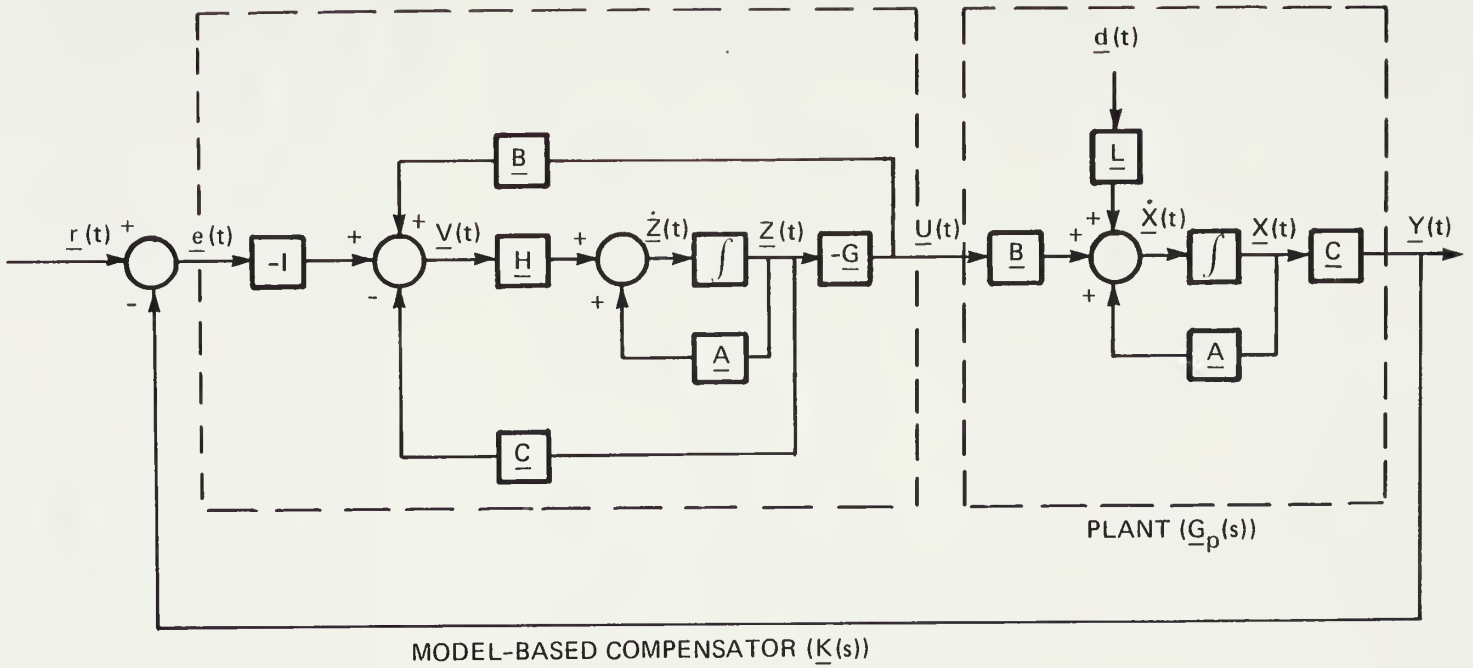

Figure 14. Model-Based Compensator in a feedback configuration.

3.5 The Filter Gain and Control Gain Matrices

It can be seen from Figure 14 that the filter and control gain matrices are the heart of the MBC. In essence the Kalman filter gain matrix, $\underline{H}$, is the input matrix into the MBC taking the error input through the MBC dynamics, which in turn passes it through the integrator having first multiplied the outputs by the appropriate gain matrix $\underline{G}$. This then generates the appropriate control input for the plant.

The $\underline{G}$ and $\underline{H}$ matrices serve a very useful purpose. Recall from Section 3.1 that the desired plant output is modeled via singular values. Setting the shape of the desired plant open loop singular values is important for good command following, disturbance and noise rejection. Once the designer has achieved a shape that meets the open loop specifications, it is important to realize them next in a closed loop configuration. The feedback configuration has the advantages of reduced sensitivity to external disturbances, as a result of a course change—for example, depth change, as well as meeting the specifications of good command following and other noise and modeling uncertainty reduction. Through the clever iterative selection of the $\underline{H}$ and $\underline{G}$ matrices via the LQG/LTR procedure this can be attained. Section 3.6 will detail how this selection is made.

3.6 Loop Shaping

This section will outline the procedure that was followed in designing the LQG-based controller with Loop Transfer Recovery [14]. A plot of the open loop singular values of $\underline{C}(S\underline{I} - \underline{A})^{-1}\underline{B}$ is given in Figure 11. Since there are three controls and three outputs, there are three lines of singular values. As one can see, there is significant separation between the maximum and minimum singular values. It is desirable that all three behave as close as possible in a tight controller design.

The first step is to shape the open loop plant singular values so they meet the desired specifications of good command following, stability and performance, as well as noise and disturbance rejection. This is done by tying the maximum, middle, and minimum singular values together at high and low frequencies. To achieve this, one must form the matrix

$$\underline{G}_{FOL}(s) = \underline{C}(S\underline{I} - \underline{A})^{-1}\underline{L} \tag{3.38}$$

where $\underline{L}$ is an arbitrary matrix that can be manipulated by the designer to ultimately give the desired loop shaping. For system at hand, we form,

$$(S\underline{I} - \underline{A}) = \begin{bmatrix} (S\underline{I} - \underline{A}_*) & -\underline{B}_* \\ \underline{0} & S\underline{I} \end{bmatrix}$$

where

$$\underline{A}_x = \begin{bmatrix} \underset{(8 \times 8)}{\underline{A}_p} & \underset{(8 \times 3)}{\underline{B}_p\underline{C}_a} \\ \underset{(3 \times 3)}{\underline{0}} & \begin{matrix} -\frac{1}{\tau} & 0 & 0 \\ 0 & -\frac{1}{\tau} & 0 \\ 0 & 0 & -\frac{1}{\tau} \end{matrix} \end{bmatrix}$$

and

$$\underline{B}_* = \begin{bmatrix} & \underline{0} & \\ & (8 \times 3) & \\ \frac{1}{\tau} & 0 & 0 \\ 0 & \frac{1}{\tau} & 0 \\ 0 & 0 & \frac{1}{\tau} \end{bmatrix}$$

Note, the $\underline{A}$ matrix of $(S\underline{I} - \underline{A})$ came from Section 3.3. The inverse of $(S\underline{I} - \underline{A})$ is

$$(S\underline{I} - \underline{A})^{-1} = \begin{bmatrix} (S\underline{I} - \underline{A}_*)^{-1} & \frac{\underline{B}_*}{S}(S\underline{I} - \underline{A}_*)^{-1} \\ \underline{0} & \frac{\underline{I}}{S} \end{bmatrix}$$

The $\underline{L}$ matrix can be broken up into two components $\underline{L}_1$ and $\underline{L}_2$ where $\underline{L}_1 = \underline{L}_{(8 \times 3)}$ and $\underline{L}_2 = \underline{L}_{(3 \times 3)}$. For low frequency shaping, $S\underline{I}$ is approximately zero. With that approximation and forming $\underline{G}_{FOL}(s)$, one gets

$$\underline{C}(S\underline{I} - \underline{A})^{-1}\underline{L} = [\underline{C}_{(3 \times 11)} \quad \underline{0}] \begin{bmatrix} -\underline{A}_*^{-1} & \frac{-\underline{A}_*^{-1}\underline{B}_*}{s} \\ \underline{0} & \frac{\underline{I}}{S} \end{bmatrix} \begin{bmatrix} \underline{L}_1 \\ \underline{L}_2 \end{bmatrix} \qquad (3.39)$$

where $\underline{C}$ is a (3×11) matrix with identity in positions (1, 6), (2, 7), and (3, 8) corresponding to the states to be controlled r, ϕ, and θ. Expanding (3.39) yields

$$\underline{C}(S\underline{I} - \underline{A})^{-1}\underline{L} = -\underline{C}_{11}\underline{A}_*^{-1}\underline{L}_1 - \frac{\underline{C}_{11}\underline{A}_*^{-1}\underline{B}_*\underline{L}_2}{S} \tag{3.40}$$

But for small s, low frequency, the second term in (3.40) dominates the first term. So $\underline{C}(S\underline{I} - \underline{A})^{-1}\underline{L}$ can be approximated by $\frac{-\underline{C}_{11}\underline{A}_*^{-1}\underline{B}_*\underline{L}_2}{S}$. Then to tie the singular values together at low frequencies we also have $\underline{G}_{FOL}(s) = \frac{\underline{I}}{S}$. Therefore

$$\underline{L}_2 = -(\underline{C}_{11}\underline{A}_*^{-1}\underline{B}_*)^{-1} \tag{3.41}$$

For high frequencies, one can approximate $(S\underline{I} - \underline{A})$ by $S\underline{I}$. Using the same procedure as above,

$$\underline{C}(S\underline{I} - \underline{A})^{-1}\underline{L} = [\underline{C}_{11} \quad \underline{0}]\begin{bmatrix} (S\underline{I})^{-1} & \frac{\underline{B}_*}{S}(S\underline{I})^{-1} \\ \underline{0} & \frac{\underline{I}}{S} \end{bmatrix}\begin{bmatrix} \underline{L}_1 \\ \underline{L}_2 \end{bmatrix} \tag{3.42}$$

Expansion of (3.42) yields

$$\underline{C}(S\underline{I} - \underline{A})^{-1}\underline{L} = \frac{\underline{C}_{11}\underline{L}_1}{S} + \frac{\underline{C}_{11}\underline{B}_*\underline{L}_2}{S^2} \tag{3.43}$$

As S gets large, high frequencies, the second term in (3.43) will be dominated by the first term. So $\underline{L}_1$ will be equal to

$$\underline{L}_1 = \left(\underline{C}_{11}^T\underline{C}_{11}\right)^{-1}\underline{C}_{11}^T = \underline{C}_{11}^T\left(\underline{C}_{11}\underline{C}_{11}^T\right)^{-1} \tag{3.44}$$

The combination of $\underline{L}_1$ and $\underline{L}_2$ now constitutes the $\underline{L}$ matrix of the overall system. The $\underline{L}$ matrix provides loop shaping and is totally under the designer's control as a free design parameter. Figure 15 shows the result of the initial open loop shaping. This, in turn, provides the desirable system profile which the closed loop compensated system should match. The resulting $\underline{L}$ matrix can be found in Appendix G. In order for the crossover frequency to be less than the critical crossover frequency of 0.1 radians per second, (natural sea spectrum is at 0.14 radians per second), it was necessary to multiply the $\underline{L}$ matrix by a scalar of 0.05.

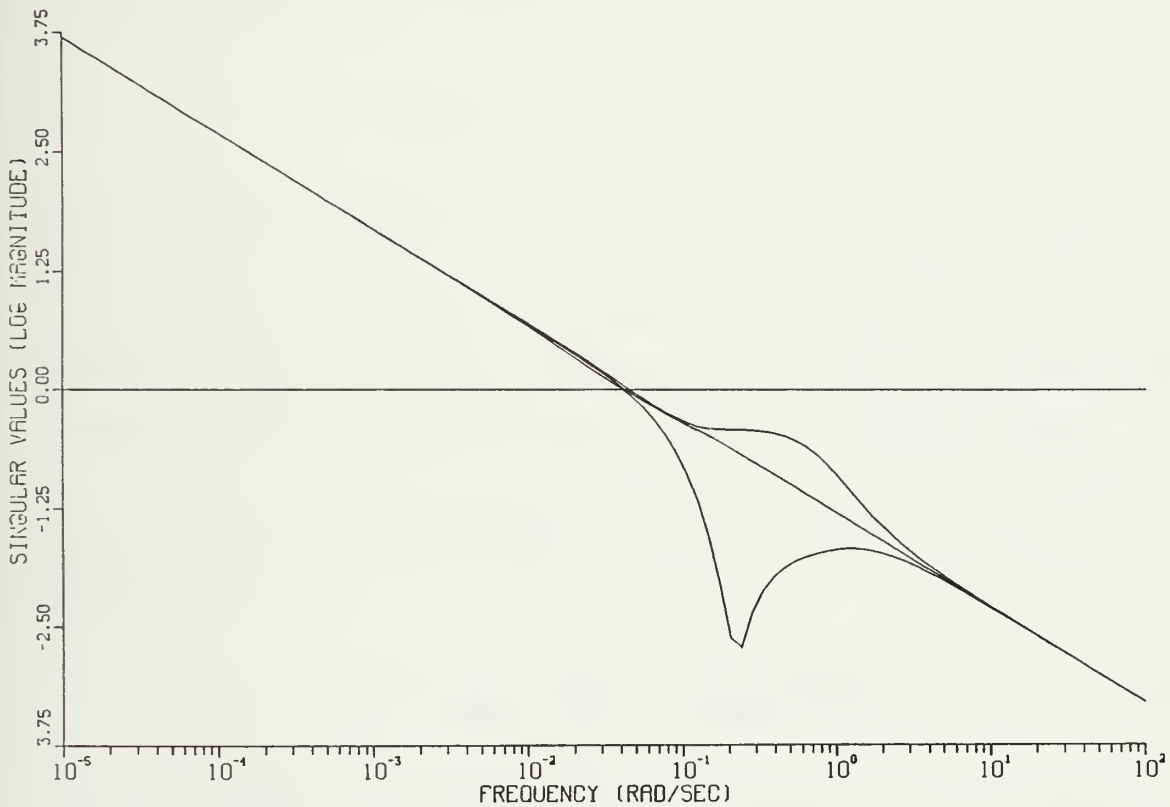

Figure 15. Singular values of $\underline{G}_{FOL}(j\omega)$.

The next step in the controller design is to determine the filter gain matrix, $\underline{H}$. To do this one solves the Filter Algebraic Riccati Equation (FARE).

$$\underline{0} = \underline{\Sigma A} + \underline{A}^T\underline{\Sigma} + \underline{\Xi} - \frac{1}{\mu}\underline{\Sigma C}^T\underline{\theta}^{-1}\underline{C\Sigma} \tag{3.45}$$

where $\underline{\theta}$ is an arbitrary (m × m) symmetric and positive definite matrix (equal to the identity here) and $\underline{\Xi}$, normally the process noise covariance matrix is now replaced by $\underline{LL}^T$. The solution to the FARE is the (n × n)$\underline{\Sigma}$ matrix. The filter gain matrix is given by,

$$\underline{H} = \frac{1}{\mu}\underline{\Sigma C}^T\underline{\Xi}^{-1} \tag{3.46}$$

If one plots the singular values of the Kalman filter,

$$\sigma_i(\underline{G}_{KF}(j\omega)) = \underline{C}(S\underline{I} - \underline{A})^{-1}\underline{H} \tag{3.47}$$

then they should pattern the profile of the singular values of $\underline{G}_{FOL}(j\omega)$. Figure 16 shows the similar profile. The DC gains, crossover frequency, and band crossover bandwidth are approximately the same. If it becomes necessary to adjust the DC gain and crossover, this can be accomplished by selecting another free parameter μ, in Eqs. (3.45) and (3.46).

The final step in the controller design is to solve the Control Algebraic Riccati Equation (CARE) to obtain the control gain matrix, $\underline{G}$. The CARE looks like

$$\underline{0} = -\underline{KA} - \underline{A}^T\underline{K} - \underline{qQ} + \underline{KBR}^{-1}\underline{B}^T\underline{K} \tag{3.48}$$

where $\underline{K}$ is an (n × n) solution. The $\underline{R}$ matrix is an (m × m) positive definite matrix (identity for our purposes), and the $\underline{Q}$ matrix is given by

$$\underline{Q} = \underline{C}^T\underline{C} \tag{3.49}$$

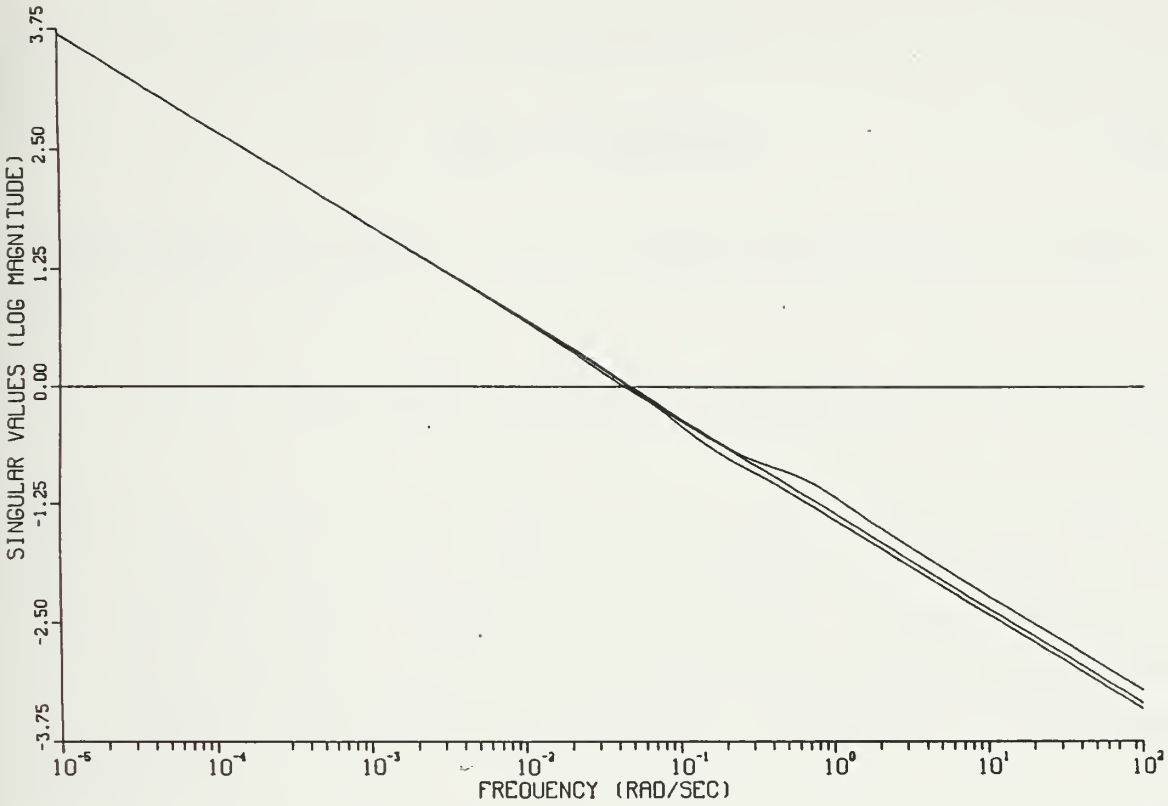

Figure 16. Singular values of $\underline{G}_{KF}(j\omega)$.

such that $[\underline{A}, \underline{C}]$ is a detectable pair. The control gain matrix $\underline{G}$ is given by

$$\underline{G} = \underline{R}^{-1}\underline{B}^{T}\underline{K} \tag{3.50}$$

The singular values of the resultant loop transfer matrix ($\sigma_i[\underline{T}(j\omega)]$) are now calculated where

$$\underline{T}(s) = \underline{G}(s)\underline{K}_{LQG}(s) \tag{3.51a}$$

or

$$\underline{T}(s) = \underline{G}p(s)\underline{K}(s) \tag{3.51b}$$

$\underline{G}(s)$ is the plant transfer matrix defined by

$$\underline{G}(s) = \underline{G}p(s)\underline{G}a(s) \tag{3.52}$$

as illustrated in Figure 7. In the frequency domain $\underline{K}_{LQG}(s)$ is given by:

$$\underline{K}_{LQG}(s) = \underline{G}(S\underline{I} - \underline{A} + \underline{BG} + \underline{HC})^{-1}\underline{H} \tag{3.53}$$

Figure 17 is a plot of the singular values of the compensated system $\underline{T}(s)$. A value of 1000 was used for q so that the three individual control singular values coincide. It is apparent by comparing $\sigma_i(\underline{T}(j\omega))$ with $\sigma_i(\underline{G}_{KF}(j\omega))$ that the DC gains are equal and crossover occurs at the same frequency. The roll-off past crossover is desired as illustrated in Figure 9.

A check was made to determine if the controller, $\underline{K}(s)$ introduced any instabilities into the system. Table 2 is a listing of poles and zeroes which indeed corroborates the fact that the design has resulted in a stable system. Appendix H contains the $\underline{A}$, $\underline{B}$, $\underline{C}$, $\underline{G}$, $\underline{H}$ and $(\underline{A} - \underline{BG} - \underline{HC})$ design matrices that will also be used in the simulation as described in Section 4.1.

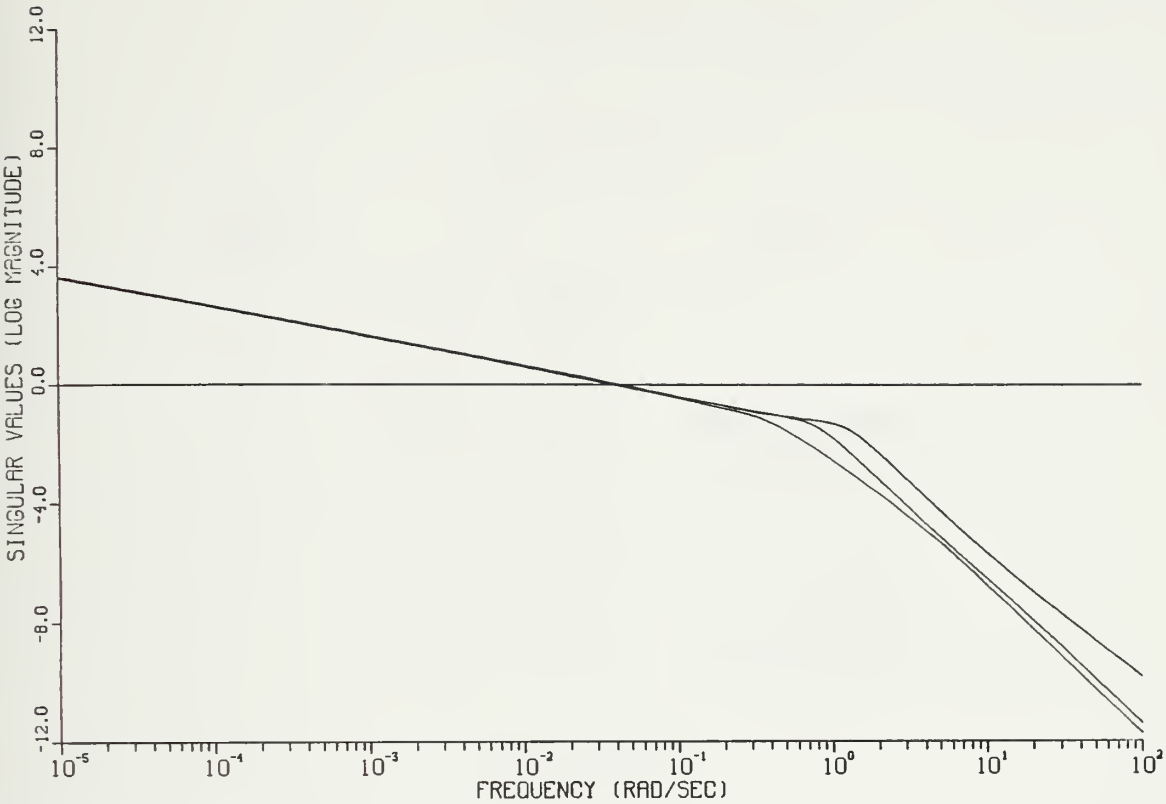

Figure 17. Singular values of $\underline{T}(j\omega)$.

Table 2. Poles and zeroes of K(s).

Unique Poles

Number	Real	Imag
1	-4.421317785E-02	
2	-1.984642130E-01	
3	-2.515003179E-01	
5	-2.283572447E-01	2.689624484E-01
7	-3.121226887E-01	7.200466481E-01
8	-8.357975180E-01	
10	-8.470467465E-01	3.140172344E-01
12	-4.856380807E-01	1.221159615E+00
14	-1.202212619E+00	5.654424752E-01

Unique Zeroes

Number		
1	-2.418544925E-02	
2	-4.342940086E-02	
3	-9.122782906E-02	
4	-1.062659914E-01	
6	-1.471524383E-01	-7.231643907E-02
7	-1.852788869E-01	
8	-5.245929103E-01	
9	-6.230977444E-01	
11	-5.179401036E-01	4.323091793E-01

CHAPTER 4

COMPENSATOR PERFORMANCE

4.1 Model Simulation

The model simulation used to test the controller involves the integration of

$$\dot{\underline{z}}(t) = (\underline{A} - \underline{BG} - \underline{HC})\underline{z}(t) - \underline{He}(t)$$

where $\underline{e}(t)$ is the error vector defined by

$$\underline{e}(t) = \underline{r}(t) - \underline{y}(t)$$

To close the loop, one can either select the linear model or nonlinear model as developed in Chapter 2. It is expected that the linear model will give good results with the nonlinear model giving acceptable results because the controller was designed from the linear model originally.

4.2 Simulation Results

Now that the controller has been designed, it is necessary to test its performance. Recall that the motivation behind this thesis was twofold: (i) design a controller from a linear model and (ii) test it on a nonlinear model, controlling r, ϕ, and θ in a turn.

The first test simulation run purpose was to check if the controller would be able to achieve zero steady state error with a command reference input of -0.368482E-02 rad/s, the nominal r value, and zero for both ϕ and θ, keeping in mind that the open loop roll for the same condition was 1.5 degrees and θ 4.0×10^{-2} degrees. With the closed loop simulation, both ϕ and θ indeed went to zero.

A second simulation run was made to command a condition that was other than the nominal r. A turning velocity equivalent to a 5 degree nominal rudder deflection was commanded with zero again for ϕ and θ. The open loop ϕ and θ for this condition were 5.5 degrees and 2.5 degrees respectively with the controller, r went to the commanded value of -0.1160E-02 rad/s, and ϕ and θ went to zero. With both simulation runs, the controller achieved zero steady state error for the three command inputs. Figure 18 contains the open loop r, ϕ and θ response runs and the closed loop simulation response with command input of -0.368482E-02 rad/s, 0°, and 0° for r, ϕ and θ respectively. Figure 19 likewise shows the open and closed loop responses for r = -0.1160E-01 rad/s and zero for ϕ and θ.

One additional benefit of the controller can be seen with depth, z. Without the controller, both open loop simulations exhibited continuous depth change throughout the run. With the controller, the vehicle sank a small amount but steadied as the run continued. Therefore the controller was able to stabilize depth loss even though depth was not a control variable.

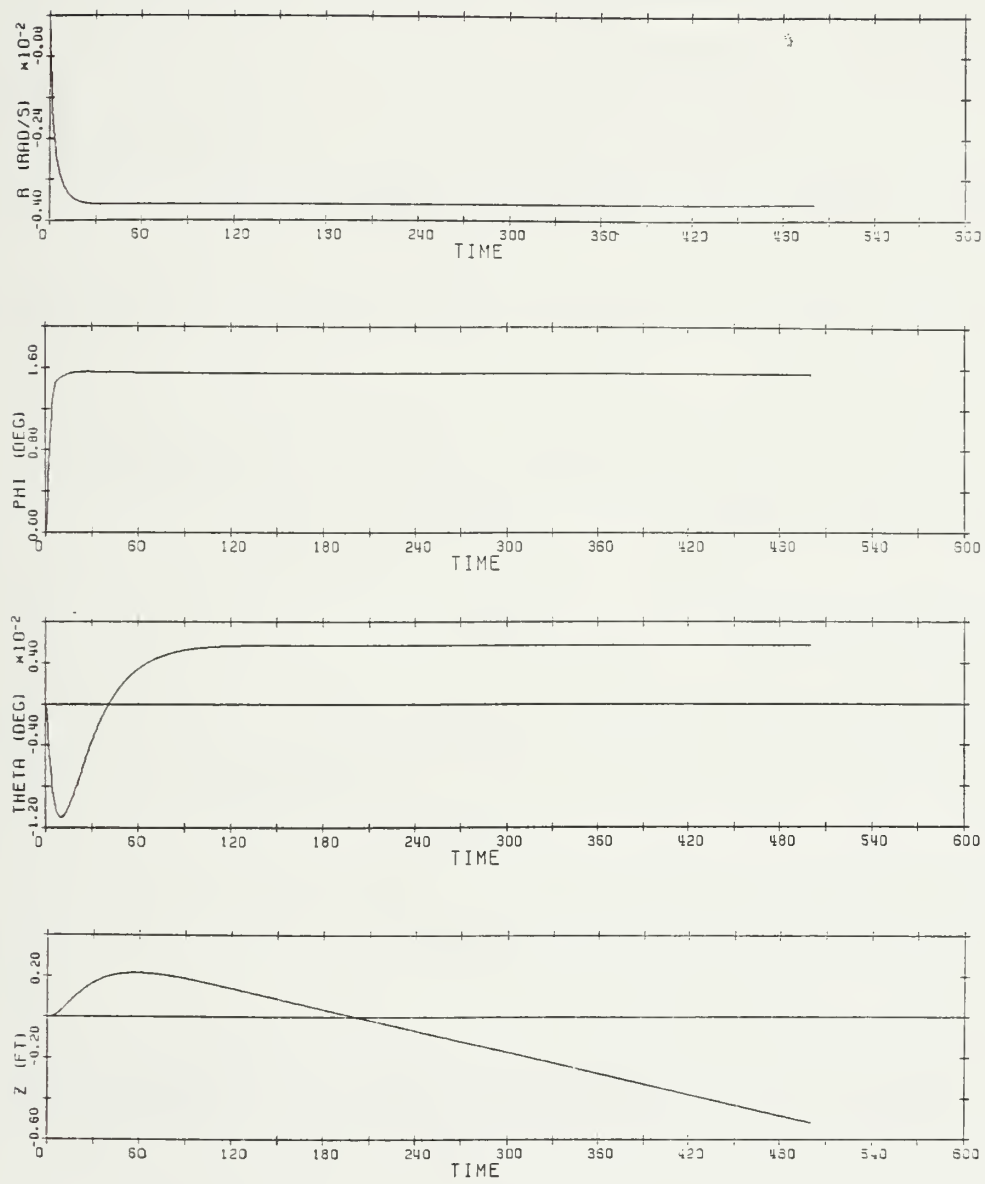

Figure 18. Open and closed loop simulation responses with command input.

$r = -0.368482E-02$ rad/s

$\phi = 0°$

$\theta = 0°$

CLOSED LOOP SIMULATION RESPONSE (2° RUDDER)

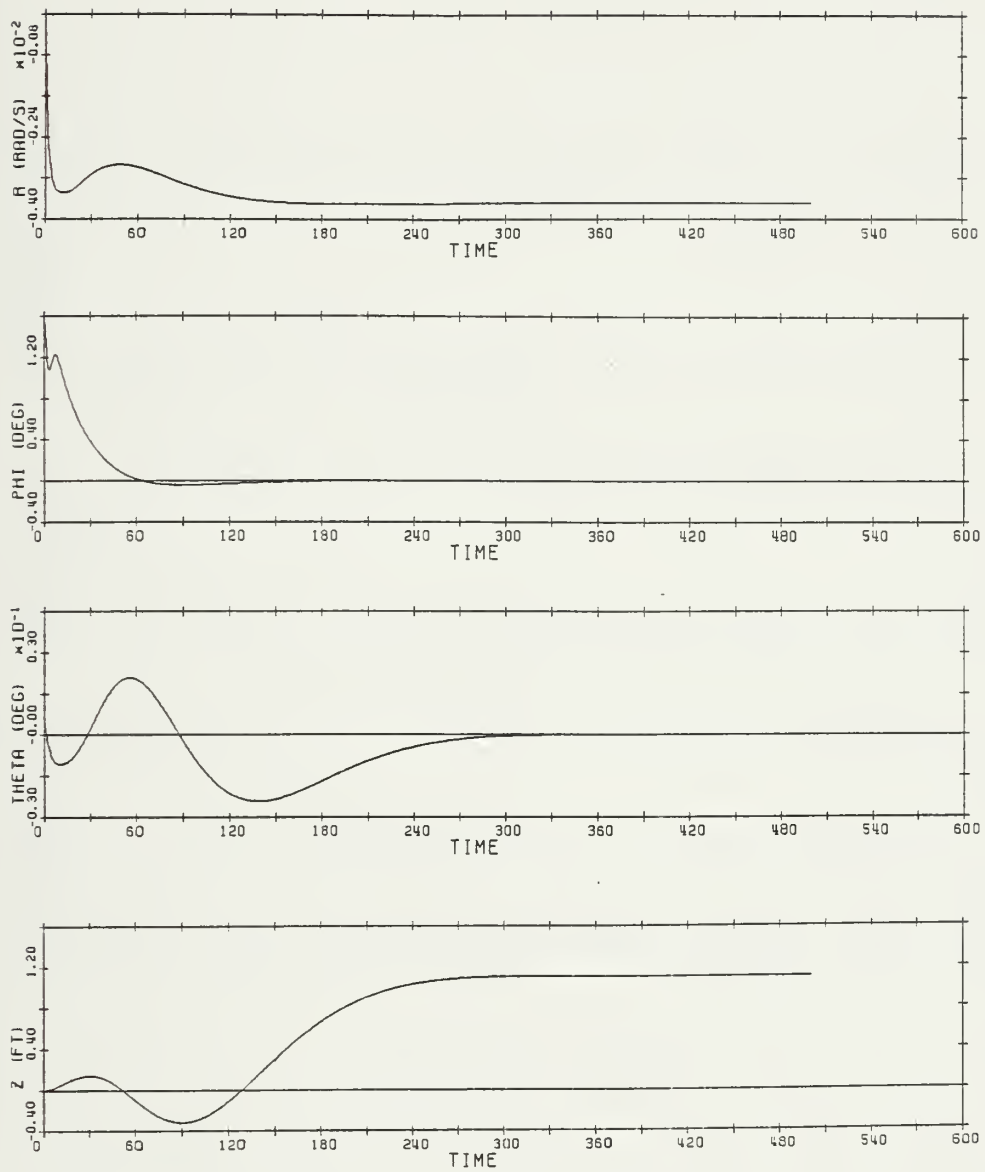

Figure 18. (Cont.)

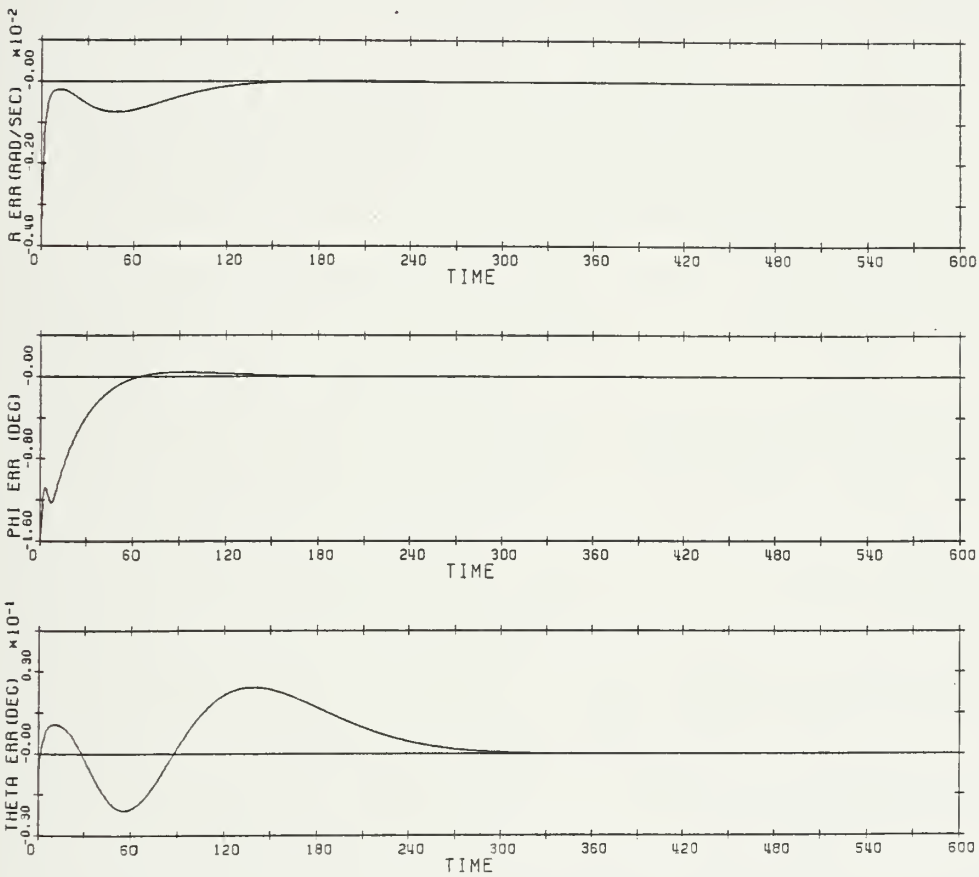

Figure 18. (Cont.)

OPEN LOOP RESPONSE

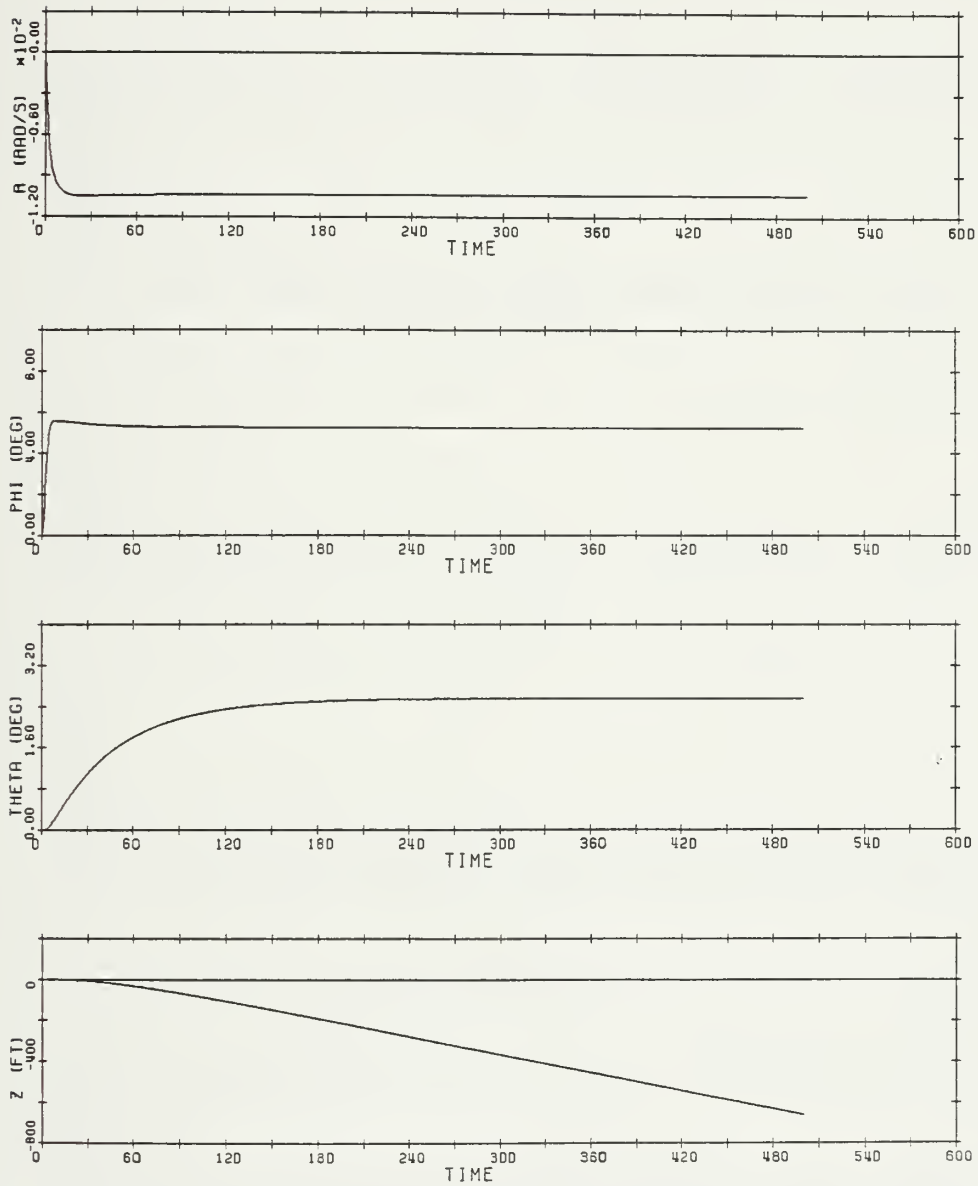

Figure 19. Open and closed loop simulation responses with command input.

$r = -0.1160E\text{-}01$ rad/s

$\phi = 0°$

$\theta = 0°$

CLOSED LOOP SIMULATION RESPONSE (5° RUDDER)

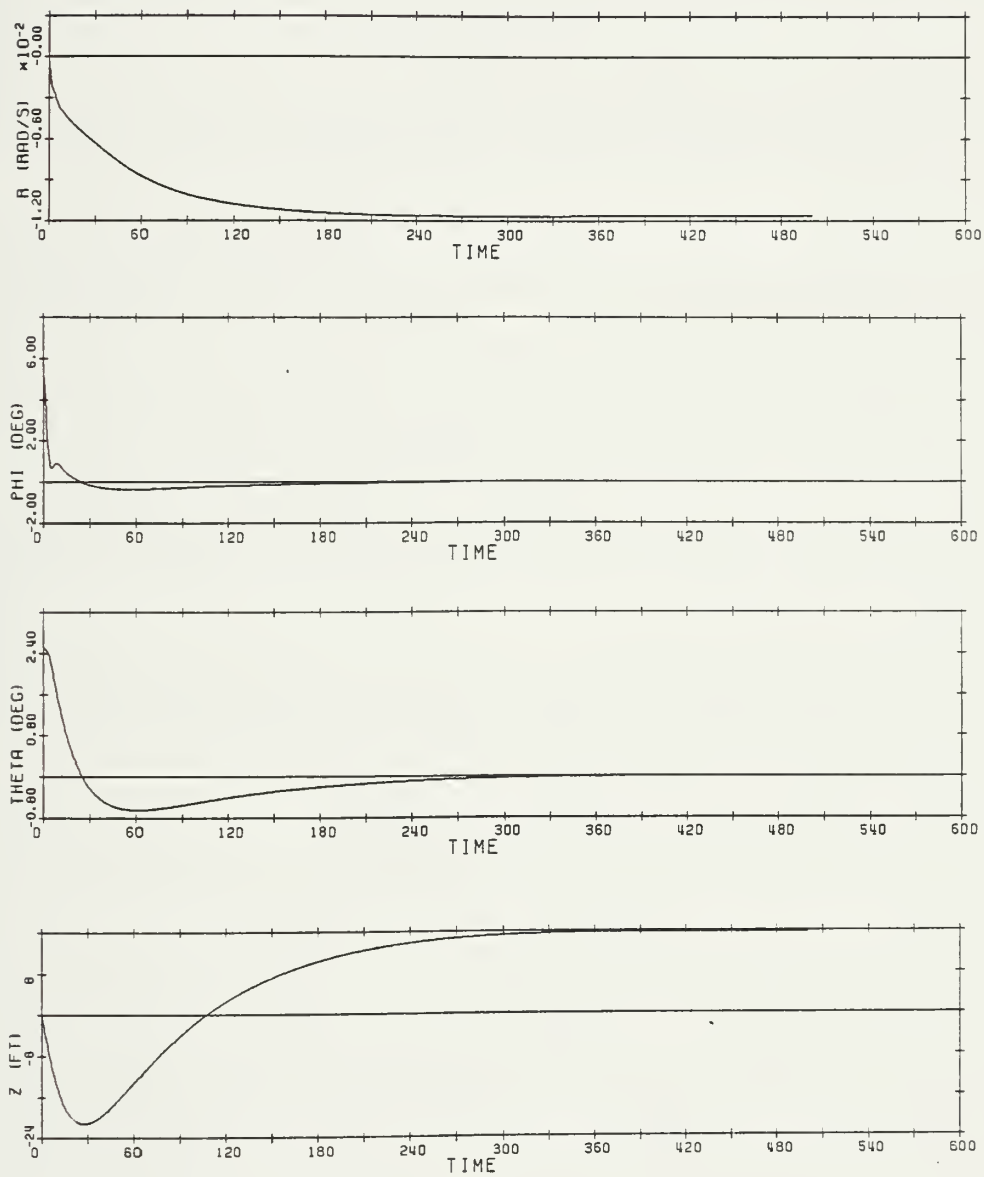

Figure 19. (Cont.)

CLOSED LOOP SIMULATION RESPONSE (CONT'D)

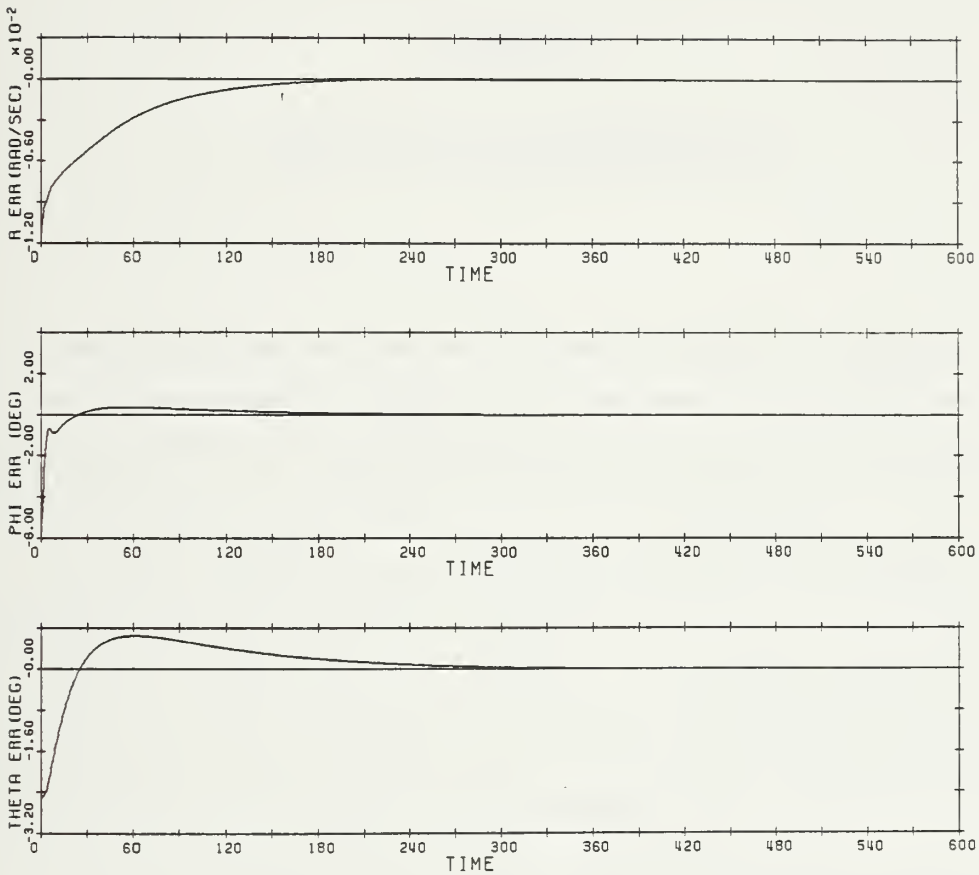

Figure 19. (Cont.)

CHAPTER 5

CONCLUSIONS AND RECOMMENDATIONS

The LQG/LTR method can be successfully used to design a controller from a linear model. Additionally the resulting controller is able to perform acceptably with zero steady state error on a nonlinear model, which more closely approximates the real world system.

The MDS configuration has demonstrated improved ability over the conventional cruciform stern in turning situations. With the ability of the vehicle to align its local reference axis to that of the global system, one is able to obtain true motions of surge, sway, heave, roll, pitch, and yaw. The advantage being improved crew comfort and quicker computer solutions to fire control problems.

It is recommended that further thesis work on this model to include depth control with the additional control surface of sailplanes. A potpourri of operating points spanning a speed range from 5 to 21 knots with rudder deflections of 5 to 30 degrees will give on a feeling for the capabilities of the MDS configured submersible. The addition of vortex shedding to the model will also improve the characteristics of the model to real world submersibles. Finally, it would be desirable to design a controller that could negotiate ordered changes in depth. With gain scheduling, the model could clearly be used as a training aid in a simulation laboratory.

REFERENCES

(1) Gerther, Hagen, "Standard Equations of Motion for Submarine Simulation", NSRDC Report 2510, June 1967.

(2) Gillard, J.H., Control System Design for an Unmanned, Untethered Underwater Vehicle, Ocean Engineer's Thesis, MIT 1982.

(3) Lamb, Sir Horace, Hydrodynamics, 6th Ed., Dover Publications, New York 1945.

(4) Newman, J.N., Marine Hydrodynamics, MIT Press 1980.

(5) Landweber, L., Johnson, J.L., Prediction of Dynamic Stability Derivatives of an Elongated Body of Revolution, David Taylor Model Basin Report C-359, May 1951.

(6) Underwood, M.J., Control of a Small Submersible with an Inverted "Y" Sternplane Arrangement, CSDL-T-803, Ocean Engineer's Thesis, MIT 1983.

(7) Abkowitz, M., Stability and Motion Control of Ocean Vehicles, MIT Press 1969.

(8) Comstock, J.P., Principles of Naval Architecture, The Society of Naval Architects and Marine Engineers, New York, NY 1967.

(9) Charles Stark Draper Laboratory Memo No.: SUB 1-1083 "Submarine Configuration and Control".

(10) Stein, G., "LQG-Based Multivariable Design: Frequency Domain Interpretation" 6.236 Notes Spring 1984.

(11) Takahashi, Rabins, Auslander, Control and Dynamic Systems, Addison-Wesley Publishing, Reading, MA, November 1972.

(12) DiStefano, Stubbernd, Williams, Feedback and Control Systems, Schaum's Outline Series, McGraw-Hill, NY 1967.

(13) Athans, M., "Model-Based Compensators for Multivariable Control Synthesis and the LQG Algorithms", 6232/820308 Spring 1982 class notes.

(14) Athans, M., "LQG-Based Designs with Loop Transfer Recovery" 6232/820419 Spring 1983 class notes.

APPENDIX A

MASS PROPERTIES

Mass	Weight	Buoyancy
75,483 slugs	2,428,300 lb_f	2,428,300 lb_f
Ixx	Iyy	Izz
3,019,300 slugs-ft^2	123,790,000 slugs-ft^2	123,790,000 slugs-ft^2
Ixy	Ixz	Iyz
0.	0.	0.
XG	YG	ZG
0.	0.	1.0 ft
XB	YB	ZB
0.	0.	0.
Xstern	Slength	
-89.75 ft	180 ft	

APPENDIX B

NONLINEAR EQUATIONS OF MOTION

Axial Force Equation

$$\begin{aligned}
m\dot{u} - my_G\dot{r} + mz_G\dot{q} = {} & mvr - mwq + mx_G(q^2 + r^2) - my_G pq - mz_G pr \\
& + \frac{\rho}{2}\ell^4\left[X'_{qq}q^2 + X'_{rr}r^2 + X'_{rp}rp\right] \\
& + \frac{\rho}{2}\ell^3\left[X'_{\dot{u}}\dot{u} + X'_{vr}vr + X'_{wq}wq\right] \\
& + \frac{\rho}{2}\ell^2\left[X'_{uu}u^2 + X'_{vv}v^2 + X'_{ww}w^2\right] \\
& + \frac{\rho}{2}\ell^2u^2\left[X'_{\delta\delta}(D1^2 + D2^2 + D3^2) + X'_{\delta b\delta b}\delta_b^2\right] \\
& + \frac{\rho}{2}\ell^2u^2\left[\text{thrcst}\left(a_i + b_i\eta + c_i\eta^2\right)\right] \\
& + \frac{\rho}{2}\ell^2(\eta - 1)\left[X'_{\delta\delta\eta}u^2(D1^2 + D2^2 + D3^2) + X'_{vv\eta}v^2 + X'_{ww\eta}w^2\right] \\
& - (W - B)\sin\theta - \text{drag}
\end{aligned}$$

Lateral Force Equation

$$\dot{mu} - mz_G\dot{p} + mx_G\dot{r} =$$

$$mwp - mur + my_G(r^2 + p^2) - mz_G gr - mx_G qp$$

$$+ \frac{\rho}{2}\ell^4\left[Y_{\dot{p}}'\dot{p} + Y_{\dot{r}}'\dot{r} + Y'_{p|p|}p|p| + Y'_{pq}pq + Y'_{qr}qr\right]$$

$$+ \frac{\rho}{2}\ell^3\left[Y_{\dot{v}}'\dot{v} + Y'_{vq}vq + Y'_{wp}wp + Y'_{wr}wr + Y'_{r}ur + Y'_{p}up\right.$$

$$+ Y'_{|r|\delta}u|r|(D1 - 0.6088D2 + 0.6088D3)$$

$$\left. + Y'_{v|r|}\frac{v}{|v|}(v^2 + w^2)^{\frac{1}{2}}|r| + Y'_{r\eta}ur(\eta - 1)\right]$$

$$+ \frac{\rho}{2}\ell^2\left[Y'_{\dot{*}}u^2 + Y'_{v}uv + Y'_{v|v|}v(v^2 + w^2)^{\frac{1}{2}}\right.$$

$$\left. + Y'_{vw}\frac{vwu}{\sqrt{u^2 + v^2 + w^2}} + Y'_{\delta}u^2(D1 - 0.6088D2 + 0.6088D3)\right]$$

$$+ \frac{\rho}{2}\ell^2(\eta - 1)\left[Y'_{v\eta}uv + Y'_{v|v|\eta}v(v^2 + w^2)^{\frac{1}{2}}\right.$$

$$\left. + Y'_{\delta\eta}u^2(D1 - 0.6088D2 + 0.6088D3)\right]$$

$$+ (W - B)\sin\phi\cos\theta$$

$$- \frac{\rho}{2}\ell^2\frac{Z_{ww}}{\int_{\ell} D(x)\,dx}\int_{\ell} H(x)v(x)\left\{[w(x)]^2 + [v(x)]^2\right\}^{\frac{1}{2}}dx$$

$$- \frac{\rho}{2}\ell^2\frac{Z_{vv}}{(\bar{x}_{fw} - x_{so})}\int_{x_{vs}}^{x_{fw}} w(x)\bar{v}_{fw}(t - \tau(x))\,dx$$

Normal Force Equation

$$
\begin{aligned}
m\dot{w} - mx_G\dot{q} + my_G\dot{p} \;=\;
&muq - mvp + mz_G(p^2 + q^2) - mx_G rp - my_G rq \\
&+ \frac{\rho}{2}\ell^4\left[Z'_{\dot{q}}\dot{q} + Z'_{p|p|}\frac{p^2u}{\sqrt{u^2+v^2+w^2}} + Z'_{r|r|}\frac{r^2u}{\sqrt{u^2+v^2+w^2}}\right. \\
&\qquad \left. + Z'_{rp}\frac{rpu}{\sqrt{u^2+v^2+w^2}}\right] \\
&+ \frac{\rho}{2}\ell^3\left[Z'_{\dot{w}}\dot{w} + Z'_{vr}\frac{vru}{\sqrt{u^2+v^2+w^2}} + Z'_{vp}vp + Z'_{q}uq\right. \\
&\qquad + Z'_{|q|\delta}u|q|(-0.7934D2 - 0.7934D3) \\
&\qquad \left. + Z'_{w|q|}\frac{w}{|w|}(v^2+w^2)^{\frac{1}{2}}|q| + Z'_{q\eta}uq(\eta - 1)\right] \\
&+ \frac{\rho}{2}\ell^2\left[Z'_{*}u^2 + Z'_{w}uw + Z'_{w|w|}w(v^2+w^2)^{\frac{1}{2}} + Z'_{|w|}u|w|\right. \\
&\qquad + Z'_{v|v|}\frac{v^2u}{\sqrt{u^2+v^2+w^2}} + Z'_{\delta}u^2(-0.7934D2 - 0.7934D3) \\
&\qquad \left. + Z'_{\delta b}u^2\delta_b + Z'_{ww}|w|\sqrt{v^2+w^2}\right] \\
&+ \frac{\rho}{2}\ell^2(\eta - 1)\left[Z'_{w\eta}uw + Z'_{w|w|\eta}w(v^2+w^2)^{\frac{1}{2}}\right. \\
&\qquad \left. + Z'_{\delta\eta}u^2(-0.7934D2 - 0.7934D3)\right] + (w - B)\cos\theta\cos\phi
\end{aligned}
$$

$$- \frac{\rho}{2} \int_{\ell} C_d D(x) w(x) \left\{ [v(x)]^2 + [w(x)]^2 \right\}^{\frac{1}{2}} dx$$

$$+ \frac{\rho}{2} \ell C_v \int_{x_{vs}}^{\bar{x}_{fw}} v(x) \bar{v}_{fw} (t - Z_x) \, dx$$

Rolling Moment Equation

$$my_G\dot{w} - mz_G\dot{v} =$$

$$-I_{xx}\dot{p} - (I_{zz} - I_{yy})gr + (\dot{r} + pq)I_{xz} - (r^2 - q^2)I_{yz} - (pr - \dot{q})I_{xy}$$

$$+ my_G uq - my_G vp - mz_G wp + mz_G ur$$

$$+ \frac{\rho}{2}\ell^5\left[K_{\dot{p}}'\dot{p} + K_{\dot{r}}'\dot{r} + K_{qr}'qr + K_{pq}'pq + K_{p|p|}'p|p|\right]$$

$$+ \frac{\rho}{2}\ell^4\left[K_p'up + K_r'ur + K_{\dot{v}}'\dot{v} + K_{vq}'vq + K_{wp}'wp + K_{wr}'wr\right]$$

$$+ \frac{\rho}{2}\ell^3\left[K_*'u^2 + K_v'uv + K_{v|v|}'v(v^2 + w^2)^{\frac{1}{2}} + K_{vw}'vw + K_\delta'u^2(D1 - D2 + D3)\right.$$

$$\left. + K_{*\eta}'u^2(\eta - 1)\right] - Propt + \left(u^2 + v_s^2 + w_s^2\right)$$

$$\left(K4S\beta_s^2 \sin 4(\phi_s - 37.5) + K8S \sin 8(\phi_s - 37.5)\right)$$

$$+ [(y_G w - y_B B)\cos\theta\cos\phi - (z_G w - z_B B)\cos\theta\sin\phi]$$

$$+ \frac{\rho}{2}\ell^2 C_v \bar{z} \int_{x_{vs}}^{\bar{x}_{fw}} w(x)\bar{v}_{fw}(t - \tau_x)\,dx$$

$$+ \frac{\rho}{2}\ell^3\left(u^2 + v_t^2 + w_t^2\right)$$

$$\left[K_{4s}\beta_s^2 \sin\left(4(\phi_s - 37.5°)\right) + \beta_s^2 K_{8s} \sin\left(8(\phi_s - 37.5°)\right)\right]$$

$$v_s = v + x_s r$$

$$w_s = w - x_s q$$

$$\phi_s = \tan^{-1}\left(-\frac{w_s}{v_s}\right)$$

$$\beta_s = \tan^{-1}\frac{\left(v_s^2 + w_s^2\right)^{\frac{1}{2}}}{u}$$

Pitching Moment Equation

$$mz_G\dot{u} - mx_G\dot{w} =$$

$$mz_G vr - mz_G wq - mx_G uq + mx_G vp - I_{yy}\dot{q} - (I_{xx} - I_{zz})rp + I_{xy}(\dot{p} + qr)$$

$$- I_{xz}(p^2 - r^2) - I_{yz}(qp - \dot{r})$$

$$+ \frac{\rho}{2}\ell^5\left[M_q'\dot{q} + \left(M'_{p|p|}p^2 + M'_{r|r|}r^2\right)\frac{u}{\sqrt{u^2 + v^2 + w^2}} + M'_{rp}rp + M'_{q|q|}q|q|\right]$$

$$+ \frac{\rho}{2}\ell^4\left[M_w'\dot{w} + M'_{vr}\frac{vru}{\sqrt{u^2 + v^2 + w^2}} + M_{vp}\frac{vpu}{\sqrt{u^2 + v^2 + w^2}} + M'_{q}uq\right.$$

$$+ M'_{|q|\delta\delta}u|q|(D1^2 - 0.6088D2^2 - 0.6088D3^2)$$

$$+ M'_{|q|\delta}u|q|(0.7934D2 + 0.7934D3) + M'_{|w|q}q(v^2 + w^2)^{\frac{1}{2}}$$

$$\left.+ M'_{q\eta}uq(\eta - 1)\right]$$

$$+ \frac{\rho}{2}\ell^3\left[M'_*u^2 + M'_wuw + M'_{w|w|}w(v^2 + w^2)^{\frac{1}{2}} + M'_{|w|}u|w|\right.$$

$$+ M'_{v|v|}\frac{v^2u}{\sqrt{u^2 + v^2 + w^2}} + M'_{\delta\delta}u^2(D1^2 - 0.6088D2^2 - 0.6088D3^2)$$

$$\left.+ M'_\delta u^2(0.7934D2 + 0.7934D3) + M'_{\delta b}u^2\delta_b + M'_{ww}|w|\sqrt{v^2 + w^2}\right]$$

$$+ \frac{\rho}{2}\ell^3(\eta - 1)\left[M'_{w\eta}uw + M'_{w|w|\eta}w(v^2 + w^2)^{\frac{1}{2}}\right.$$

$$+ M'_{\delta\delta\eta}u^2(D1^2 - 0.6088D2^2 - 0.6088D3^2)$$

$$\left.+ M'_{\delta\eta}u^2(0.7934D2 + 0.7934D3)\right]$$

$$- (x_G w - x_B B) \cos\theta \cos\phi - (z_G w - z_B B) \sin\theta$$

$$+ \frac{\rho}{2} C_d \int_{\ell} C_d x D(x) w(x) \left\{ [w(x)]^2 + [v(x)]^2 \right\}^{\frac{1}{2}} dx$$

$$- \frac{\rho}{2} \ell C_v \int_{x_{vs}}^{\bar{x}_{fw}} x v(x) \bar{v}_{fw}(t - \tau_x) \, dx$$

Yawing Moment Equation

$$
\begin{aligned}
mx_G\dot{v} - my_G\dot{u} = \;& mx_G wp - mx_G ur - my_G vr + my_G wq - I_{zz}\dot{r} - (I_{yy} - I_{xx})pq + I_{yz}(\dot{q} + rp) \\
& - I_{xy}(q^2 - p^2) - I_{xq}(rq - \dot{p}) \\
& + \frac{\rho}{2}\ell^5\left[N'_{\dot{r}}\dot{r} + N'_{\dot{p}}\dot{p} + N'_{pq}pq + N'_{qr}qr + N'_{r|r|}r|r|\right] \\
& + \frac{\rho}{2}\ell^4\Big[N'_{\dot{v}}\dot{v} + N'_{wr}wr + N'_{wp}wp + N'_{vq}vq + N'_{p}up + N'_{r}ur \\
& \qquad + N'_{|r|\delta\delta}u|r|(0.7934D2^2 - 0.7934D3^2) \\
& \qquad + N'_{|r|\delta}u|r|(D1 - 0.6088D2 + 0.6088D3) + N'_{|v|r}r(v^2 + w^2)^{\frac{1}{2}} \\
& \qquad + N'_{r\eta}ur(\eta - 1)\Big] \\
& + \frac{\rho}{2}\ell^3\Bigg[N'_{*}u^2 + N'_{v}uv + N'_{v|v|}v(v^2 + w^2)^{\frac{1}{2}} + N'_{vw}\frac{vwu}{\sqrt{u^2 + v^2 + w^2}} \\
& \qquad + N'_{\delta\delta}u^2(0.7934D2^2 - 0.7934D3^2) \\
& \qquad + N'_{\delta}u^2(D1 - 0.6088D2 + 0.6088D3)\Bigg] \\
& + \frac{\rho}{2}\ell^3(\eta - 1)\Big[N'_{v\eta}uv + N'_{v|v|\eta}v(v^2 + w^2)^{\frac{1}{2}} \\
& \qquad + N'_{\delta\delta\eta}u^2(0.7934D2^2 - 0.7934D3^2) \\
& \qquad + N'_{\delta\eta}u^2(D1 - 0.6088D2 + 0.6088D3)\Big] \\
& + (x_G w - x_B B)\cos\theta\sin\phi + (y_G w - y_B B)\sin\theta
\end{aligned}
$$

$$- \frac{\rho}{2} C_d \int_{\ell} xH(x)v(x)\left\{[v(x)]^2 + [w(x)]^2\right\}^{\frac{1}{2}} dx$$

$$- \frac{\rho}{2} \ell C_v \int_{x_{vs}}^{\bar{x}_{fw}} xw(x)\bar{v}_{fw}(t - \tau_x) dx$$

Auxiliary Equations

$$U^2 = u^2 + v^2 + w^2$$

$$\dot{z}_D = -u \sin\theta + v \cos\theta \sin\phi + w \cos\theta \cos\phi$$

$$\dot{\phi} = p + \dot{\psi} \sin\theta$$

$$\dot{\theta} = \frac{q - \dot{\psi} \cos\theta \sin\phi}{\cos\phi}$$

$$\dot{\psi} = \frac{r + \dot{\theta} \sin\phi}{\cos\theta \cos\phi}$$

APPENDIX C

LINEARIZED EQUATIONS OF MOTION

Axial Force

$$[m - x_{\dot{u}}]\Delta\dot{u} - my_G\Delta\dot{r} + mz_G\Delta\dot{q} =$$

$$\Delta u\left[2u_o\left\{x_{uu} + a_i + b_i\eta + c_i\eta^2\right\} + 2u_o x_{\delta\delta}\left(D_{10}^2 + D_{20}^2 + D_{30}^2\right)\right.$$

$$\left. + 2u_o X_{\delta b\delta b}\delta_{bo}^2 + 2u_o(\eta_o - 1)X_{\delta\delta\eta}\left(D_{10}^2 + D_{20}^2 + D_{30}^2\right)\right]$$

$$+ \Delta v[mr_o + X_{vr}r_o + 2V_oX_{vv} + 2V_o(\eta_o - 1)X_{vv\eta}]$$

$$+ \Delta w[-mq_o + X_{wq}q_o + 2w_oX_{ww} + 2w_oX_{ww\eta}(\eta_o - 1)]$$

$$+ \Delta p[-my_Gq_o - mz_Gr_o + X_{rp}r_o]$$

$$+ \Delta q[-mw_o + 2q_omx_G - my_Gp_o + 2q_ox_{qq} + X_{wq}w_o]$$

$$+ \Delta r[mv_o + 2mx_Gr_o - mz_Gp_o + 2r_oX_{rr} + X_{rp}p_o + x_{vr}v_o]$$

$$- \Delta\theta[(W - B)\cos\theta_o]$$

$$+ \Delta\delta_b\left[2\delta_{bo}X_{\delta b\delta b}u_o^2\right]$$

$$+ \Delta D_1\left[2D_{10}\left\{\left(X_{\delta\delta}u_o^2 + X_{\delta\delta\eta}u_o^2(\eta_o - 1)\right)\right\}\right]$$

$$+ \Delta D_2\left[2D_{20}\left\{\left(X_{\delta\delta}u_o^2 + X_{\delta\delta\eta}u_o^2(\eta_o - 1)\right)\right\}\right]$$

$$+ \Delta D_3\left[2D_{30}\left\{\left(X_{\delta\delta}u_o^2\right) + X_{\delta\delta\eta}u_o^2(\eta_o - 1)\right\}\right]$$

$$+ \Delta\eta\left[X_{\delta\delta\eta}u_o^2\left(D_{10}^2 + D_{20}^2 + D_{30}^2\right) + X_{vv\eta}v_o^2 + X_{ww\eta}w_o^2 + u_o^2(b_i + 2c_i\eta_o)\right]$$

Lateral Force

$$[m - Y_{\dot{v}}]\Delta\dot{v} - [mz_G + Y_{\dot{p}}]\Delta\dot{p} + [mx_G - Y_{\dot{r}}]\Delta\dot{r} =$$

$$\Delta u\Bigg[-mr_o + Y_r r_o + Y_o p_o + Y'_{|r|\delta}|r_o|(D_{10} - 0.6088D_{20} + 0.6088D_{30})$$

$$+ Y_{r\eta} r_o(\eta_o - 1) + Y_v u_o + 2u_o\Big\{Y_* + Y_\delta(D_{10} - 0.6088D_{20} + 0.6088D_{30})$$

$$+ Y_{\delta\eta}(D_{10} - 0.6088D_{20} + 0.6088D_{30})(\eta_o - 1)\Big\} + Y_{v\eta} v_o(\eta_o - 1)$$

$$+ Y_{vw}\frac{v_o w_o\left(v_o^2 + w_o^2\right)}{\left(u_o^2 + v_o^2 + w_o^2\right)^{\frac{3}{2}}}\Bigg]$$

$$+ \Delta v\Bigg[Y_{vq} q_o + Y_{v|v|}\left\{\left(v_o^2 + w_o^2\right)^{-\frac{1}{2}}\frac{v_o^2}{|v_o|}|r_o|\right\} + Y_v u_o$$

$$+ Y_{v|v|}\frac{2u_o^2 + w_o^2}{\sqrt{u_o^2 + w_o^2}} + \frac{Y_{vw} u_o w_o\left(u_o^2 + w_o^2\right)}{\left(u_o^2 + v_o^2 + w_o^2\right)^{\frac{3}{2}}} + Y_{v\eta} u_o(\eta_o - 1)$$

$$+ Y_{v|v|\eta}(\eta_o - 1)\frac{2u_o^2 + w_o^2}{\sqrt{v_o^2 + w_o^2}} + \frac{\partial Y_{CRFW}}{\partial v}\Bigg]$$

$$+ \Delta w\Bigg[mp_o + Y_{wp} p_o + Y_{wr} r_o + Y_{v|r|}\frac{v_o}{|v_o|}\left(v_o^2 + w_o^2\right)^{-\frac{1}{2}} w_o|r_o|$$

$$+ Y_{v|v|} v_o\left(v_o^2 + w_o^2\right)^{-\frac{1}{2}} w_o + Y_{vw}\frac{u_o v_o\left(u_o^2 + v_o^2\right)}{\left(u_o^2 + v_o^2 + w_o^2\right)^{\frac{3}{2}}}$$

$$+ Y_{v|v|\eta}(\eta_o - 1) v_o\left(v_o^2 + w_o^2\right)^{-\frac{1}{2}} w_o + \frac{\partial Y_{CRFW}}{\partial w}\Bigg]$$

$$+ \Delta p[mw_o + 2p_o my_G - mx_G q_o + 2|p_o|Y_{p|p|} + Y_{pq}q_o + Y_{wp}w_o + Y_p u_o]$$

$$+ \Delta q\left[-mz_G r_o - mx_G p_o + Y_{pq}p_o + Y_{qr}r_o + Y_{vq}v_o + \frac{\partial Y_{CRFW}}{\partial q}\right]$$

$$+ \Delta r\Bigg[-mu_o - mz_G q_o + Y_{qr}q_o + Y_{wr}w_o + Y_r u_o$$

$$+ Y_{|r|\delta}u_o(D_{10} - 0.6088D_{20} + 0.6088D_{30})\frac{|r_o|}{r_o}$$

$$+ Y_{v|r|}\frac{|r_o|}{|v_o|}\left(v_o^2 + w_o^2\right)^{\frac{1}{2}}\frac{v_o}{r_o} + Y_{r\eta}u_o(\eta_o - 1) + \frac{\partial Y_{CRFW}}{\partial r}\Bigg]$$

$$+ \Delta\phi[(W - B)\cos\phi_o \cos\theta_o]$$

$$- \Delta\theta[(W - B)\sin\phi_o \sin\theta_o]$$

$$+ \Delta D_1\left[Y_{|r|\delta}u_o|r_o| + Y_\delta u_o^2 + Y_{\delta\eta}u_o^2(\eta_o - 1)\right]$$

$$+ \Delta D_2\left[-0.6088Y_{|r|\delta}u_o|r_o| - 0.6088Y_\delta u_o^2 - Y_{\delta\eta}u_o^2(\eta_o - 1)0.6088\right]$$

$$+ \Delta D_3\left[0.6088Y_{|r|\delta}u_o|r_o| + 0.6088Y_\delta u_o^2 + 0.6088Y_{\delta\eta}u_o^2(\eta_o - 1)\right]$$

$$+ \Delta\eta\Bigg[Y_{r\eta}u_o r_o + Y_{v\eta}u_o v_o + Y_{v|v|\eta}v_o\left(v_o^2 + w_o^2\right)^{\frac{1}{2}}$$

$$+ Y_{\delta\eta}u_o^2(D_{10} - 0.6088D_{20} + 0.6088D_{30})\Bigg]$$

where

$$\frac{\partial Y_{CRFW}}{\partial v} = \frac{\rho}{2}\left(-\ell^2\frac{Zww}{\int_\ell D(x)\,dx}\right)\int_\ell H(x)\frac{\left(w_o^2(x) + 2v_o^2(x)\right)}{\sqrt{v_o^2(x) + w_o^2(x)}}\,dx$$

$$\frac{\partial Y_{CRFW}}{\partial w} = \frac{\rho}{2}\left(-\ell^2 \frac{Zww}{\int_{\ell} D(x)\,dx}\right)\int_{\ell} H(x)\,\frac{v_o(x)w_o(x)}{\sqrt{v_o^2(x) + w_o^2(x)}}\,dx$$

$$\frac{\partial Y_{CRFW}}{\partial q} = \frac{\rho}{2}\left(\ell^2 \frac{Zww}{\int_{\ell} D(x)\,dx}\right)\int_{\ell} x\,\frac{H(x)v_o(x)w_o(x)}{\sqrt{v_o^2(x) + w_o^2(x)}}\,dx$$

$$\frac{\partial Y_{CRFW}}{\partial r} = \frac{\rho}{2}\left(-\ell^2 \frac{Zww}{\int_{\ell} D(x)\,dx}\right)\int_{\ell} x\,H(x)\,\frac{\left(2v_o^2(x) + w_o^2(x)\right)}{\sqrt{v_o^2(x) + w_o^2(x)}}$$

Normal Force

$$[m - Z_{\dot{w}}]\Delta\dot{w} - [mx_G + Z_{\dot{q}}]\Delta\dot{q} + my_G\Delta\dot{p} =$$

$$\Delta u\Bigg[mq_o + Z_q q_{qo} + Z_{|q|\delta}|q_o|(-0.7934D_{20} - 0.7934D_{30}) + Z_{q\eta}q_o(\eta_o - 1)$$

$$+ 2u_o Z_* + Z_w w_o + Z_{|w|}|w_o| + 2u_o Z_\delta(-0.7934D_{20} - 0.7934D_{30})$$

$$+ 2u_o Z_{\delta b}\delta b_o + Z_{w\eta}w_o(\eta_o - 1) + 2u_o Z_{\delta\eta}(-0.7934D_{20} - 0.7934D_{30})$$

$$+ \left(Z_{p|p|}p_o^2 + Z_{r|r|}r_o^2 + Z_{rp}r_o p_o + Z_{vr}v_o r_o + Z_{v|v|}v_o^2\right)$$

$$\frac{v_o^2 + w_o^2}{\left(u_o^2 + v_o^2 + w_o^2\right)^{\frac{3}{2}}}\Bigg]$$

$$+ \Delta v\Bigg[-mp_o + Z_{vr}\frac{r_o u_o}{\left(u_o^2 + v_o^2 + w_o^2\right)^{\frac{3}{2}}} + Z_{vp}p_o$$

$$+ Z_{w|q|}\frac{w_o}{|w_o|}\left(v_o^2 + w_o^2\right)^{-\frac{1}{2}}v_o|q_o| + Z_{w|w|}w_o v_o\left(v_o^2 + w_o^2\right)^{-\frac{1}{2}}$$

$$+ \left(Z_{p|p|}p_o^2 + Z_{r|r|}r_o^2 + Z_{rp}p_o r_o\right)\frac{u_o v_o}{\left(u_o^2 + v_o^2 + w_o^2\right)^{\frac{3}{2}}}$$

$$+ Z_{v|v|}\frac{\left(2v_o u_o\left(u_o^2 + w_o^2\right) + v_o^2 u_o\right)}{\left(u_o^2 + v_o^2 + w_o^2\right)}$$

$$+ Z_{w|w|\eta}q_o v_o(\eta_o - 1)\left(v_o^2 + w_o^2\right)^{-\frac{1}{2}}$$

$$+ Z_{ww}\frac{|w_o|v_o}{\sqrt{v_o^2 + w_o^2}} + \frac{\partial Z_{CRFW}}{\partial v}\Bigg]$$

$$+ \Delta w \Bigg[Z_{w|q|} |q_o w_o| \left(v_o^2 + w_o^2\right)^{-\frac{1}{2}} + Z_w u_o + Z_{w|w|} \frac{v_o^2 + 2w_o^2}{\sqrt{v_o^2 + w_o^2}}$$

$$- \left(Z_{p|p|} p_o^2 + Z_{r|r|} r_o^2 + Z_{rp} r_o p_o + Z_{v|v|} v_o^2 + Z_{vr} v_o r_o\right)$$

$$\frac{u_o w_o}{\left(u_o^2 + v_o^2 + w_o^2\right)^{\frac{3}{2}}} + Z_{|w|} \frac{u_o w_o}{|w_o|} + Z_{w\eta} u_o (\eta_o - 1) + Z_{w|w|\eta} \frac{v_o^2 + 2w_o^2}{\sqrt{v_o^2 + w_o^2}}$$

$$+ Z_{ww} \frac{w_o}{|w_o|} \frac{v_o^2 + 2w_o^2}{\sqrt{v_o^2 + w_o^2}} + \frac{\partial Z_{CRFW}}{\partial w} \Bigg]$$

$$+ \Delta p \Bigg[-m v_o + 2 p_o m z_G - m x_G r_o + \left(2 p_o Z_{p|p|} + Z_{rp} r_o\right) \frac{u_o}{\sqrt{u_o^2 + v_o^2 + w_o^2}}$$

$$+ Z_{vp} v_o \Bigg]$$

$$+ \Delta q \Bigg[m u_o + 2 q_o m z_G - m y_G r_o + Z_q u_o$$

$$+ Z_{|q|\delta} u_o \frac{|q_o|}{q_o} (-0.7934 D_{20} - 0.7934 D_{30})$$

$$+ Z_{w|q|} \frac{|q_o|}{|w_o|} \frac{w_o}{q_o} \sqrt{v_o^2 + w_o^2} + Z_{q\eta} u_o (\eta_o - 1)$$

$$+ Z_{w|w|\eta} (\eta_o - 1) \sqrt{v_o^2 + w_o^2} + \frac{\partial Z_{CRFW}}{\partial q} \Bigg]$$

$$+ \Delta r \Bigg[-m x_G p_o - m y_G q_o + \left(2 r_o Z_{r|r|} + Z_{rp} p_o + Z_{vr} v_o\right) \frac{u_o}{\sqrt{u_o^2 + v_o^2 + w_o^2}}$$

$$+ \frac{\partial Z_{CRFW}}{\partial r} \Bigg]$$

$$- \Delta\phi[(W - B) \cos \theta_o \sin \phi_o]$$

$$- \Delta\theta[(W - B) \sin \theta_o \cos \phi_o]$$

$$+ \Delta\delta b\left[Z_{\delta b} u_o^2\right]$$

$$+ \Delta D_2\left[0.7934\left(Z_{|q|\delta} u_o |q_o| + Z_\delta u_o^2 + Z_{\delta\eta} u_o^2(\eta_o - 1)\right)\right]$$

$$+ D_3\left[0.7934\left(Z_{|q|\delta} u_o |q_o| + Z_\delta u_o^2 + Z_{\delta\eta} u_o^2(\eta_o - 1)\right)\right]$$

$$+ \Delta\eta\left[z_{q\eta} u_o q_o + Z_{w\eta} u_o w_o + Z_{w|w|\eta} w_o \left(v_o^2 + w_o^2\right)^{\frac{1}{2}}\right.$$

$$\left. + Z_{\delta\eta} u_o^2(-0.7934 D_{20} - 0.7934 D_{30})\right]$$

where

$$\frac{\partial Z_{CRFW}}{\partial v} = \frac{\rho}{2}\left(-\ell^2 \frac{Z_{ww}}{\int_\ell D(x)\, dx}\right) \int_\ell D(x) \frac{w_o(x) v_o(x)}{\sqrt{v_o^2(x) + w_o^2(x)}}\, dx$$

$$\frac{\partial Z_{CRFW}}{\partial w} = \frac{\rho}{2}\left(-\ell^2 \frac{Z_{ww}}{\int_\ell D(x)\, dx}\right) \int_\ell D(x) \frac{\left(v_o^2(x) + 2w_o^2(x)\right)}{\sqrt{v_o^2(x) + w_o^2(x)}}\, dx$$

$$\frac{\partial Z_{CRFW}}{\partial q} = \frac{\rho}{2}\left(-\ell^2 \frac{Z_{ww}}{\int_\ell D(x)\, dx}\right) \int_\ell x\, D(x) \frac{\left(v_o^2(x) + 2w_o^2(x)\right)}{\sqrt{v_o^2(x) + w_o^2(x)}}\, dx$$

$$\frac{\partial Z_{CRFW}}{\partial r} = \frac{\rho}{2}\left(-\ell^2 \frac{Z_{ww}}{\int_\ell D(x)\, dx}\right) \int_\ell x \frac{D(x) w_o(x) v_o(x)}{\sqrt{v_o^2(x) + w_o^2(x)}}\, dx$$

Rolling Moment

$$-[mz_G + K_v^{\cdot}]\Delta\dot{v} + my_G\Delta\dot{w} + [I_{xx} - K_p^{\cdot}]\Delta\dot{p} - I_{xy}\Delta\dot{q} - [I_{xz} + K_r^{\cdot}]\Delta\dot{r} =$$

$$\Delta u\Big[my_G q_o + mz_G r_o + K_p p_o + K_r r_o + 2u_o K_* + K_v v_o$$

$$+ 2u_o K_\delta (D_{10} - D_{20} + D_{30}) + 2u_o K_{*\eta}(\eta_o - 1)$$

$$+ 2u_o \beta_{so}^2 (K_{4s} \sin 4(\phi_{so} - 37.5°) + K_{8s} \sin 8(\phi_{so} - 37.5°))$$

$$- 2\beta_{so}\sqrt{v_{so}^2 + w_{so}^2}\,(K_{4s} \sin 4(\phi_{so} - 37.5°)$$

$$+ K_{8s} \sin 8(\phi_{so} - 37.5°))\Big]$$

$$+ \Delta v\Bigg[-my_G p_o + K_{vq} q_o + K_v u_o + K_{v|v|} \frac{w_o^2 + 2v_o^2}{\sqrt{v_o^2 + w_o^2}} + K_{vw} w_o$$

$$+ 2v_{so}\beta_{so}^2 (K_{4s} \sin 4(\phi_{so} - 37.5°) + K_{8s} \sin 8(\phi_{so} - 37.5°))$$

$$+ \frac{2u_o \beta_{so} v_{so}}{\sqrt{v_{so}^2 + w_o^2}} (K_{4s} \sin 4(\phi_{so} - 37.5°) + K_{8s} \sin 8(\phi_{so} - 37.5°))$$

$$+ \left(\frac{u_o^2 + v_{so}^2 + w_{so}^2}{w_{so}^2 + v_{so}^2}\right) \beta_{so}^2 w_{so} (4K_{4s} \cos 4(\phi_{so} - 37.5°)$$

$$+ 8K_{8s} \cos 8(\phi_{so} - 37.5°))\Bigg]$$

$$+ \Delta w\Bigg[-mz_G p_o + K_{wp} p_o + K_{wr} r_o + K_{v|v|} \frac{v_o w_o}{\sqrt{v_o^2 + w_o^2}} + K_{vw} v_o$$

$$+ 2w_{so}\beta_{so} (K_{4s} \sin 4(\phi_{so} - 37.5°) + K_{8s} \sin 8(\phi_{so} - 37.5°))$$

$$+\frac{2u_o\beta_{so}w_{so}}{\sqrt{v_{so}^2+w_{so}^2}}(K_{4s}\sin 4(\phi_{so}-37.5°)+K_{8s}\sin 8(\phi_{so}-37.5°))$$

$$-\frac{\left(u_o^2+v_{so}^2+w_{so}^2\right)}{\left(w_{so}^2+v_{so}^2\right)}\beta_{so}^2v_{so}(4K_{4s}\cos 4(\phi_{so}-37.5°)$$

$$+8K_{8s}\cos 8(\phi_{so}-37.5°))\Bigg]$$

$$+\Delta p[I_{yz}q_o-I_{xy}r_o-my_Gv_o-mz_Gw_o+K_{pq}q_o+2|p_o|K_{p|p|}+K_pu_o$$

$$+K_{wp}w_o]$$

$$+\Delta q\Bigg[-(I_{zz}-I_{yy})r_o+I_{yz}p_o-2q_oI_{yz}+my_Gu_o+K_{qr}r_o+K_{pq}p_o$$

$$+K_{vq}v_o+\left(\frac{-2u_o\beta_{so}x_{so}w_{so}}{\sqrt{v_{so}^2+w_{so}^2}}-2w_{so}\beta_{so}^2x_{so}\right)$$

$$(K_{4s}\sin 4(\phi_{so}-37.5°)+K_{8s}\sin 8(\phi_{so}-37.5°))$$

$$+\frac{\left(u_o^2+v_{so}^2+w_{so}^2\right)x_{so}v_{so}\beta_{so}^2}{v_{so}^2+w_{so}^2}(4K_{4s}\cos 4(\phi_{so}-37.5°)$$

$$+8K_{8s}\cos 8(\phi_{so}-37.5°))\Bigg]$$

$$+\Delta r\Bigg[-(I_{zz}-I_{yy})q_o-2r_oI_{yz}-I_{xy}p_o+mz_Gu_o+K_{qr}q_o+K_ru_o$$

$$+K_{wr}w_o+\frac{2\beta_{so}u_ox_{so}v_{so}}{\sqrt{v_{so}^2+w_{so}^2}}(K_{4s}\sin 4(\phi_{so}-37.5°)$$

$$+K_{8s}\sin 8(\phi_{so}-37.5°))+2\beta_{so}^2v_{so}x_{so}(K_{4s}\sin 4(\phi_{so}-37.5°)$$

$$+K_{8s}\sin 8(\phi_{so}-37.5°))+\frac{w_{so}x_{so}\beta_{so}^2\left(u_o^2+v_{so}^2+w_{so}^2\right)}{w_{so}^2+v_{so}^2}$$

$$(4K_{4s} \cos 4(\phi_{so} - 37.5°) + 8K_{8s} \cos 8(\phi_{so} - 37.5°))\Big]$$

$$+ \Delta\phi[-(y_G w - y_B B) \cos \theta_o \sin \phi_o - (z_G w - z_B B) \cos \theta_o \cos \phi_o]$$

$$+ \Delta\theta[-(y_G w - y_B B) \sin \theta_o \cos \phi_o + (z_G w - z_B B) \sin \theta_o \sin \phi_o]$$

$$+ \Delta D_1\left[K_\delta u_o^2\right]$$

$$+ \Delta D_2\left[-K_\delta u_o^2\right]$$

$$+ \Delta D_3\left[K_\delta u_o^2\right]$$

$$+ \Delta\eta\left[K_{*\eta} u_o^2\right]$$

Pitching Moment

$$mz_G\Delta\dot{u} - [mx_G + M_{\dot{w}}]\Delta\dot{w} - I_{xy}\Delta\dot{p} + [I_{yy} - M_{\dot{q}}]\Delta\dot{q} - I_{yz}\Delta\dot{r} =$$

$$+ \Delta u\Bigg[-mx_G q_o + M_q q_o + M_{|q|\delta\delta}|q_o|\left(D_{10}^2 - 0.6088D_{20}^2 - 0.6088D_{30}^2\right)$$

$$+ M_{|q|\delta}|q_o|(0.7934D_{20} + 0.7934D_{30}) + M_{q\eta}q_o(\eta_o - 1) + 2u_oM_*$$

$$+ M_w w_o + M_{|w|}|w_o| + 2u_oM_{\delta\delta}\left(D_{10}^2 - 0.6088D_{20}^2 - 0.6088D_{30}^2\right)$$

$$+ 2u_oM_\delta(0.7934D_{20} + 0.7934D_{30}) + 2u_oM_{\delta b}\delta b_o + M_{w\eta}w_o(\eta_o - 1)$$

$$+ 2u_oM_{\delta\delta\eta}\left(D_{10}^2 - 0.6088D_{20}^2 - 0.6088D_{30}^2\right)$$

$$+ 2u_oM_{\delta\eta}(0.7934D_{20} + 0.7934D_{30}) + \left(M_{p|p|}p_o^2 + M_{r|r|}r_o^2\right.$$

$$\left. + M_{vr}v_o r_o + M_{v|v|}v_o^2\right)\frac{v_o^2 + w_o^2}{\left(u_o^2 + v_o^2 + w_o^2\right)^{\frac{3}{2}}}\Bigg]$$

$$+ \Delta v\Bigg[mz_G r_o + mx_G p_o + M_{|w|q}\frac{q_o v_o}{\sqrt{v_o^2 + w_o^2}} + M_{w|w|}\frac{v_o w_o}{\sqrt{v_o^2 + w_o^2}}$$

$$- \left(M_{p|p|}p_o^2 + M_{r|r|}r_o^2\right)\frac{u_o v_o}{\left(u_o^2 + v_o^2 + w_o^2\right)^{\frac{3}{2}}} + (M_{vr}r_o + M_{vp}p_o)$$

$$\frac{u_o\left(u_o^2 + w_o^2\right)}{\left(u_o^2 + v_o^2 + w_o^2\right)^{\frac{3}{2}}} + M_{v|v|}\frac{v_o\left(2\left(u_o^2 + w_o^2\right) + v_o^2\right)}{\left(u_o^2 + v_o^2 + w_o^2\right)^{\frac{3}{2}}}$$

$$+ M_{w|w|\eta}\frac{(\eta_o - 1)v_o w_o}{\sqrt{v_o^2 + w_o^2}} + M_{ww}\frac{|w_o|v_o}{\sqrt{v_o^2 + w_o^2}}\quad\frac{\partial M_{CRFW}}{\partial v}\Bigg]$$

$$+ \Delta w \Bigg[-mz_G q_o + M_{|w|q} \frac{q_o w_o}{\sqrt{v_o^2 + w_o^2}} + M_w u_o + M_{w|w|} \frac{v_o^2 + 2w_o^2}{\sqrt{v_o^2 + w_o^2}}$$

$$- \left(M_{p|p|} p_o^2 + M_{r|r|} r_o^2 + M_{v|v|} v_o^2 + M_{vp} v_o p_o + M_{vr} v_o r_o \right)$$

$$\frac{u_o w_o}{\left(u_o^2 + v_o^2 + w_o^2 \right)^{\frac{3}{2}}} + M_{|w|} u_o \frac{w_o}{|w_o|} + M_{w\eta} u_o (\eta_o - 1)$$

$$+ M_{w|w|\eta} (\eta_o - 1) \frac{v_o^2 + 2w_o^2}{\sqrt{v_o^2 + w_o^2}} + M_{ww} \frac{w_o}{|w_o|} \frac{v_o^2 + 2w_o^2}{\sqrt{v_o^2 + w_o^2}} + \frac{\partial M_{CRFW}}{\partial w} \Bigg]$$

$$+ \Delta p \Bigg[mx_G v_o - (I_{xx} - I_{zz}) r_o - 2P_o I_{xz} - I_{yz} q_o + 2M_{p|p|} \frac{p_o u_o}{\sqrt{u_o^2 + v_o^2 + w_o^2}}$$

$$+ M_{rp} r_o + M_{vp} \frac{u_o}{\sqrt{u_o^2 + v_o^2 + w_o^2}} \Bigg]$$

$$+ \Delta q \Bigg[-mz_G w_o - mx_G u_o + I_{xy} r_o - I_{yz} p_o + 2M_{q|q|} |q_o| + M_q u_o$$

$$+ M_{|q|\delta\delta} \frac{u_o q_o}{|q_o|} \left(D_{10}^2 - 0.6088 D_{20}^2 - 0.6088 D_{30}^2 \right)$$

$$+ M_{|q|\delta} \frac{u_o q_o}{|q_o|} (0.7934 D_{20} + 0.7934 D_{30}) + M_{|w|q} \sqrt{v_o^2 + w_o^2}$$

$$+ M_{q\eta} u_o (\eta_o - 1) + \frac{\partial M_{CRFW}}{\partial q} \Bigg]$$

$$+ \Delta r \Bigg[mz_G v_o + I_{xy} q_o + 2I_{xz} r_o + 2M_{r|r|} \frac{r_o u_o}{\sqrt{u_o^2 + v_o^2 + w_o^2}} + M_{rp} p_o$$

$$+ M_{vr} \frac{u_o v_o}{\sqrt{u_o^2 + v_o^2 + w_o^2}} - (I_{xx} - I_{zz})P_o + \frac{\partial M_{CRFW}}{\partial r}\Bigg]$$

$$+ \Delta\phi[(x_G w - x_B B) \cos\theta_o \sin\theta_o]$$

$$+ \Delta\theta[(x_G w - x_B B) \sin\theta_o \cos\phi_o - (z_G w - z_B B) \cos\theta_o]$$

$$+ \Delta\delta b\left[M_{\delta b} u_o^2\right]$$

$$+ \Delta D_1\left[2M_{|q|\delta\delta} u_o |q_o| D_{10} + 2M_{\delta\delta} u_o^2 D_{10} + 2M_{\delta\delta\eta} u_o^2 D_{10}(\eta_o - 1)\right]$$

$$+ \Delta D_2\Big[-1.2176M_{|q|\delta\delta} u_o |q_o| D_{20} + 0.7934M_{|q|\delta} u_o |q_o| - 1.2176M_{\delta\delta} u_o^2 D_{20}$$
$$+ 0.7934M_{\delta} u_o^2 - 1.2176M_{\delta\delta\eta}(\eta_o - 1) u_o^2 D_{20}$$
$$+ 0.7934M_{\delta\eta} u_o^2 (\eta_o - 1)\Big]$$

$$+ \Delta D_3\Big[-1.2176M_{|q|\delta\delta} u_o |q_o| D_{30} + 0.7934M_{|q|\delta} u_o |q_o| - 1.2176M_{\delta\delta} u_o^2 D_{30}$$
$$+ 0.7934M_{\delta} u_o^2 - 1.2176M_{\delta\delta\eta}(\eta_o - 1) u_o^2 D_{30}$$
$$+ 0.7934M_{\delta\eta} u_o^2 (\eta_o - 1)\Big]$$

$$+ \Delta\eta\Big[M_{q\eta} u_o q_o + M_{w\eta} u_o w_o + M_{w|w|\eta} w_o \sqrt{v_o^2 + w_o^2}$$
$$+ M_{\delta\delta\eta} u_o^2 \left(D_{10}^2 - 0.6088 D_{20}^2 - 0.6088 D_{30}^2\right)$$
$$+ M_{\delta\eta} u_o^2 (0.7934 D_{20} + 0.7934 D_{30})\Big]$$

where:

$$\frac{\partial M_{CRFW}}{\partial v} = \frac{\rho}{2}\left(\ell^2 \frac{Z_{ww}}{\int_{\ell} D(x)\,dx}\right)\int_{\ell} \frac{D(x)w_o(x)v_o(x)}{\sqrt{v_o^2(x) + w_o^2(x)}}\,dx$$

$$\frac{\partial M_{CRFW}}{\partial w} = \frac{\rho}{2}\left(\ell^2 \frac{Z_{ww}}{\int_{\ell} D(x)\,dx}\right)\int_{\ell} x\,D(x)\,\frac{\left(v_o^2(x) + 2w_o^2(x)\right)}{\sqrt{v_o^2(x) + w_o^2(x)}}\,dx$$

$$\frac{\partial M_{CRFW}}{\partial q} = \frac{\rho}{2}\left(-\ell^2 \frac{Z_{ww}}{\int_{\ell} D(x)\,dx}\right)\int_{\ell} x^2\,D(x)\,\frac{\left(v_o^2(x) + 2w_o^2(x)\right)}{\sqrt{v_o^2(x) + w_o^2(x)}}\,dx$$

$$\frac{\partial M_{CRFW}}{\partial r} = \frac{\rho}{2}\left(\ell^2 \frac{Z_{ww}}{\int_{\ell} D(x)\,dx}\right)\int_{\ell} x^2\,D(x)\,\frac{w_o(x)v_o(x)}{\sqrt{v_o^2(x) + w_o^2(x)}}\,dx$$

Yawing Moment

$$-my_G\dot{\Delta u} + [mx_G - N_{\dot{v}}]\dot{\Delta v} - [I_{xz} + N_{\dot{p}}]\dot{\Delta p} - I_{yz}\dot{\Delta q} + [I_{zz} - N_{\dot{r}}]\dot{\Delta r} =$$

$$\Delta u\Bigg[-mx_G r_o + N_p p_o + N_r r_o + N_{|r|\delta\delta}\left(0.7934D_{20}^2 - 0.7934D_{30}^2\right)$$

$$+ N_{vw}\frac{v_o w_o\left(v_o^2 + w_o^2\right)}{\left(u_o^2 + v_o^2 + w_o^2\right)^{\frac{3}{2}}} + N_{|r|\delta|r_o|}(D_{10} - 0.6088D_{20} + 0.6088D_{30})$$

$$+ N_{rq} r_o(\eta_o - 1) + 2u_o N_* + N_v v_o + 2u_o N_{\delta\delta}\left(0.7934D_{20}^2 - 0.7934D_{30}^2\right)$$

$$+ 2u_o N_\delta(D_{10} - 0.6088D_{20} + 0.6088D_{30}) + N_{v\eta} v_o(\eta_o - 1)$$

$$+ 2u_o N_{\delta\delta\eta}(\eta_o - 1)\left(0.7934D_{20}^2 - 0.7934D_{30}^2\right)$$

$$+ 2u_o N_{\delta\eta}(\eta_o - 1)(D_{10} - 0.6088D_{20} + 0.6088D_{30})\Bigg]$$

$$+ \Delta v\Bigg[-my_G r_o + N_{vq} q_o + N_{|v|r}\frac{r_o v_o}{\sqrt{v_o^2 + w_o^2}} + N_v u_o + N_{v|v|}\frac{2v_o^2 + w_o^2}{\sqrt{v_o^2 + w_o^2}}$$

$$+ N_{vw}\frac{u_o w_o\ u_o^2 + w_o^2}{\left(u_o^2 + v_o^2 + w_o^2\right)^{\frac{3}{2}}} + N_{v\eta} u_o(\eta_o - 1) + N_{v|v|\eta}\frac{2v_o^2 + w_o^2}{\sqrt{v_o^2 + w_o^2}}$$

$$+ \frac{\partial N_{CRFW}}{\partial v}\Bigg]$$

$$+ \Delta w\Bigg[mx_G p_o + my_G q_o + N_{wr} r_o + N_{wp} p_o + N_{|v|r}\frac{r_o w_o}{\sqrt{v_o^2 + w_o^2}}$$

$$+ N_{v|v|}\frac{v_o w_o}{\sqrt{v_o^2 + w_o^2}} + N_{vw}\frac{u_o v_o\left(u_o^2 + v_o^2\right)}{\left(u_o^2 + v_o^2 + w_o^2\right)^{\frac{3}{2}}}$$

$$+ N_{v|v|\eta} \frac{(\eta_o - 1)v_o w_o}{\sqrt{v_o^2 + w_o^2}} + \frac{\partial N_{CRFW}}{\partial w}\Bigg]$$

$$+ \Delta p[mx_G w_o - (I_{yy} - I_{xx})q_o + I_{yz} r_o + 2I_{xy} p_o + N_{pq} q_o + N_{wp} w_o + N_p u_o]$$

$$+ \Delta q\Bigg[my_G w_o - (I_{yy} - I_{xx})p_o - 2I_{xy} q_o - I_{xy} r_o + N_{pq} p_o + N_{qr} r_o + N_{vq} v_o + \frac{\partial N_{CRFW}}{\partial q}\Bigg]$$

$$+ \Delta r\Bigg[-mx_G u_o - my_G v_o + I_{yz} p_o - I_{xz} q_o + N_{qr} q_o + 2N_{r|r|}|r_o| + N_{wr} w_o + N_r u_o + N_{|r|\delta\delta} \frac{u_o r_o}{|r_o|}\left(0.7934D_{20}^2 - 0.7934D_{30}^2\right) + N_{|r|\delta} \frac{u_o r_o}{|r_o|}(D_{10} - 0.6088D_{20} + 0.6088D_{30}) + N_{|v|r}\sqrt{v_o^2 + w_o^2} + N_{r\eta} u_o(\eta_o - 1) + \frac{\partial N_{CRFW}}{\partial r}\Bigg]$$

$$+ \Delta\phi[(x_G w - x_B B)\cos\theta_o \cos\phi_o]$$

$$+ \Delta\theta[-(x_G w - x_B B)\sin\theta_o \sin\phi_o + (y_G w - y_B B)\cos\theta_o]$$

$$+ \Delta\delta_1\left[-N_{|r|\delta} u_o |r_o| + N_\delta u_o^2 + N_{\delta\eta} u_o^2\right]$$

$$+ \Delta\delta_2\Big[1.5868N_{|r|\delta\delta} u_o |r_o| D_{20} - 0.6088N_{|r|\delta} u_o |r_o| + 1.5868N_{\delta\delta} u_o^2 D_{20} - 0.6088N_\delta u_o^2 + 1.5868N_{\delta\delta\eta} u_o^2 D_{20} - 0.6088N_{\delta\eta} u_o^2\Big]$$

$$+ \Delta\delta_3\Big[-1.5868N_{|r|\delta\delta} u_o |r_o| + 0.6088N_{|r|\delta} u_o |r_o| - 1.5868N_{\delta\delta} u_o^2 D_{30} + 0.6088N_\delta u_o^2 - 1.5868N_{\delta\delta\eta} u_o^2 D_{30} + 0.6088N_{\delta\eta} u_o^2\Big]$$

$$+ \Delta\eta\Big[N_{r\eta}u_o r_o + N_{v\eta}u_o v_o + N_{v|v|\eta}v_o\sqrt{v_o^2 + w_o^2}$$

$$+ N_{\delta\delta\eta}u_o^2\left(0.7934D_{20}^2 - 0.7934D_{30}^2\right)$$

$$+ N_{\delta\eta}u_o^2(D_{10} - 0.6088D_{20} + 0.6088D_{30})\Big]$$

where:

$$\frac{\partial N_{CRFW}}{\partial v} = \frac{\rho}{2}\left(-\ell^2\frac{Z_{ww}}{\int_\ell D(x)\,dx}\right)\int_\ell x\,H(x)\,\frac{\left(w_o^2(x) + 2v_o^2(x)\right)}{\sqrt{v_o^2(x) + w_o^2(x)}}\,dx$$

$$\frac{\partial N_{CRFW}}{\partial w} = \frac{\rho}{2}\left(-\ell^2\frac{Z_{ww}}{\int_\ell D(x)\,dx}\right)\int_\ell x\,H(x)\,\frac{v_o(x)w_o(x)}{\sqrt{v_o^2(x) + w_o^2(x)}}\,dx$$

$$\frac{\partial N_{CRFW}}{\partial q} = \frac{\rho}{2}\left(\ell^2\frac{Z_{ww}}{\int_\ell D(x)\,dx}\right)\int_\ell x^2\,H(x)\,\frac{v_o(x)w_o(x)}{\sqrt{v_o^2(x) + w_o^2(x)}}\,dx$$

$$\frac{\partial N_{CRFW}}{\partial r} = \frac{\rho}{2}\left(-\ell^2\frac{Z_{ww}}{\int_\ell D(x)\,dx}\right)\int_\ell x^2\,H(x)\,\frac{\left(w_o^2(x) + 2v_o^2(x)\right)}{\sqrt{v_o^2(x) + w_o^2(x)}}\,dx$$

APPENDIX D

SUMMARY OF NON-DIMENSIONALIZING FACTORS AND DIMENSIONALIZED HYDRODYNAMIC COEFFICIENTS

NOTATION [1]

Symbol	Dimensionless Form	Definition
I_x	$I'_x = \frac{I_x}{\frac{1}{2}\rho\ell^5}$	Moment of inertia of submarine about x axis
I_y	$I'_y = \frac{I_y}{\frac{1}{2}\rho\ell^5}$	Moment of inertia of submarine about y axis
I_z	$I'_z = \frac{I_z}{\frac{1}{2}\rho\ell^5}$	Moment of inertia of submarine about z axis
I_{xy}	$I'_{xy} = \frac{I_{xy}}{\frac{1}{2}\rho\ell^5}$	Product of inertia about xy axis
I_{yz}	$I'_{yz} = \frac{I_{yz}}{\frac{1}{2}\rho\ell^5}$	Product of inertia about yz axes
I_{zx}	$I'_{zx} = \frac{I_{zx}}{\frac{1}{2}\rho\ell^5}$	Product of inertia about zx axes
K_*	$K'_* = \frac{K_*}{\frac{1}{2}\rho\ell^3U^2}$	Rolling moment when body angle (α, β) and control surface angles are zero

Symbol	Dimensionless Form	Definition
$K_{*\eta}$	$K'_{*\eta} = \frac{K_{*\eta}}{\frac{1}{2}\rho\ell^3U^2}$	Coefficient used in representing K_* as a function of $(\eta-1)$
K_p	$K'_p = \frac{K_p}{\frac{1}{2}\rho\ell^4U}$	First order coefficient used in representing K as a function of p
$K_{\dot{p}}$	$K'_{\dot{p}} = \frac{K_{\dot{p}}}{\frac{1}{2}\rho\ell^5}$	Coefficient used in representing K as a function of $\dot{p}$
$K_{p\|p\|}$	$K'_{p\|p\|} = \frac{K_{p\|p\|}}{\frac{1}{2}\rho\ell^5}$	Second order coefficient used in representing K as a function of p
K_{pq}	$K'_{pq} = \frac{K_{pq}}{\frac{1}{2}\rho\ell^5}$	Coefficient used in representing K as a function of the product pq
K_{qr}	$K'_{qr} = \frac{K_{qr}}{\frac{1}{2}\rho\ell^5}$	Coefficient used in representing K as a function of the product qr
K_r	$K'_r = \frac{K_r}{\frac{1}{2}\rho\ell^4U}$	First order coefficient used in representing K as a function of r
$K_{\dot{r}}$	$K'_{\dot{r}} = \frac{K_{\dot{r}}}{\frac{1}{2}\rho\ell^5}$	Coefficient used in representing K as a function of $\dot{r}$
K_v	$K'_v = \frac{K_v}{\frac{1}{2}\rho\ell^3U}$	First order coefficient used in representing K as a function of v

Symbol	Dimensionless Form	Definition
$K_{\dot{v}}$	$K_{\dot{v}}' = \frac{K_{\dot{v}}}{\frac{1}{2}\rho\ell^4}$	Coefficient used in representing K as a function of $\dot{v}$
$K_{v\|v\|}$	$K'_{v\|v\|} = \frac{K_{v\|v\|}}{\frac{1}{2}\rho\ell^3}$	Second order coefficient used in representing K as a function of v
K_{vq}	$K'_{vq} = \frac{K_{vq}}{\frac{1}{2}\rho\ell^4}$	Coefficient used in representing K as a function of the product vq
K_{vw}	$K'_{vw} = \frac{K_{vw}}{\frac{1}{2}\rho\ell^3}$	Coefficient used in representing K as a function of the product vw
K_{wp}	$K'_{wp} = \frac{K_{wp}}{\frac{1}{2}\rho\ell^4}$	Coefficient used in representing K as a function of the product wp
K_{wr}	$K'_{wr} = \frac{K_{wr}}{\frac{1}{2}\rho\ell^4}$	Coefficient used in representing K as a function of the product wr
K_{δ}	$K'_{\delta} = \frac{K_{\delta r}}{\frac{1}{2}\rho\ell^3U^2}$	First order coefficient used in representing K as a function of δ_r
ℓ	$\ell' = 1$	Overall length of submarine
m	$m' = \frac{m}{\frac{1}{2}\rho\ell^3}$	Mass of submarine, including water in free-flooding spaces
M_*	$M'_* = \frac{M_*}{\frac{1}{2}\rho\ell^3U^2}$	Pitching moment when body angles (α, β) and control surface angles are zero

Symbol	Dimensionless Form	Definition
$M_{p\|p\|}$	$M'_{p\|p\|} = \frac{M_{p\|p\|}}{\frac{1}{2}\rho\ell^5}$	Second order coefficient used in representing M as a function of p. First order coefficient is zero.
M_q	$M'_q = \frac{M_q}{\frac{1}{2}\rho\ell^4 U}$	First order coefficient used in representing M as a function of q
$M_{\dot{q}}$	$M_{\dot{q}}' = \frac{M_{\dot{q}}}{\frac{1}{2}\rho\ell^5}$	Coefficient used in representing M as a function of $\dot{q}$
$M_{q\|q\|}$	$M'_{q\|q\|} = \frac{M_{q\|q\|}}{\frac{1}{2}\rho\ell^5}$	Second order coefficient used in representing M as a function of q
$M_{\|q\|\delta}$	$M'_{\|q\|\delta} = \frac{M_{\|q\|\delta}}{\frac{1}{2}\rho\ell^4 U}$	Coefficient used in representing M_δ as a function q
M_{rp}	$M'_{rp} = \frac{M_{rp}}{\frac{1}{2}\rho\ell^5}$	Coefficient used in representing M as a function of the product rp
$M_{r\|r\|}$	$M'_{r\|r\|} = \frac{M_{r\|r\|}}{\frac{1}{2}\rho\ell^5}$	Second order coefficient used in representing M as a function of r. First order coefficient is zero
M_{vr}	$M'_{vr} = \frac{M_{vr}}{\frac{1}{2}\rho\ell^4}$	Coefficient used in representing M as a function of the product vr
$M_{v\|v\|}$	$M'_{v\|v\|} = \frac{M_{v\|v\|}}{\frac{1}{2}\rho\ell^3}$	Second order coefficient used in representing M as a function of v

NOTATION (Cont.)

Symbol	Dimensionless Form	Definition
M_w	$M'_w = \frac{M_w}{\frac{1}{2}\rho\ell^3 U}$	First order coefficient used in representing M as a function of w
$M_{w\eta}$	$M'_{w\eta} = \frac{M_{w\eta}}{\frac{1}{2}\rho\ell^3 U}$	First order coefficient used in representing M_w as a function of $(\eta - 1)$
$M_{\dot{w}}$	$M_{\dot{w}}' = \frac{M_{\dot{w}}}{\frac{1}{2}\rho\ell^4}$	Coefficient used in representing M as a function of $\dot{w}$
$M_{\|w\|}$	$M'_{\|w\|} = \frac{M_{\|w\|}}{\frac{1}{2}\rho\ell^4}$	First order coefficient used in representing M as a function of w; equal to zero for symmetrical function
$M_{\|w\|q}$	$M'_{\|w\|q} = \frac{M_{\|w\|q}}{\frac{1}{2}\rho\ell^4}$	Coefficient used in representing M_q as a function of w
$M_{w\|w\|}$	$M'_{w\|w\|} = \frac{M_{w\|w\|}}{\frac{1}{2}\rho\ell^3}$	Second order coefficient used in representing M as a function of w
$M_{w\|w\|\eta}$	$M'_{w\|w\|\eta} = \frac{M_{w\|w\|\eta}}{\frac{1}{2}\rho\ell^3}$	First order coefficient used in representing $M_{w\|w\|}$ as a function of $(\eta - 1)$
$M_{\delta b}$	$M'_{\delta b} = \frac{M_{\delta b}}{\frac{1}{2}\rho\ell^3 U^2}$	First order coefficient used in representing M as a function of δ_b
M_δ	$M'_\delta = \frac{M_\delta}{\frac{1}{2}\rho\ell^3 U^2}$	First order coefficient used in representing M as a function of δ

Symbol	Dimensionless Form	Definition
$M_{\delta\eta}$	$M'_{\delta\eta} = \frac{M_{\delta\eta}}{\frac{1}{2}\rho\ell^3U^2}$	First order coefficient used in representing M_δ as a function of $(\eta - 1)$
N_*	$N'_* = \frac{N_*}{\frac{1}{2}\rho\ell^3U^2}$	Yawing moment when body angles (α, β) and control surface angles are zero
N_p	$N'_p = \frac{N_p}{\frac{1}{2}\rho\ell^4U}$	First order coefficient used in representing N as a function of p
$N_{\dot{p}}$	$N_{\dot{p}}' = \frac{N_{\dot{p}}}{\frac{1}{2}\rho\ell^5}$	Coefficient used in representing N as a function of $\dot{p}$
N_{pq}	$N'_{pq} = \frac{N_{pq}}{\frac{1}{2}\rho\ell^5}$	Coefficient used in representing N as a function of the product pq
N_{qr}	$N'_{qr} = \frac{N_{qr}}{\frac{1}{2}\rho\ell^5}$	Coefficient used in representing N as a of the product qr
N_r	$N'_r = \frac{N_r}{\frac{1}{2}\rho\ell^4U}$	First order coefficient used in representing N as a function of r
$N_{r\eta}$	$N'_{r\eta} = \frac{N_{r\eta}}{\frac{1}{2}\rho\ell^4U}$	First order coefficient used in representing N_r as a function of $(\eta - 1)$
$N_{\dot{r}}$	$N_{\dot{r}}' = \frac{N_{\dot{r}}}{\frac{1}{2}\rho\ell^5}$	Coefficient used in representing N as a function of $\dot{r}$

Symbol	Dimensionless Form	Definition
$N_{r\|r\|}$	$N'_{r\|r\|} = \frac{N_{r\|r\|}}{\frac{1}{2}\rho\ell^5}$	Second order coefficient used in representing N as a function of r
$N_{\|r\|\delta r}$	$N'_{\|r\|\delta r} = \frac{N_{\|r\|\delta r}}{\frac{1}{2}\rho\ell^4 U}$	Coefficient used in representing $N_{\delta r}$ as a function of r
N_v	$N'_v = \frac{N_v}{\frac{1}{2}\rho\ell^3 U}$	First order coefficient used in representing N as a function of v
$N_{v\eta}$	$N'_{v\eta} = \frac{N_{v\eta}}{\frac{1}{2}\rho\ell^3 U}$	First order coefficient used in representing N_v as a function of $(\eta - 1)$
$N_{\dot{v}}$	$N_{\dot{v}}' = \frac{N_{\dot{v}}}{\frac{1}{2}\rho\ell^4}$	Coefficient used in representing N as a function of $\dot{v}$
N_{vq}	$N'_{vq} = \frac{N_{vq}}{\frac{1}{2}\rho\ell^4}$	Coefficient used in representing N as a function of the product vq
$N_{\|v\|r}$	$N'_{\|v\|r} = \frac{N_{\|v\|r}}{\frac{1}{2}\rho\ell^4}$	Coefficient used in representing N_r as a function of v
$N_{v\|v\|}$	$N'_{v\|v\|} = \frac{N_{v\|v\|}}{\frac{1}{2}\rho\ell^3}$	Second order coefficient used in representing N as a function of v
$N_{v\|v\|\eta}$	$N'_{v\|v\|\eta} = \frac{N_{v\|v\|\eta}}{\frac{1}{2}\rho\ell^3}$	First order coefficient used in representing $N_{v\|v\|}$ as a function of $(\eta - 1)$

NOTATION (Cont.)

Symbol	Dimensionless Form	Definition
N_{vw}	$N'_{vw} = \frac{N_{vw}}{\frac{1}{2}\rho\ell^3}$	Coefficient used in representing N as a function of the product vw
N_{wp}	$N'_{wp} = \frac{N_{wp}}{\frac{1}{2}\rho\ell^4}$	Coefficient used in representing N as a function of the product wp
N_{wr}	$N'_{wr} = \frac{N_{wr}}{\frac{1}{2}\rho\ell^4}$	Coefficient used in representing N as a function of the product wr
$N_{\delta r}$	$N'_{\delta r} = \frac{N_{\delta r}}{\frac{1}{2}\rho\ell^3 U^2}$	First order coefficient used in representing N as a function of δ_r
$N_{\delta r\eta}$	$N'_{\delta r\eta} = \frac{N_{\delta r\eta}}{\frac{1}{2}\rho\ell^3 U^2}$	First order coefficient used in representing $N_{\delta r}$ as a function of $(\eta - 1)$
p	$p' = \frac{p\ell}{U}$	Angular velocity component about x axis relative to fluid (roll)
$\dot{p}$	$\dot{p}' = \frac{\dot{p}\ell^2}{U^2}$	Angular acceleration component about x axis relative to fluid
q	$q' = \frac{q\ell}{U}$	Angular velocity component about y axis relative to fluid (pitch)
$\dot{q}$	$\dot{q}' = \frac{\dot{q}\ell^2}{U^2}$	Angular acceleration component about y axis relative to fluid
r	$r' = \frac{r\ell}{U}$	Angular velocity component about z axis relative to fluid (yaw)

NOTATION (Cont.)

Symbol	Dimensionless Form	Definition
$\dot{r}$	$\dot{r}' = \frac{\dot{r}\ell^2}{U^2}$	Angular acceleration component about z axis relative to fluid
U	$U' = \frac{U}{U}$	Linear velocity of origin of body axes relative to fluid
u	$u' = \frac{u}{U}$	Component of U in direction of the x axis
$\dot{u}$	$\dot{u}' = \frac{\dot{u}\ell}{U^2}$	Time rate of change of u in direction of the x axis
u_c	$u_c' = \frac{u_c}{U}$	Command speed: steady value of ahead speed component u for a given propeller rpm when body angles (α, β) and control surface angles are zero. Sign changes with propeller reversal.
v	$v' = \frac{v}{U}$	Component of U in direction of the y axis
$\dot{v}$	$\dot{v}' = \frac{\dot{v}\ell}{U^2}$	Time rate of change of v in direction of the y axis
w	$w' = \frac{w}{U}$	Component of U in direction of the z axis
$\dot{w}$	$\dot{w}' = \frac{\dot{w}\ell}{U^2}$	Time rate of change of w in direction of the z axis
x	$x' = \frac{x}{\ell}$	Longitudinal body axis; also the coordinate of a point relative to the origin of body axes
x_B	$x_B' = \frac{x_B}{\ell}$	The x coordinate of CB

Symbol	Dimensionless Form	Definition
x_G	$x'_G = \frac{x_G}{\ell}$	The x coordinate of CG
x_o	$x'_o = \frac{x_o}{\ell}$	A coordinate of the displacement of CG relative to the origin of a set of fixed axes
X_{qq}	$X'_{qq} = \frac{X_{qq}}{\frac{1}{2}\rho\ell^4}$	Second order coefficient used in representing X as a function of q. First order coefficient is zero
X_{rp}	$X'_{rp} = \frac{X_{rp}}{\frac{1}{2}\rho\ell^4}$	Coefficient used in representing X as a function of the product rp
X_{rr}	$X'_{rr} = \frac{X_{rr}}{\frac{1}{2}\rho\ell^4}$	Second order coefficient used in representing X as a function of r. First order coefficient is zero.
$X_{\dot{u}}$	$X_{\dot{u}}' = \frac{X_{\dot{u}}}{\frac{1}{2}\rho\ell^3}$	Coefficient used in representing X as a function of $\dot{u}$
X_{uu}	$X'_{uu} = \frac{X_{uu}}{\frac{1}{2}\rho\ell^2}$	Second order coefficient used in representing X as a function of u in the non-propelled case. First order coefficient is zero.
X_{vr}	$X'_{vr} = \frac{X_{vr}}{\frac{1}{2}\rho\ell^3}$	Coefficient used in representing X as a function of the product vr
X_{vv}	$X'_{vv} = \frac{X_{vv}}{\frac{1}{2}\rho\ell^2}$	Second order coefficient used in representing X as a function of v. First order coefficient is zero.

Symbol	Dimensionless Form	Definition
$X_{vv\eta}$	$X'_{vv\eta} = \frac{X_{vv\eta}}{\frac{1}{2}\rho\ell^2}$	First order coefficient used in representing X_{vv} as a function of $(\eta - 1)$
X_{wq}	$X'_{wq} = \frac{X_{wq}}{\frac{1}{2}\rho\ell^3}$	Coefficient used in representing X as a function of the product wq
X_{ww}	$X'_{ww} = \frac{X_{ww}}{\frac{1}{2}\rho\ell^2}$	Second order coefficient used in representing X as a function of w. First order coefficient is zero
$X_{ww\eta}$	$X'_{ww\eta} = \frac{X_{ww\eta}}{\frac{1}{2}\rho\ell^2}$	First order coefficient used in representing X_{ww} as a function of $(\eta - 1)$
$X_{\delta b\delta b}$	$X'_{\delta b\delta b} = \frac{X_{\delta b\delta b}}{\frac{1}{2}\rho\ell^2U^2}$	Second order coefficient used in representing X as a function of δ_b. First order coefficient is zero.
$X_{\delta r\delta r}$	$X'_{\delta r\delta r} = \frac{X_{\delta r\delta r}}{\frac{1}{2}\rho\ell^2U^2}$	Second order coefficient used in representing X as a function of δ_r. First order coefficient is zero.
$X_{\delta r\delta r\eta}$	$X'_{\delta r\delta r\eta} = \frac{X_{\delta r\delta r\eta}}{\frac{1}{2}\rho\ell^2U^2}$	First order coefficient used in representing $X_{\delta r\delta r}$ as a function of $(\eta - 1)$
$X_{\delta s\delta s}$	$X'_{\delta s\delta s} = \frac{X_{\delta s\delta s}}{\frac{1}{2}\rho\ell^2U^2}$	Second order coefficient used in representing X as a function of δ_s. First order coefficient is zero.
$X_{\delta s\delta s\eta}$	$X'_{\delta s\delta s\eta} = \frac{X_{\delta s\delta s\eta}}{\frac{1}{2}\rho\ell^2U^2}$	First order coefficient used in representing $X_{\delta s\delta s}$ as a function of $(\eta - 1)$

Symbol	Dimensionless Form	Definition
y	$y' = \frac{y}{\ell}$	Lateral body axis; also the coordinate of a point relative to the origin of body axes
y_B	$y'_B = \frac{y_B}{\ell}$	The y coordinate of CB
y_G	$y'_G = \frac{y_G}{\ell}$	The y coordinate of CG
y_o	$y'_o = \frac{y_o}{\ell}$	A coordinate of the displacement of CG relative to the origin of a set of fixed axes
Y_*	$Y'_* = \frac{Y}{\frac{1}{2}\rho\ell^2U^2}$	Lateral force when body angles (α, β) and control surface angles are zero
Y_p	$Y'_p = \frac{Y_p}{\frac{1}{2}\rho\ell^3U}$	First order coefficient used in representing Y as a function of p
$Y_{\dot{p}}$	$Y'_{\dot{p}} = \frac{Y_{\dot{p}}}{\frac{1}{2}\rho\ell^4}$	Coefficient used in representing Y as a function of $\dot{p}$
$Y_{p\|p\|}$	$Y'_{p\|p\|} = \frac{Y_{p\|p\|}}{\frac{1}{2}\rho\ell^4}$	Second order coefficient used in representing Y as a function of p
Y_{pq}	$Y'_{pq} = \frac{Y_{pq}}{\frac{1}{2}\rho\ell^4}$	Coefficient used in representing Y as a function of the product pq

Symbol	Dimensionless Form	Definition
Y_{qr}	$Y'_{qr} = \frac{Y_{qr}}{\frac{1}{2}\rho\ell^4}$	Coefficient used in representing Y as a function of the product qr
Y_r	$Y'_r = \frac{Y_r}{\frac{1}{2}\rho\ell^3 U}$	First order coefficient used in representing Y as a function of r
$Y_{r\eta}$	$Y'_{r\eta} = \frac{Y_{r\eta}}{\frac{1}{2}\rho\ell^3 U}$	First order coefficient used in representing Y_r as a function of $(\eta - 1)$
$Y_{\dot{r}}$	$Y_{\dot{r}}' = \frac{Y_{\dot{r}}}{\frac{1}{2}\rho\ell^4}$	Coefficient used in representing Y as a function of $\dot{r}$
$Y_{\|r\|\delta r}$	$Y'_{\|r\|\delta r} = \frac{Y_{\|r\|\delta r}}{\frac{1}{2}\rho\ell^3 U}$	Coefficient used in representing $Y_{\delta r}$ as a function of r
Y_v	$Y'_v = \frac{Y_v}{\frac{1}{2}\rho\ell^2 U}$	First order coefficient used in representing Y as a function of v
$Y_{v\eta}$	$Y'_{v\eta} = \frac{Y_{v\eta}}{\frac{1}{2}\rho\ell^2 U}$	First order coefficient used in representing Y_v as a function of $(\eta - 1)$
$Y_{\dot{v}}$	$Y_{\dot{v}}' = \frac{Y_{\dot{v}}}{\frac{1}{2}\rho\ell^3}$	Coefficient used in representing Y as a function of $\dot{v}$
Y_{vq}	$Y'_{vq} = \frac{Y_{vq}}{\frac{1}{2}\rho\ell^3}$	Coefficient used in representing Y as a function of the product vq

Symbol	Dimensionless Form	Definition
$Y_{v\|r\|}$	$Y'_{v\|r\|} = \frac{Y_{v\|r\|}}{\frac{1}{2}\rho\ell^3}$	Coefficient used in representing Y_v as a function of r
$Y_{v\|v\|}$	$Y'_{v\|v\|} = \frac{Y_{v\|v\|}}{\frac{1}{2}\rho\ell^3}$	Second order coefficient used in representing Y as a function of v
$Y_{v\|v\|\eta}$	$Y'_{v\|v\|\eta} = \frac{Y_{v\|v\|\eta}}{\frac{1}{2}\rho\ell^2}$	First order coefficient used in representing $Y_{v\|v\|}$ as a function of $(\eta - 1)$
Y_{vw}	$Y'_{vw} = \frac{Y_{vw}}{\frac{1}{2}\rho\ell^2}$	Coefficient used in representing Y as a function of the product vw
Y_{wp}	$Y'_{wp} = \frac{Y_{wp}}{\frac{1}{2}\rho\ell^3}$	Coefficient used in representing Y as a function of the product wp
Y_{wr}	$Y'_{wr} = \frac{Y_{wr}}{\frac{1}{2}\rho\ell^3}$	Coefficient used in representing Y as a function of the product wr
$Y_{\delta r}$	$Y'_{\delta r} = \frac{Y_{\delta r}}{\frac{1}{2}\rho\ell^2U^2}$	First order coefficient used in representing Y as a function of δr
$Y_{\delta r\eta}$	$Y'_{\delta r\eta} = \frac{Y_{\delta r\eta}}{\frac{1}{2}\rho\ell^2U^2}$	First order coefficient used in presenting $Y_{\delta r}$ as a function of $(\eta - 1)$
z	$z' = \frac{z}{\ell}$	Normal body axis; also the coordinate of a point relative to the origin of body axes

NOTATION (Cont.)

Symbol	Dimensionless Form	Definition
z_B	$z'_B = \frac{z_B}{\ell}$	The z coordinate of CB
z_G	$z'_G = \frac{z_G}{\ell}$	The z coordinate of CG
z_o	$z'_o = \frac{z_o}{\ell}$	A coordinate of the displacement of CG relative to the origin of a set of fixed axes
Z_*	$Z'_* = \frac{Z_*}{\frac{1}{2}\rho\ell^2U^2}$	Normal force when body angles (α, β) and control surface angles are zero
$Z_{p\|p\|}$	$Z'_{p\|p\|} = \frac{Z_{p\|p\|}}{\frac{1}{2}\rho\ell^4}$	Second order coefficient used in representing Z as a function of p. First order coefficient is zero
Z_q	$Z'_q = \frac{Z_q}{\frac{1}{2}\rho\ell^3U}$	First order coefficient used in representing Z as a function of q
$Z_{\dot{q}}$	$Z'_{\dot{q}} = \frac{Z_{\dot{q}}}{\frac{1}{2}\rho\ell^4}$	Coefficient used in representing Z as a function of $\dot{q}$
$Z_{\|q\|\delta s}$	$Z'_{\|q\|\delta s} = \frac{Z_{\|q\|\delta s}}{\frac{1}{2}\rho\ell^3U}$	Coefficient used in representing $Z_{\delta s}$ as a function of q
Z_{rp}	$Z'_{rp} = \frac{Z_{rp}}{\frac{1}{2}\rho\ell^4}$	Coefficient used in representing Z as a function of the product rp

NOTATION (Cont.)

Symbol	Dimensionless Form	Definition
$Z_{r\|r\|}$	$Z'_{r\|r\|} = \frac{Z_{r\|r\|}}{\frac{1}{2}\rho\ell^4}$	Second order coefficient used in representing Z as a function of r. First order coefficient is zero
Z_w	$Z'_w = \frac{Z_w}{\frac{1}{2}\rho\ell^2 U}$	First order coefficient used in representing Z as a function of w
$Z_{q\eta}$	$Z'_{q\eta} = \frac{Z_{q\eta}}{\frac{1}{2}\rho\ell^3 U}$	First order coefficient used in representing Z_q as a function of $(\eta - 1)$
$Z_{w\eta}$	$Z'_{w\eta} = \frac{Z_{w\eta}}{\frac{1}{2}\rho\ell^2 U}$	First order coefficient used in representing Z_w as a function of $(\eta - 1)$
$Z_{\dot{w}}$	$Z'_{\dot{w}} = \frac{Z_{\dot{w}}}{\frac{1}{2}\rho\ell^3}$	Coefficient used in representing Z as a function of $\dot{w}$
$Z_{\|w\|}$	$Z'_{\|w\|} = \frac{Z_{\|w\|}}{\frac{1}{2}\rho\ell^2 U}$	First order coefficient used in representing Z as a function of w; equal to zero for symmetrical function
$Z_{w\|q\|}$	$Z'_{w\|q\|} = \frac{Z_{w\|q\|}}{\frac{1}{2}\rho\ell^3}$	Coefficient used in representing Z_w as a function of q
$Z_{w\|w\|}$	$Z'_{w\|w\|} = \frac{Z_{w\|w\|}}{\frac{1}{2}\rho\ell^2}$	Second order coefficient used in representing Z as a function of w
$Z_{w\|w\|\eta}$	$Z'_{w\|w\|\eta} = \frac{Z_{w\|w\|\eta}}{\frac{1}{2}\rho\ell^2}$	First order coefficient used in representing $Z_{w\|w\|}$ as a function of $(\eta - 1)$

Symbol	Dimensionless Form	Definition
Z_{ww}	$Z'_{ww} = \frac{Z_{ww}}{\frac{1}{2}\rho \ell^2}$	Second order coefficient used in representing Z as a function of w; equal to zero for symmetrical function
$Z_{\delta b}$	$Z'_{\delta b} = \frac{Z_{\delta b}}{\frac{1}{2}\rho \ell^2 U^2}$	First order coefficient used in representing Z as a function of δ_b
$Z_{\delta s}$	$Z'_{\delta s} = \frac{Z_{\delta s}}{\frac{1}{2}\rho \ell^2 U^2}$	First order coefficient used in representing Z as a function of δ_s
$Z_{\delta s\eta}$	$Z'_{\delta s\eta} = \frac{Z_{\delta s\eta}}{\frac{1}{2}\rho \ell^2 U^2}$	First order coefficient used in representing $Z_{\delta s}$ as a function of $(\eta - 1)$
δ_b		Deflection of bowplane or sailplane
δ_r		Deflection of rudder
δ_s		Deflection of sternplane
η		The ratio $\frac{u_c}{U} \equiv u'_c$
θ		Angle of pitch
ψ		Angle of yaw
ϕ		Angle of roll
a_i, b_i, c_i		Sets of constants used in the representation of propeller thrust in the axial equation

Axial Coefficients

XQQ	XRR	XRP	XUDOT
-138568.	-11547.	54588.	-1819.584
XVR	XWQ	XUU	XVV
63161.	-58728.	0	154.872
XWW	XDD	XVVN	XWWN
120.204	-188.02	0	0
XDDN	XDBDB		
0	-91.044		

Lateral Coefficients

YRDOT	YPDOT	YPABP	YQR
-39890.	-72433.	0	0
YVDOT	YVQ	YWP	YWR
-79122.	0	58728.	0
YR	YP	YABRD	YVABR
41705.	-4549.	0	0
YSTAR	YV	YVABV	YVW
0	-1043.	-2054.2	0
YD	YRN	YVN	YVABVN
185.036	0	0	0
YDN	YPQ		
43.371	138568.		

Normal Coefficients

ZQDOT	ZPABP	ZRABR	ZRP
-170000.	0	0	0
ZWDOT	ZVR	ZVP	ZQ
-69459.	0	-33067.	-42148.
ZABQDD	ZWABQ	ZSTAR	ZW
0	0	0	-1044.3
ZWABW	ZABW	ZVABV	ZD
0	-8.97	0	248.054
ZQN	ZWN	ZWABWN	ZDN
0	0	0	31.34
ZDB	ZABQD	ZWW	
-175.90	0	15.99	

Rolling Coefficients

KPDOT	KRDOT	KQR	KPQ
-1133000.	-906993.	-2796560.	0
KPABP	KP	KR	KVDOT
0	-153265.	-398900.	-15746.
KVQ	KWP	KWR	KSTAR
0	53283.	0	0
KV	KVABV	KVW	KD
-3423.	0	0	1568.
KSTARN	K4S	K8S	
0	1281.4	0	

Pitching Coefficients

MQDOT	MPABP	MRABR	MRP
-124300000.	0	0	29666000.
MQABQ	MWDOT	MVR	MWW
0	-170600.	0	-1595.6
MQ	MABQDD	MABQD	MABWQ
-4066000.	0	0	0
MSTAR	MW	MWABW	MABW
0	221.62	-35873.	-239.72
MVABV	MDD	MD	MQN
0	0	-23438.	0
MWN	MWABWN	MDDN	MDN
0	0	0	-3058.
MDB			
4222.			

Yawing Coefficients

NRDOT	NPDOT	NPQ	NQR
-128800000.	-434600.	-97313000.	0
NRABR	NVDOT	NWR	NWP
0	-39800.	0	-138558.
NVQ	NP	NR	NABRDD
0	-62986.	-3766000.	0
NABRD	NABVR	NSTAR	NV
0	0	0	-12661.
NVABV	NVW	NDD	ND
49980.	0	0	-9798.
NRN	NVN	NVABVN	NDDN
0	0	0	0
NDN			
-4374			
CDCRSS			
.56889			

APPENDIX E

DESCRIPTION OF PROPULSION MODELS AND NOMINAL POINT DETERMINATION

There are two propulsion models an RPS and an eta propulsion model. The RPS model is a first order differential equation in terms of RPS (revolutions per second) and is considered the more accurate model of the two. The eta propulsion model is a simplified version of the RPS model in that it is a first order differential representation where eta (η) is defined as $\frac{u_c}{U}$. U is the actual speed of the submersible and u_c is the commanded forward velocity. The eta model is important because it was the model that was linearized and included in the linear equations of motion.

In order to find a nominal point, the final values of the states (u, v, w, p, q, r, phi and theta) from the RPS integration are used as an initial point with the eta model integration. The nonlinear equations are again integrated, however, using the eta propulsion model. A search routine is used to search for a nominal point (a local equilibrium point where the derivatives of the state variables are zero). To get some idea how good the nominal point is, the accelerations associated with each of the states are calculated. As a rule of thumb, accelerations should be less than 10^{-6}. The equilibrium point for this model is listed below.

```
XDOT (1)  =  -0.134572E-10
XDOT (2)  =  -0.132110E-07
XDOT (3)  =  -0.130859E-08
XDOT (4)  =  -0.297533E-08
XDOT (5)  =   0.137816E-10
XDOT (6)  =   0.999896E-10
XDOT (7)  =  -0.568434E-13
XDOT (8)  =   0.145519E-10

      u  =   0.351355E+02
      v  =   0.317284E+00
      w  =  -0.678508E-02
      p  =   0.368353E-06
      q  =  -0.996159E-04
      r  =  -0.368482E-02
    phi  =   0.154856E+01
  theta  =   0.572548E-02
    psi  =  -0.211141E+02
      z  =  -0.170338E+00
     DB  =  0
     D1  =   2.0
     D2  =   0.5
     D3  =  -0.4744
```

APPENDIX F

MODAL ANALYSIS MATRICES

OBSERVABILITY(T*C)

-2.1290E-05	7.1583E-05	4.8423E-03	5.2630E-05	3.2220E-03	3.2220E-03	1.3762E-03	-2.7719E-02
0.0000E+00	0.0000E+00	0.0000E+00	0.0000E+00	6.9118E-03	-6.9118E-03	0.0000E+00	0.0000E+00
2.6489E-03	-2.0743E-03	-1.9729E-02	2.4111E-03	-5.6558E-01	-5.6558E-01	-6.4347E-03	2.6790E-01
0.0000E+00	0.0000E+00	0.0000E+00	0.0000E+00	7.0275E-02	-7.0275E-02	0.0000E+00	0.0000E+00
-7.8555E-01	1.6809E-03	1.3494E-02	3.3456E-02	1.4757E-03	1.4757E-03	6.7821E-02	4.3741E-03
0.0000E+00	0.0000E+00	0.0000E+00	0.0000E+00	3.1573E-04	-3.1573E-04	0.0000E+00	0.0000E+00

CONTROLLABILITY(T^{-1}*B)

-1.5311E-02	2.3498E-01	2.1431E-01
-8.0762E-11	7.1922E-11	-7.5965E-11
4.2570E-01	-6.0879E-02	7.5270E-02
1.1603E-10	-9.0817E-11	1.1762E-10
-3.2682E+00	2.0472E+00	-1.7453E+00
-3.6227E-09	2.9746E-09	-3.3771E-09
1.0639E+00	-7.2540E-02	1.1276E+00
1.1672E-10	1.1699E-10	-7.2679E-11
3.0824E-01	-1.0009E-01	3.1597E-02
9.6169E-01	-8.6784E-01	8.3702E-01
3.0824E-01	-1.0009E-01	3.1597E-02
-9.6169E-01	8.6784E-01	-8.3702E-01
-1.6724E-01	2.3913E+00	2.2465E+00
1.7908E-10	-1.7178E-10	1.6932E-10
1.5552E+00	-6.7186E-01	4.8629E-01
-4.4036E-09	3.4853E-09	-3.2005E-09

DIAGONAL A MATRIX($T^{-1}*A*T$)

-2.0293E-02 -4.8182E-11 7.3209E-10 -4.3965E-10 -2.1759E-10 -2.9193E-10 -7.0223E-09 -4.9357E-09
 8.0822E-15 3.1627E-15 9.9136E-13 2.5088E-14 3.1149E-09 -3.1450E-09 9.1370E-13 -4.9420E-12

-9.8699E-09 -4.3774E-02 -3.8043E-09 9.8277E-10 -6.5464E-08 -6.5325E-08 -3.1495E-09 1.1828E-07
-3.7401E-14 -1.4489E-14 -2.0391E-12 -5.7494E-14 6.3310E-09 -6.3132E-09 -4.2576E-12 1.2084E-11

-1.4485E-09 1.4366E-10 -1.8040E-01 5.4190E-10 1.3579E-08 1.0251E-08 -6.1731E-09 -1.8558E-09
 5.6934E-13 2.2166E-13 4.8451E-11 1.5575E-12 -5.4467E-09 4.3286E-09 7.3613E-11 -1.2185E-10

-5.2042E-09 -3.5774E-10 4.4974E-09 -1.8432E-01 1.4152E-08 1.4424E-08 1.0565E-08 -5.5337E-08
-5.9672E-14 -6.8722E-14 2.9312E-13 9.8037E-14 7.0181E-08 -7.0659E-08 -1.3197E-11 -3.9280E-11

-1.3921E-09 -3.2740E-10 -1.0737E-09 1.6470E-11 -5.0851E-01 3.4939E-09 8.8439E-10 -1.1038E-09
-7.2923E-10 -3.5568E-10 1.7830E-10 1.6958E-10 5.2247E-01 -1.7384E-08 1.8838E-09 1.0024E-08

-1.3999E-09 -3.3429E-10 -1.0920E-09 3.6241E-11 -8.2512E-09 -5.0851E-01 5.8881E-10 3.0062E-09
 7.7433E-10 3.4266E-10 -1.9646E-10 -1.4578E-10 2.4680E-08 -5.2247E-01 -1.9305E-09 -6.7210E-09

-1.3967E-09 -4.2439E-10 1.4827E-09 -2.5007E-10 -1.1268E-08 -1.1079E-08 -6.2278E-01 2.4002E-08
 4.4808E-14 -1.5415E-14 -2.1257E-12 4.2141E-15 -1.8744E-09 1.9342E-09 -6.6594E-13 2.1903E-11

-8.4933E-09 2.2854E-10 -8.5856E-09 9.8674E-10 -8.2833E-09 -1.3066E-08 4.4007E-09 -6.5837E-01
-3.8694E-13 3.7923E-13 2.6495E-11 -1.1123E-12 -6.8672E-10 1.1121E-09 1.1026E-11 -2.8917E-10

EIGENVALUES

-2.0293E-02 -4.3774E-02 -1.8040E-01 -1.8432E-01 -5.0851E-01 -5.0851E-01 -6.2278E-01 -6.5837E-01
 0.0000E+00 0.0000E+00 0.0000E+00 0.0000E+00 5.2247E-01 -5.2247E-01 0.0000E+00 0.0000E+00

EIGENVECTOR (T)

2.1339E-02	-9.9996E-01	-5.3213E-02	9.0521E-03	2.8894E-03	2.8894E-03	4.3930E-02	2.2700E-02
0.0000E+00	0.0000E+00	0.0000E+00	0.0000E+00	-1.5787E-03	1.5787E-03	0.0000E+00	0.0000E+00
1.6640E-02	-8.5246E-03	-9.3374E-01	-6.6859E-03	6.6396E-01	6.6396E-01	3.9225E-02	-9.4647E-01
0.0000E+00	0.0000E+00	0.0000E+00	0.0000E+00	1.8760E-01	-1.8760E-01	0.0000E+00	0.0000E+00
6.1799E-01	-2.7814E-03	-3.5312E-01	-9.9935E-01	1.6231E-01	1.6231E-01	9.9503E-01	4.2817E-04
0.0000E+00	0.0000E+00	0.0000E+00	0.0000E+00	7.5758E-03	-7.5758E-03	0.0000E+00	0.0000E+00
-2.9495E-03	9.6991E-05	3.6084E-03	-3.2107E-04	2.5089E-01	2.5089E-01	4.2573E-03	-1.7636E-01
0.0000E+00	0.0000E+00	0.0000E+00	0.0000E+00	-3.3123E-01	3.3123E-01	0.0000E+00	0.0000E+00
1.5937E-02	-6.4024E-05	-2.2315E-03	-6.1764E-03	1.2570E-03	1.2570E-03	-4.2192E-02	-4.6181E-03
0.0000E+00	0.0000E+00	0.0000E+00	0.0000E+00	5.3841E-04	-5.3841E-04	0.0000E+00	0.0000E+00
-2.1290E-05	7.1583E-05	4.8423E-03	5.2630E-05	3.2220E-03	3.2220E-03	1.3762E-03	-2.7719E-02
0.0000E+00	0.0000E+00	0.0000E+00	0.0000E+00	6.9118E-03	-6.9118E-03	0.0000E+00	0.0000E+00
2.6489E-03	-2.0743E-03	-1.9729E-02	2.4111E-03	-5.6558E-01	-5.6558E-01	-6.4347E-03	2.6790E-01
0.0000E+00	0.0000E+00	0.0000E+00	0.0000E+00	7.0275E-02	-7.0275E-02	0.0000E+00	0.0000E+00
-7.8555E-01	1.6809E-03	1.3494E-02	3.3456E-02	1.4757E-03	1.4757E-03	6.7821E-02	4.3741E-03
0.0000E+00	0.0000E+00	0.0000E+00	0.0000E+00	3.1573E-04	-3.1573E-04	0.0000E+00	0.0000E+00

APPENDIX G

L MATRIX

MATRIX (14, 3)

	1	2	3
1)	0.0	0.0	0.0
2)	0.0	0.0	0.0
3)	0.0	0.0	0.0
4)	0.0	0.0	0.0
5)	0.0	0.0	0.0
6)	1.000000000000E+00	0.0	0.0
7)	0.0	1.000000000000E+00	0.0
8)	0.0	0.0	1.000000000000E+00
9)	0.0	0.0	0.0
10)	0.0	0.0	0.0
11)	0.0	0.0	0.0
12)	-1.835420480000E+01	-1.403831751000E+00	-2.723467750000E-02
13)	-1.192239258000E+01	-1.310703360000E+00	-7.691884516000E-02
14)	1.174827457000E+01	1.333686037000E+00	-4.335761088000E-02

APPENDIX H

$\underline{A}$, $\underline{B}$, $\underline{C}$, $\underline{G}$, $\underline{H}$, ($\underline{A}$-$\underline{BG}$-$\underline{HC}$) Matrices

A Matrix

-.43703E-01	-.53404E-02	-.19627E-02	0.30208E-02	0.58597E+00	0.57035E+00	0.00000E+00	0.95681E-02	0.00000E+00	0.00000E+00
0.89727E-03	-.22647E+00	0.15542E-03	-.10595E+01	0.30690E-02	-.81203E+01	-.11801E-01	0.31879E-07	0.00000E+00	0.00000E+00
-.37634E-04	0.82501E-04	-.23967E+00	-.23519E+00	0.90297E+01	-.25858E-02	0.00000E+00	0.11493E-01	0.00000E+00	0.00000E+00
0.96494E-03	-.49312E-02	-.79457E-03	-.10884E+01	-.69357E-01	-.27370E+01	-.58498E+00	0.15803E-05	0.00000E+00	0.00000E+00
0.12087E-04	0.30283E-05	0.21655E-02	-.20736E-02	-.58766E+00	-.19458E-03	0.00000E+00	-.97988E-02	0.00000E+00	0.00000E+00
-.22000E-04	-.19154E-02	-.16146E-05	-.66321E-02	0.10729E-05	-.54105E+00	0.10084E-02	-.27241E-08	0.00000E+00	0.00000E+00
0.00000E+00	0.00000E+00	0.00000E+00	0.10000E+01	0.27005E-05	0.99892E-04	-.42170E-13	-.36862E-02	0.00000E+00	0.00000E+00
0.00000E+00	0.00000E+00	0.00000E+00	0.00000E+00	0.99963E+00	-.27024E-01	0.36862E-02	0.00000E+00	0.00000E+00	0.00000E+00
0.00000E+00	0.00000E+00	0.00000E+00	0.00000E+00	0.27024E-01	0.99963E+00	-.42201E-09	-.36835E-06	0.00000E+00	0.00000E+00
-.99929E-04	0.27024E-01	0.99963E+00	0.00000E+00	0.00000E+00	0.00000E+00	0.31735E+00	-.35135E+02	0.00000E+00	0.00000E+00

B Matrix

-.215440E-01	-.209685E+00	0.427809E-01	0.144939E+00
0.000000E+00	0.161060E+01	-.984213E+00	0.980796E+00
-.152405E+01	-.748881E-04	0.185478E+01	0.185481E+01
0.000000E+00	0.504720E+00	-.489763E+00	0.486870E+00
0.220634E-01	0.638497E-04	-.974812E-01	-.975123E-01
0.000000E+00	-.703860E-01	0.431656E-01	-.301455E-01
0.000000E+00	0.000000E+00	0.000000E+00	0.000000E+00
0.000000E+00	0.000000E+00	0.000000E+00	0.000000E+00
0.000000E+00	0.000000E+00	0.000000E+00	0.000000E+00
0.000000E+00	0.000000E+00	0.000000E+00	0.000000E+00

C Matrix

0.00000E+00 0.00000E+00 0.00000E+00 0.00000E+00 0.00000E+00 0.10000E+01 0.00000E+00 0.00000E+00 0.00000E+00 0.00000E+00

0.00000E+00 0.00000E+00 0.00000E+00 0.00000E+00 0.00000E+00 0.00000E+00 0.10000E+01 0.00000E+00 0.00000E+00 0.00000E+00

0.00000E+00 0.00000E+00 0.00000E+00 0.00000E+00 0.00000E+00 0.00000E+00 0.00000E+00 0.10000E+01 0.00000E+00 0.00000E+00

G Matrix

0.15816E-01 0.14311E-01 -.14297E-01 0.95255E+01 -.10595E+01 -.33810E+02 0.81237E+01 -.14499E+00 0.11301E+02 -.93887E+01 0.90394E+01

-.18555E-01 0.27972E-01 -.10442E+00 -.93526E+01 -.31351E+02 0.31021E+02 -.80153E+01 -.21579E+02 -.99367E+01 0.15076E+02 -.28894E+01

0.16665E-01 -.33897E-01 -.13009E+00 0.91554E+01 -.33087E+02 -.28501E+02 0.75740E+01 -.21733E+02 0.95800E+01 -.29445E+01 0.14584E+02

0.11471E+01 -.69737E+00 0.67680E+00

-.69737E+00 0.15898E+01 -.35287E-01

0.67680E+00 -.35287E-01 0.15676E+01

H Matrix

0.31210E+01 0.33565E+00 -.12059E-01

-.22603E+01 -.11363E+00 0.31632E-01

-.16450E-01 -.48118E-02 -.30074E-01

-.15437E-02 0.72488E-03 0.23951E-04

0.10297E-02 -.58425E-04 -.20399E-03

0.40199E-01 0.81856E-03 -.74136E-03

0.81856E-03 0.62840E-01 0.49473E-04

-.74136E-03 0.49473E-04 0.46174E-01

-.74151E+00 -.13081E+00 0.14382E-01

-.48248E+00 -.10102E+00 0.74060E-02

0.47533E+00 0.10123E+00 -.11341E-01

-.91921E+00 -.37831E-01 0.27406E-01

-.59788E+00 -.44504E-01 0.14876E-01

0.58904E+00 0.45955E-01 -.20617E-01

A-BG-HC Matrix

-.43703E-01 -.53404E-02 -.19627E-02 0.30208E-02 0.58597E+00 -.25507E+01 -.33565E+00 0.21627E-01 -.20968E+00 0.42781E-01 0.14494E+00

0.89727E-03 -.22646E+00 0.15542E-03 -.10595E+01 0.30690E-02 -.58600E+01 0.10183E+00 -.31632E-01 0.16106E+01 -.98421E+00 0.98080E+00

-.37634E-04 0.82501E-04 -.23967E+00 -.23519E+00 0.90297E+01 0.13864E-01 0.48118E-02 0.41567E-01 -.74888E-04 0.18548E+01 0.18548E+01

0.96494E-03 -.49312E-02 -.79456E-03 -.10884E+01 -.69357E-01 -.27354E+01 -.58571E+00 -.22371E-04 0.50472E+00 -.48976E+00 0.48687E+00

0.12087E-04 0.30283E-05 0.21655E-02 -.20736E-02 -.58766E+00 -.12243E-02 0.58425E-04 -.95948E-02 0.63850E-04 -.97481E-01 -.97512E-01

-.22000E-04 -.19154E-02 -.16146E-05 -.66321E-02 0.10729E-05 -.58125E+00 0.18981E-03 0.74135E-03 -.70386E-01 0.43166E-01 -.30145E-01

0.00000E+00 0.00000E+00 0.00000E+00 0.10000E+01 0.27005E-05 -.71867E-03 -.62840E-01 -.37356E-02 0.00000E+00 0.00000E+00 0.00000E+00

0.00000E+00 0.00000E+00 0.00000E+00 0.00000E+00 0.99963E+00 -.26283E-01 0.36367E-02 -.46174E-01 0.00000E+00 0.00000E+00 0.00000E+00

0.00000E+00 0.00000E+00 0.00000E+00 0.00000E+00 0.00000E+00 0.74151E+00 0.13081E+00 -.14382E-01 -.10000E+00 0.00000E+00 0.00000E+00

0.00000E+00 0.00000E+00 0.00000E+00 0.00000E+00 0.00000E+00 0.48248E+00 0.10102E+00 -.74060E-02 0.00000E+00 -.10000E+00 0.00000E+00

0.00000E+00 0.00000E+00 0.00000E+00 0.00000E+00 0.00000E+00 -.47533E+00 -.10123E+00 0.11341E-01 0.00000E+00 0.00000E+00 -.10000E+00

-.15816E-01 -.14311E-01 0.14297E-01 -.95255E+01 0.10595E+01 0.34729E+02 -.80858E+01 0.11758E+00 -.11301E+02 0.93887E+01 -.90394E+01

0.18555E-01 -.27972E-01 0.10442E+00 0.93526E+01 0.31351E+02 -.30423E+02 0.80598E+01 0.21564E+02 0.99367E+01 -.15076E+02 0.28894E+01

-.16665E-01 0.33897E-01 0.13009E+00 -.91554E+01 0.33087E+02 0.27912E+02 -.76199E+01 0.21754E+02 -.95800E+01 0.29445E+01 -.14584E+02

0.00000E+00 0.00000E+00 0.00000E+00

0.00000E+00 0.00000E+00 0.00000E+00

0.00000E+00 0.00000E+00 0.00000E+00

0.00000E+00 0.00000E+00 0.00000E+00

0.00000E+00 0.00000E+00 0.00000E+00

0.00000E+00 0.00000E+00 0.00000E+00

0.00000E+00 0.00000E+00 0.00000E+00

0.00000E+00 0.00000E+00 0.00000E+00

0.10000E+00 0.00000E+00 0.00000E+00

0.00000E+00 0.10000E+00 0.00000E+00

0.00000E+00 0.00000E+00 0.10000E+00

-.11471E+01 0.69737E+00 -.67680E+00

0.69737E+00 -.15898E+01 0.35287E-01

-.67680E+00 0.35287E-01 -.15676E+01

207067
Thesis
H2897 Harris
Automatic control of
a submersible.